



CRYSTAL2PLATE

**How does plate tectonics work:
From crystal-scale processes to mantle
convection with self-consistent plates**



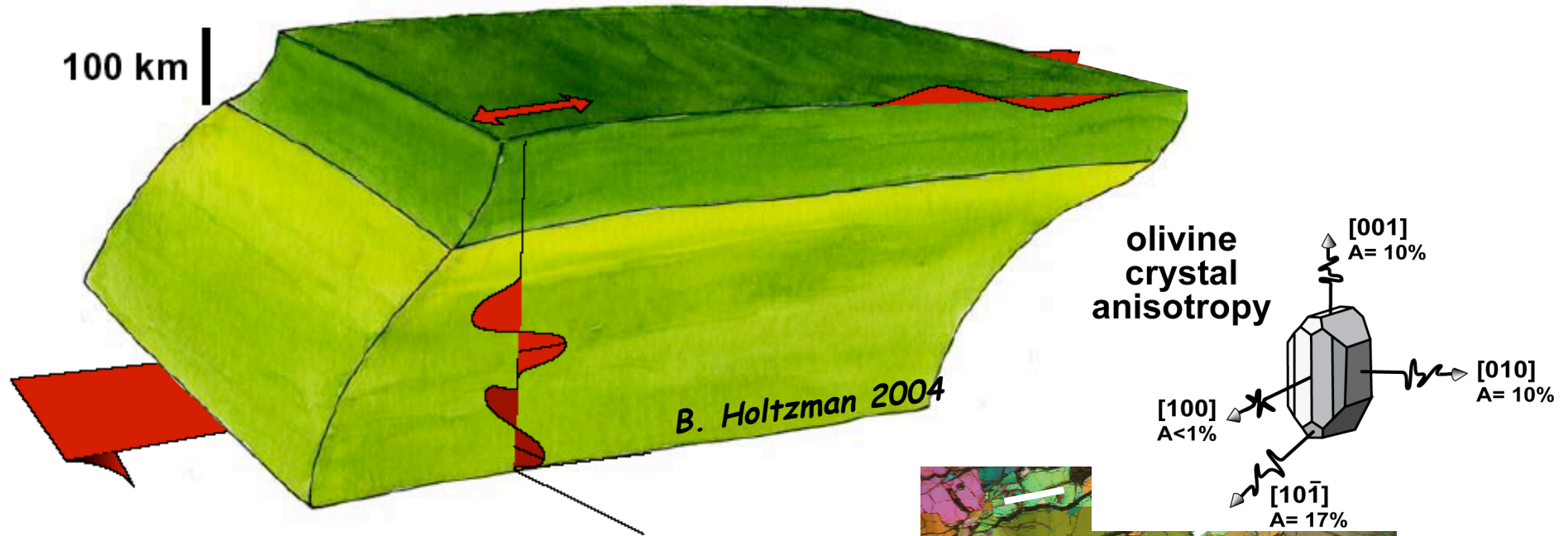
Numerical models of CPO evolution...

Andréa Tommasi

***Short course on "Microstructures, textures & anisotropy"
Geosciences Montpellier (F) - 28 June - 2 July, 2010***

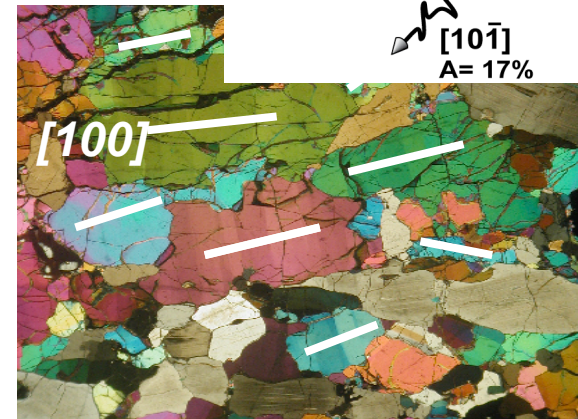


how do we "see" mantle deformation?



fast seismic axis = flow direction

**P & Rayleigh propagation,
S-wave polarisation**



Can we go farther? Quantify the anisotropy produced by mantle flow at different depths or geodynamic environments (ridges, subduction zones...)



Multi-scale models of mantle deformation and seismic anisotropy

JOURNAL OF GEOPHYSICAL RESEARCH, VOL. 98, NO. B10, PAGES 17,757-17,771, OCTOBER 10, 1993

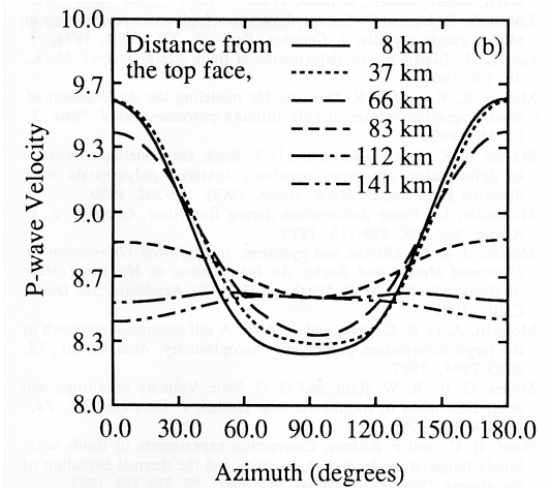
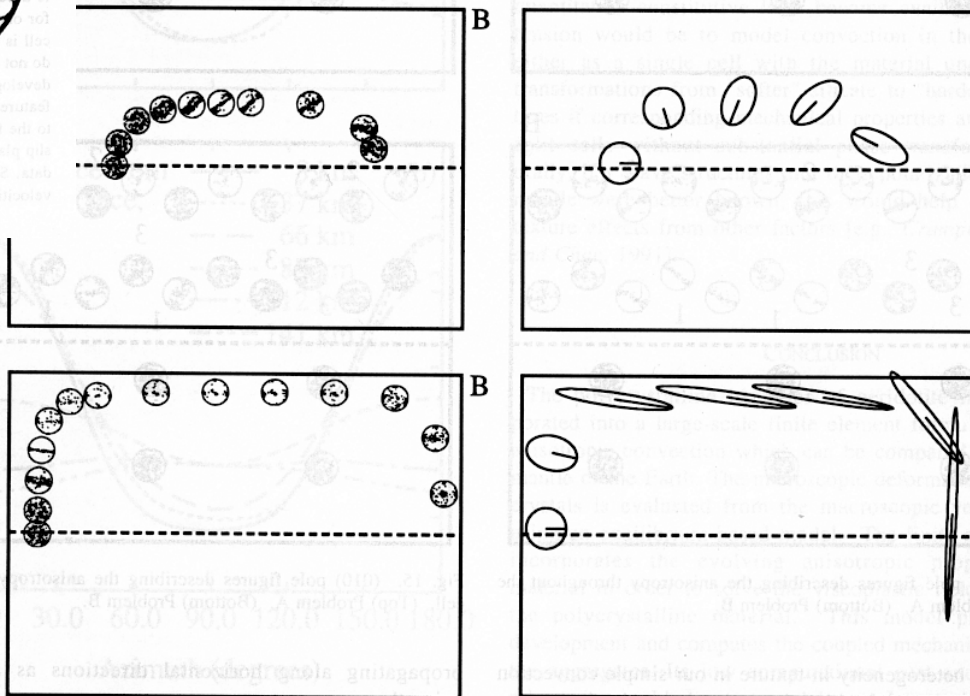
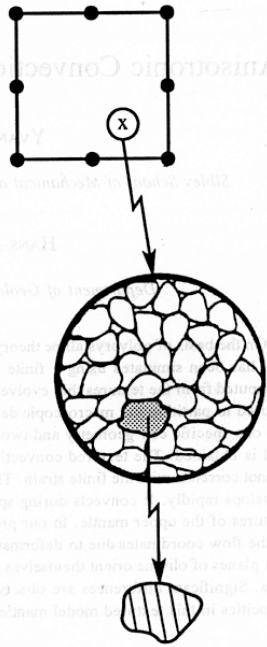
Anisotropic Convection With Implications for the Upper Mantle

YVAN B. CHASTEL AND PAUL R. DAWSON

Sibley School of Mechanical and Aerospace Engineering, Cornell University, Ithaca, New York

HANS-RUDOLF WENK AND KRISTIN BENNETT

Department of Geology and Geophysics, University of California, Berkeley



Multi-scale models of mantle deformation and seismic anisotropy

Teleseismic imaging of subaxial flow at mid-ocean ridges: traveltime effects of anisotropic mineral texture in the mantle

Donna K. Blackman,¹ J.-Michael Kendall,^{2,*} Paul R. Dawson,³
H.-Rudolph Wenk,⁴ Donald Boyce³ and Jason Phipps Morgan¹

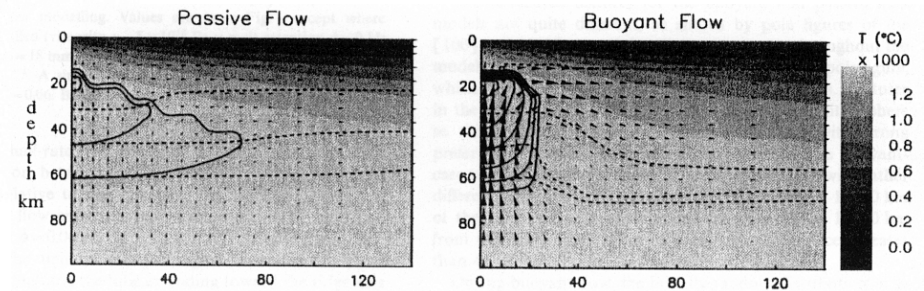
¹ IGPP, Scripps Institution of Oceanography, La Jolla, CA 92093-0225, USA

² Department of Physics, University of Toronto, Toronto, Ontario, Canada

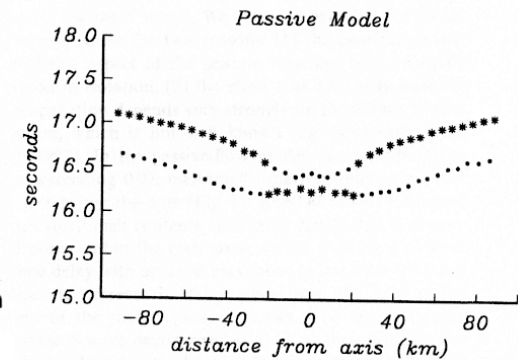
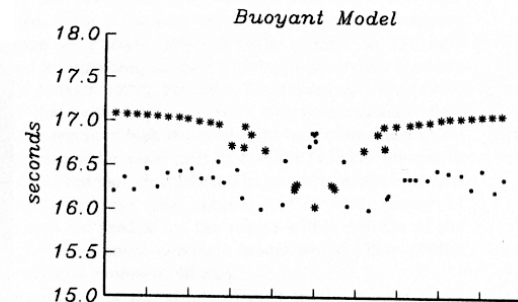
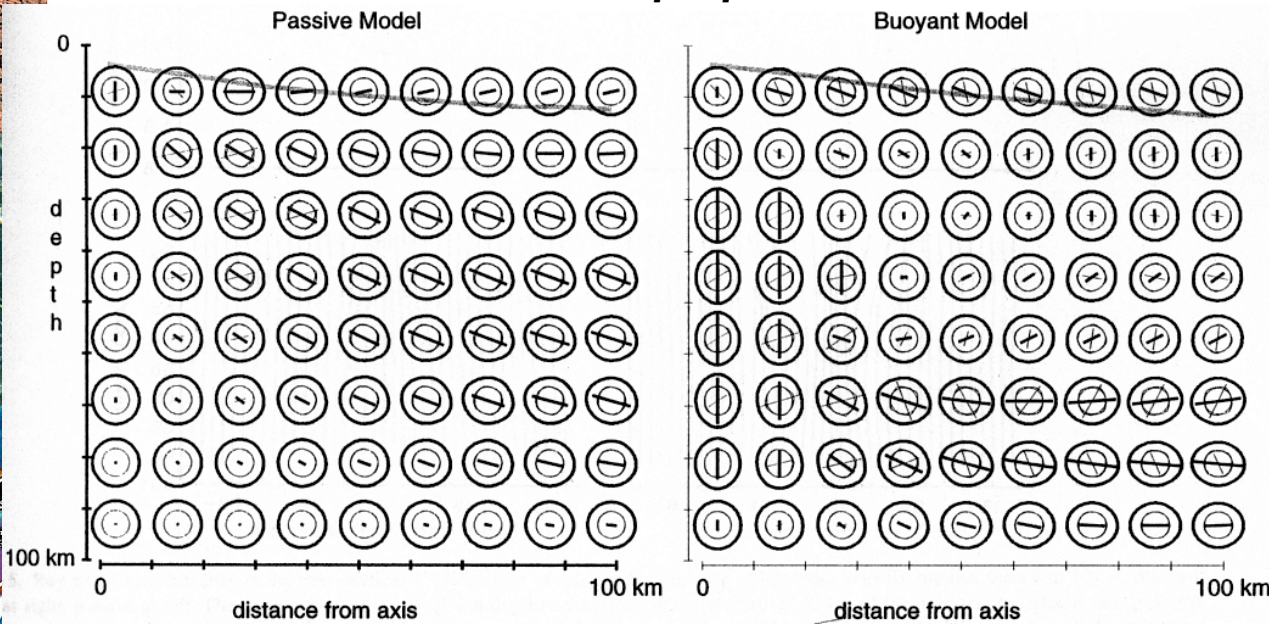
³ Sibley School of Mechanical & Aerospace Engineering, Cornell University, Ithaca, NY 14853-7501, USA

⁴ Department of Geology & Geophysics, University of California, Berkeley, CA 94720, USA

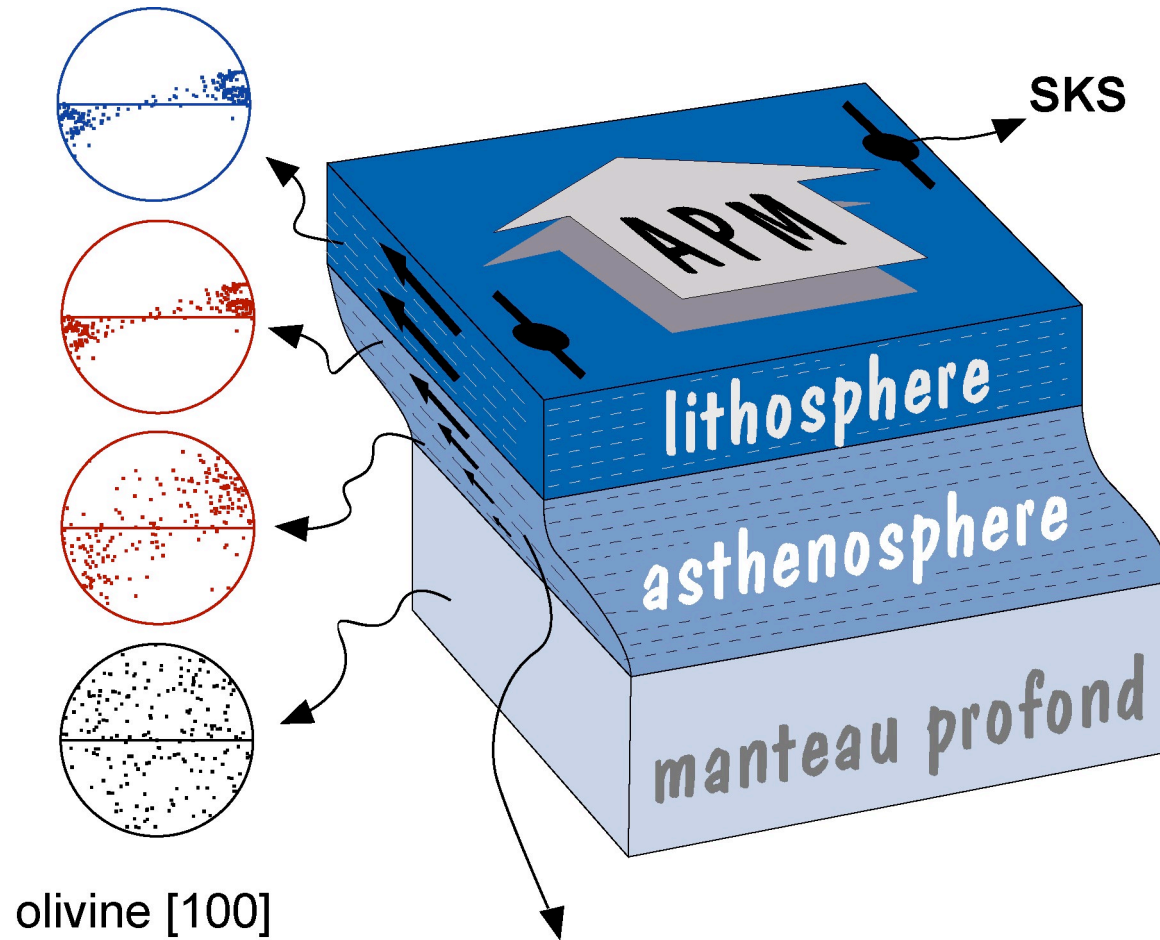
mantle flow modeling



seismic properties



Seismic anisotropy in oceanic basins

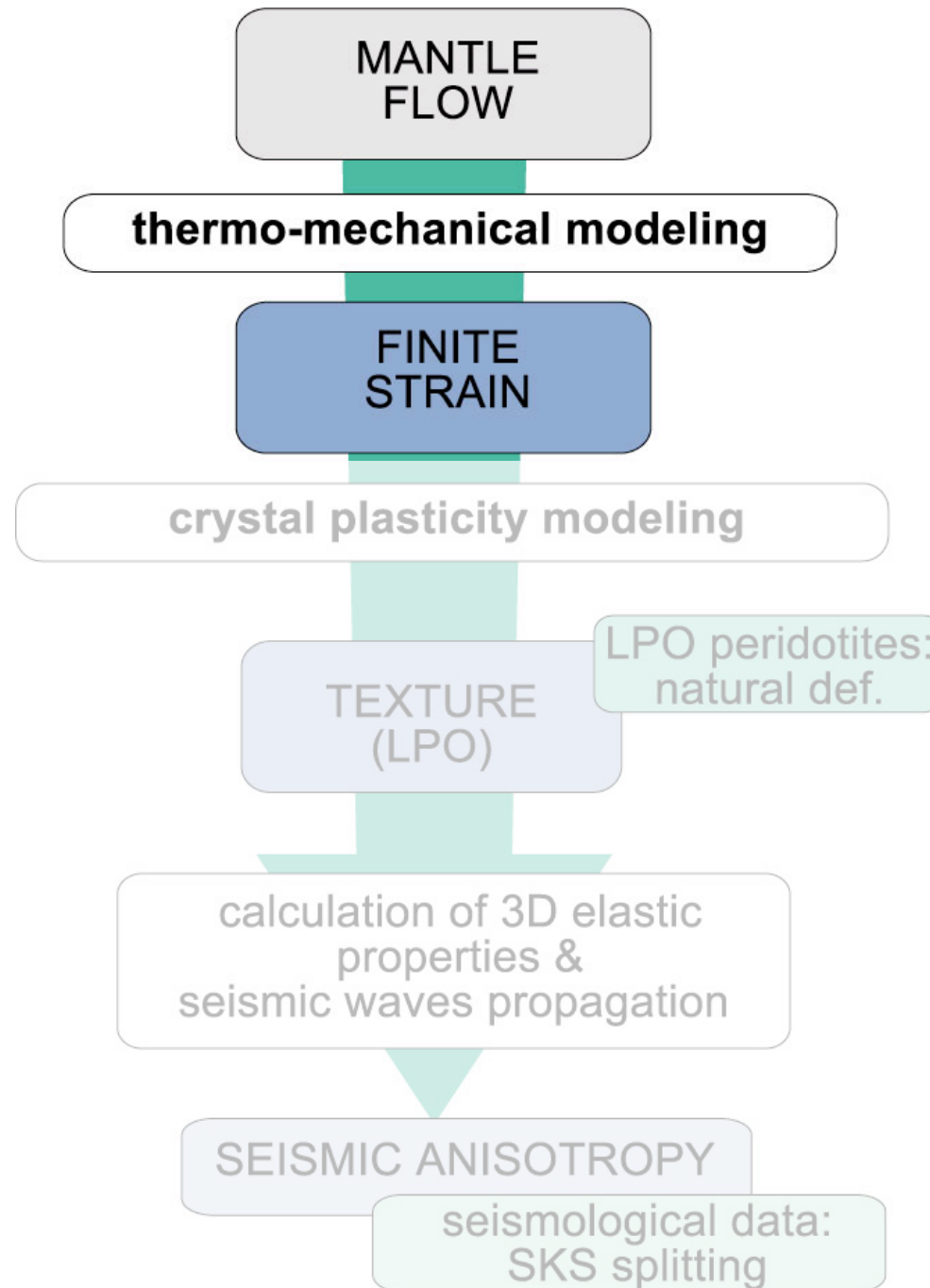


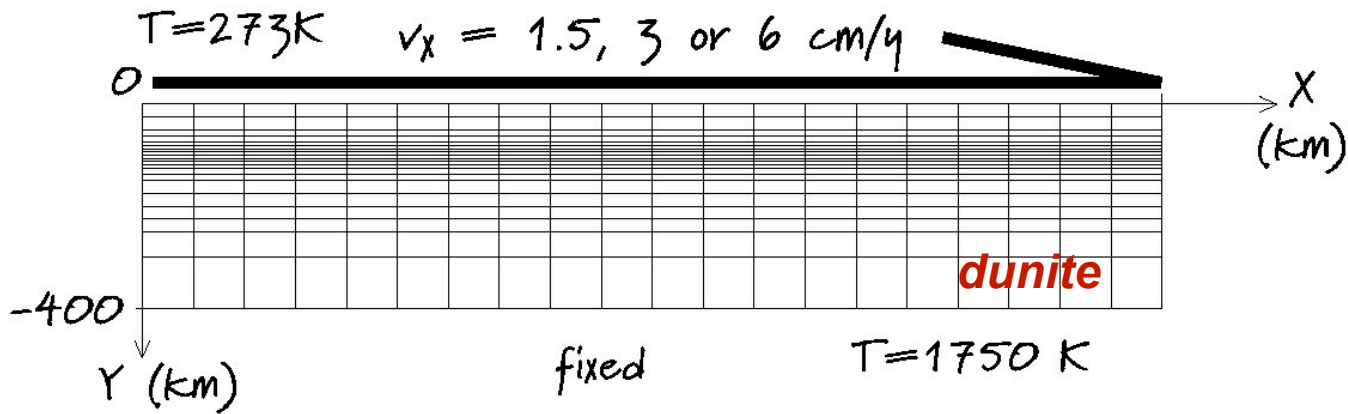
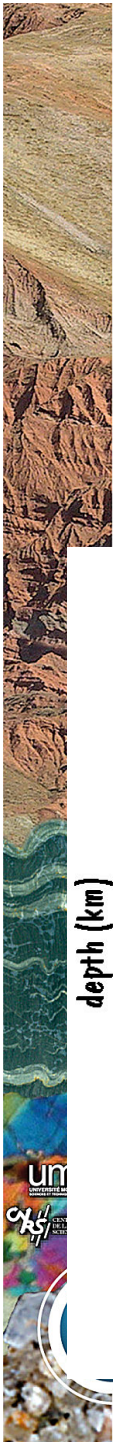
olivine [100]

Strain field:
horizontal shear // APM

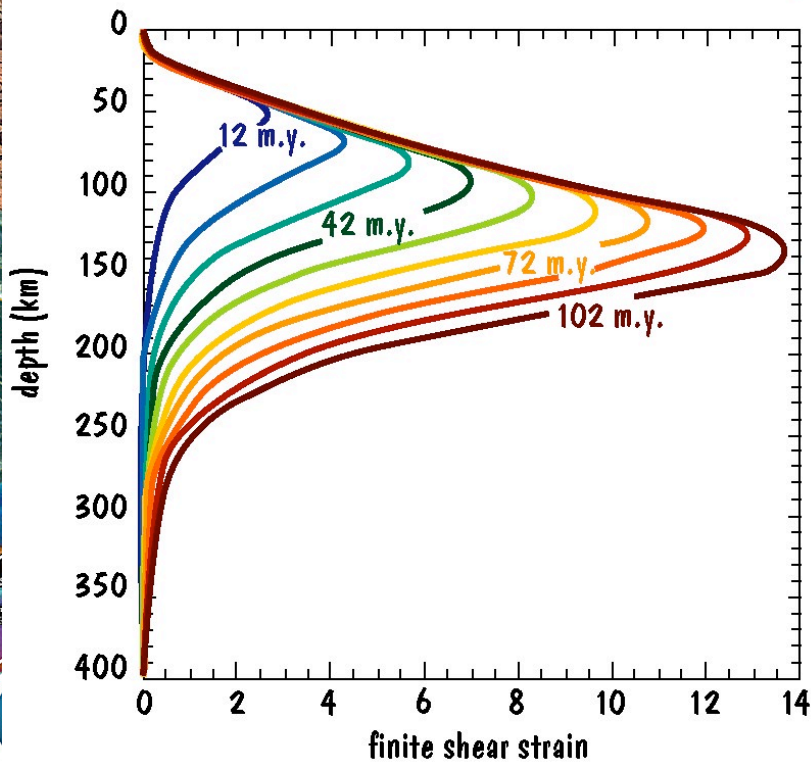
Tommasi et al. 1995 GRL, Tommasi 1998 EPSL, Rumpker et al. 1999 JGR







finite shear strain profiles ($dv = 1.5 \text{ cm/y}$)



finite strain = $F(v_x, \text{age})$

- ✓ viscous drag : strain & LPO development in the asthenosphere
- ✓ cooling : freezes LPO in the lithosphere



MANTLE FLOW

thermo-mechanical modeling

FINITE STRAIN

crystal plasticity modeling

TEXTURE (LPO)

LPO peridotites:
natural def.

calculation of 3D elastic properties & seismic waves propagation

SEISMIC ANISOTROPY

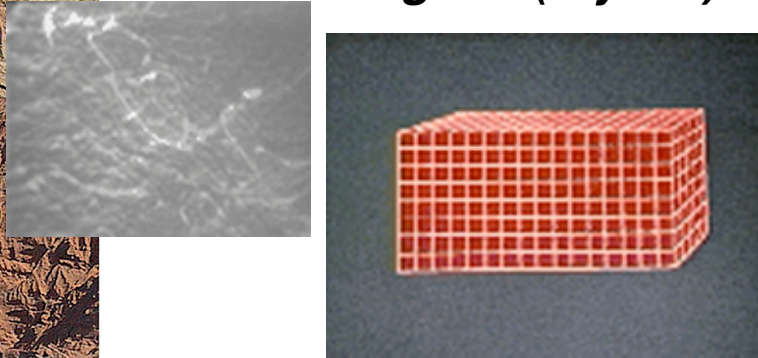
seismological data:
SKS splitting



Modeling the deformation & crystal orientation evolution

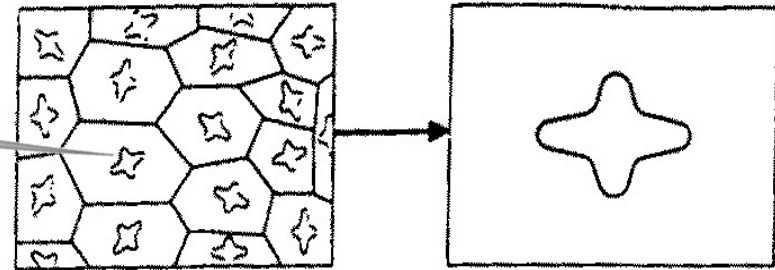
VPSC: Molinari et al. 1987, Lebensohn & Tomé 1993
 Drex: Kaminsky & Ribe 2001, 2003

within a grain (crystal):



strain = motion of dislocations on well-defined crystal planes & directions

rock (polycrystal) deformation:

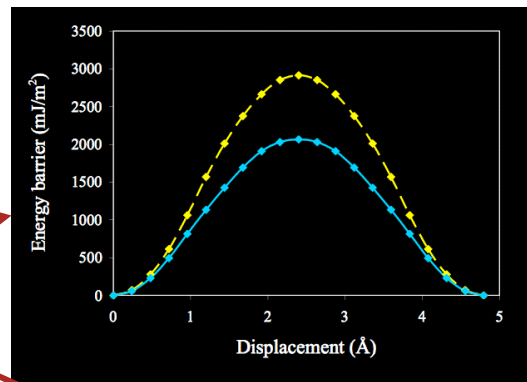


behavior of the aggregate (rock) = average of crystals' behaviors

$$\dot{\epsilon}_{ij} = \langle \dot{\epsilon}_{ij} \rangle \quad \Sigma_{ij} = \langle \sigma_{ij} \rangle$$

$$\dot{\epsilon}_{kl} - \dot{E}_{kl} = -M_{ijkl} (\sigma_{ij} - \Sigma_{ij})$$

$$\dot{\gamma}^s = \left(\frac{\tau_r^s}{\tau_0^s} \right)^n$$



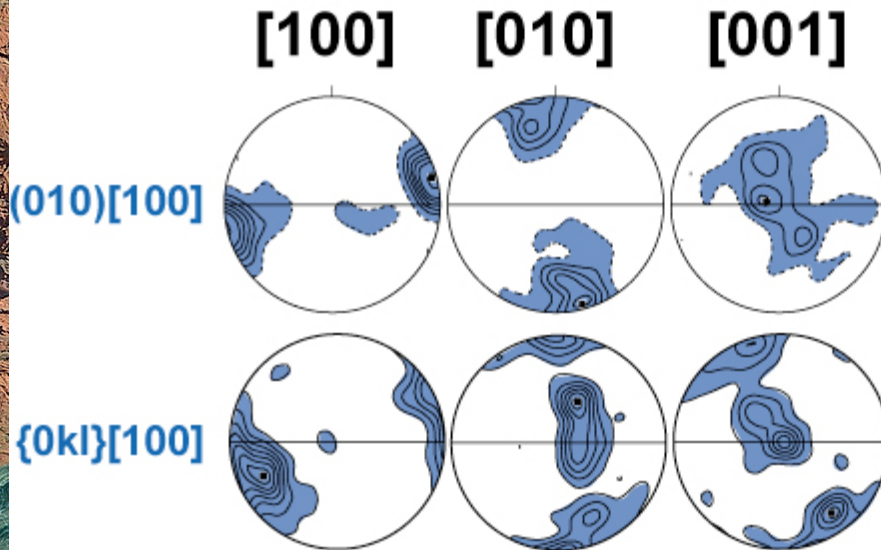
input parameters: slip systems' strength, initial texture, and macroscopic sollicitation (stress or velocity gradient tensor)
 output: evolution of crystallographic orientations and macroscopic response (strain rate or stress tensor)

Olivine CPO:

Naturally deformed peridotites:

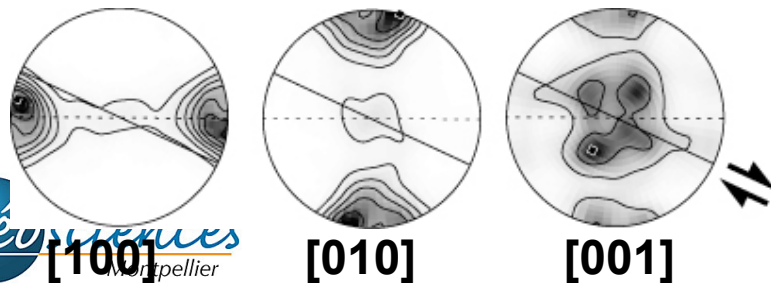
olivine LPO database (Montpellier): >300 samples

~ 80% of the samples



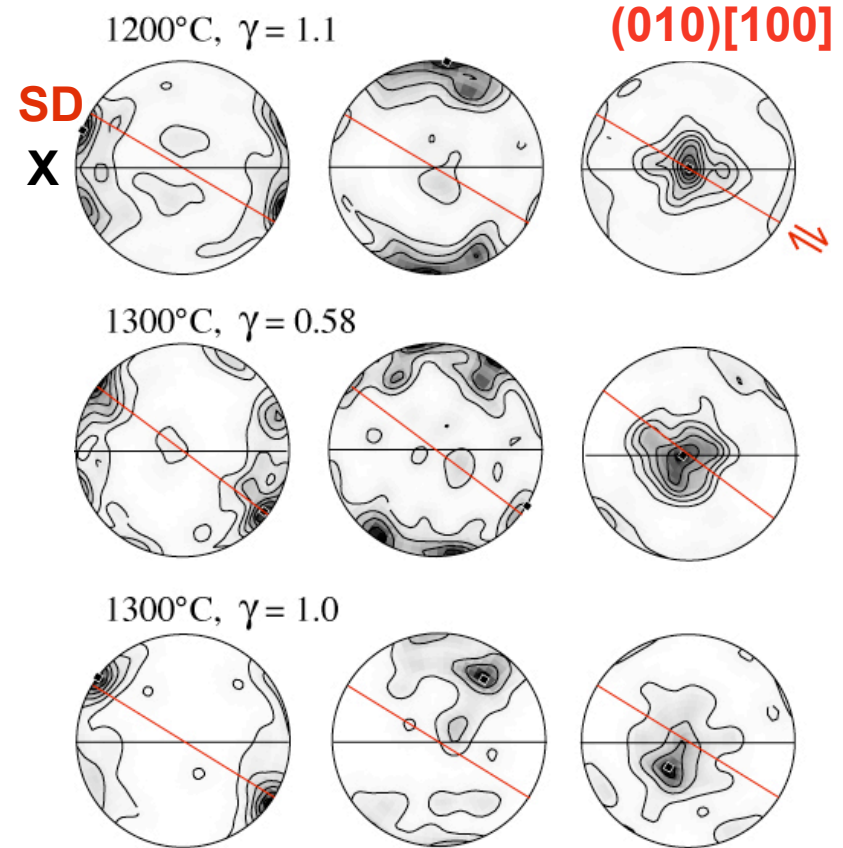
CPO/SPO asymmetry: simple shear

Polycrystal plasticity models:

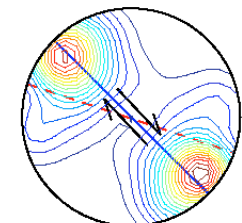


Experimental deformation: simple shear

Zhang & Karato (1995) Nature



dynamic recrystallization:
faster reorientation of
[100] // SD



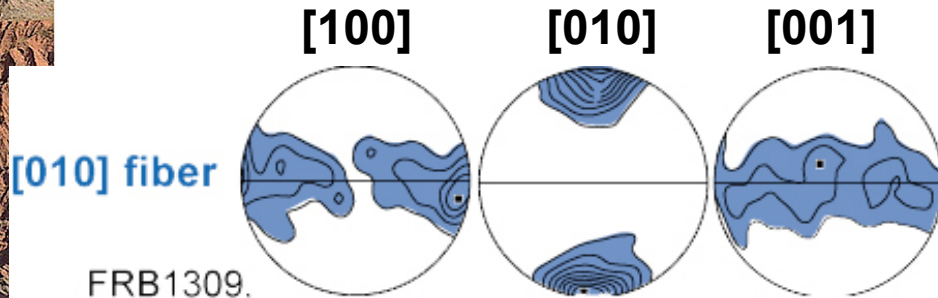
Kamisinski & Ribe 2001 EPSL



Naturally deformed peridotites

olivine LPO database (Montpellier): >300 samples

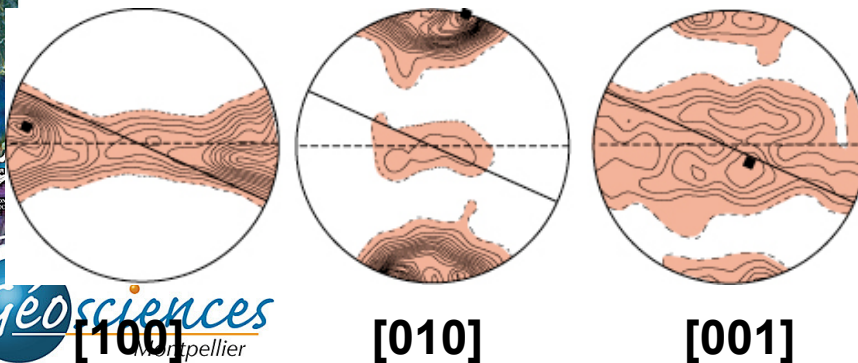
20-30% of the samples (continental)



FRB1309,
kimberlitic xenolith,
Kapvaal craton

axial compression
or transpression

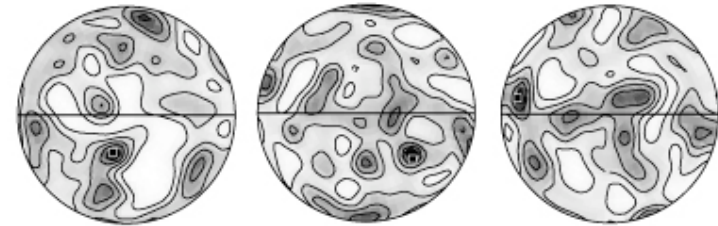
Polycrystal plasticity models:
transpression



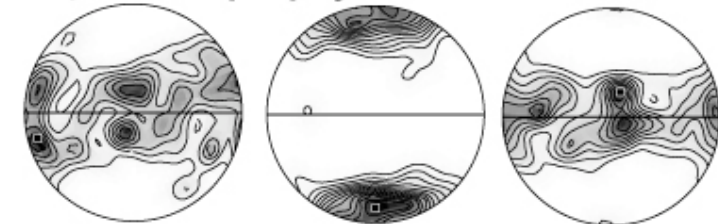
Experimental deformation: axial compression

Nicolas et al. (1973) *Am. J. Sci.*

initial LPO



$\epsilon_{eq} = 0.58$ - porphyroclasts



$\epsilon_{eq} = 0.58$ - recrystallized grains



[100]

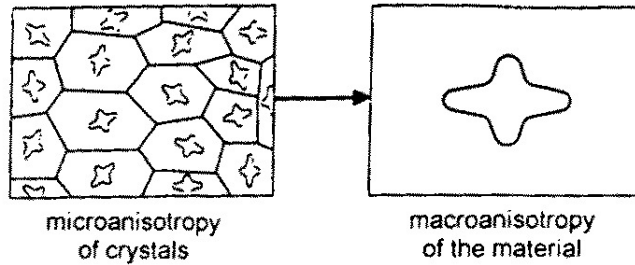
[010]

[001]

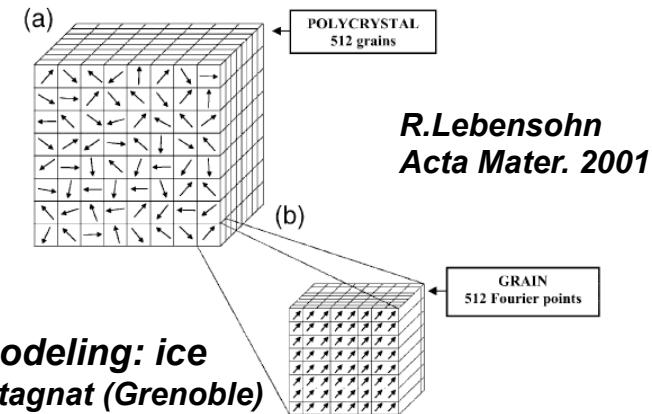


Modeling plastic deformation & development of CPO at the "rock" scale: polycrystalline aggregate

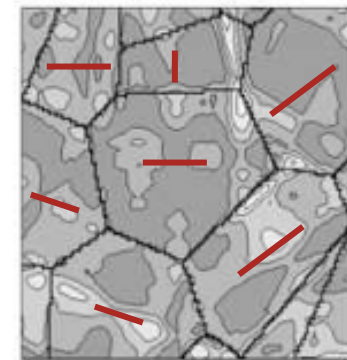
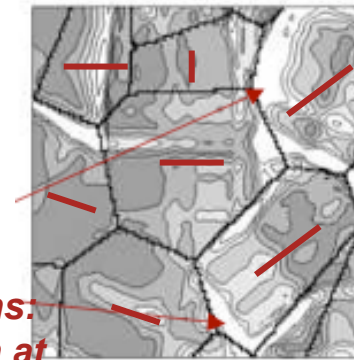
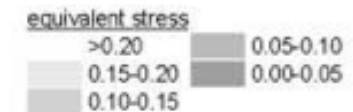
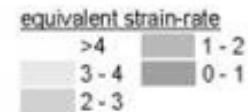
homogeneization models:



Fast-Fourier Transform

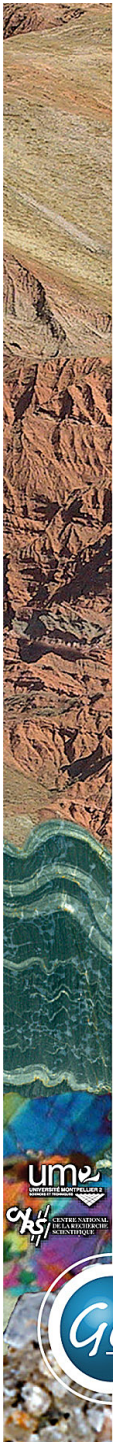


FFT modeling: ice
M. Montagnat (Grenoble)
R. Lebensohn



**easy glide orientations:
high strain at
grain boundaries**

- Sachs 1928: stress equilibrium
- Taylor 1938: homogeneous strain
- Lister 1978: Taylor in Earth Sciences
- Molinari et al. 1987: VPSC
- Wenk et al. 1989: VPSC in Earth Sciences
- Ribe & Yu 1991: strain fluctuations min.
- Lebensohn & Tomé 1993: anisotropic SC
- Wenk et al. 1997: VPSC + **recrystallization**
- Kaminski & Ribe 2001: **DRex**



MANTLE
FLOW

thermo-mechanical modeling

FINITE
STRAIN

crystal plasticity modeling

TEXTURE
(LPO)

LPO peridotites:
natural def.

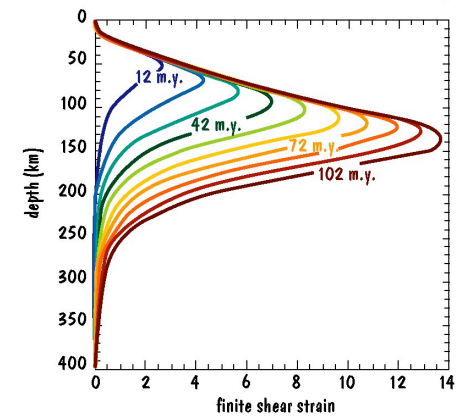
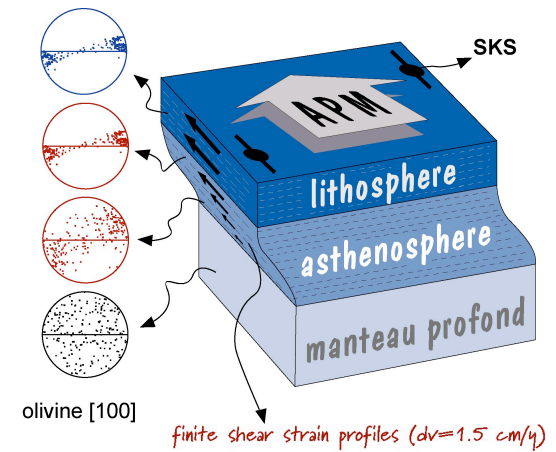
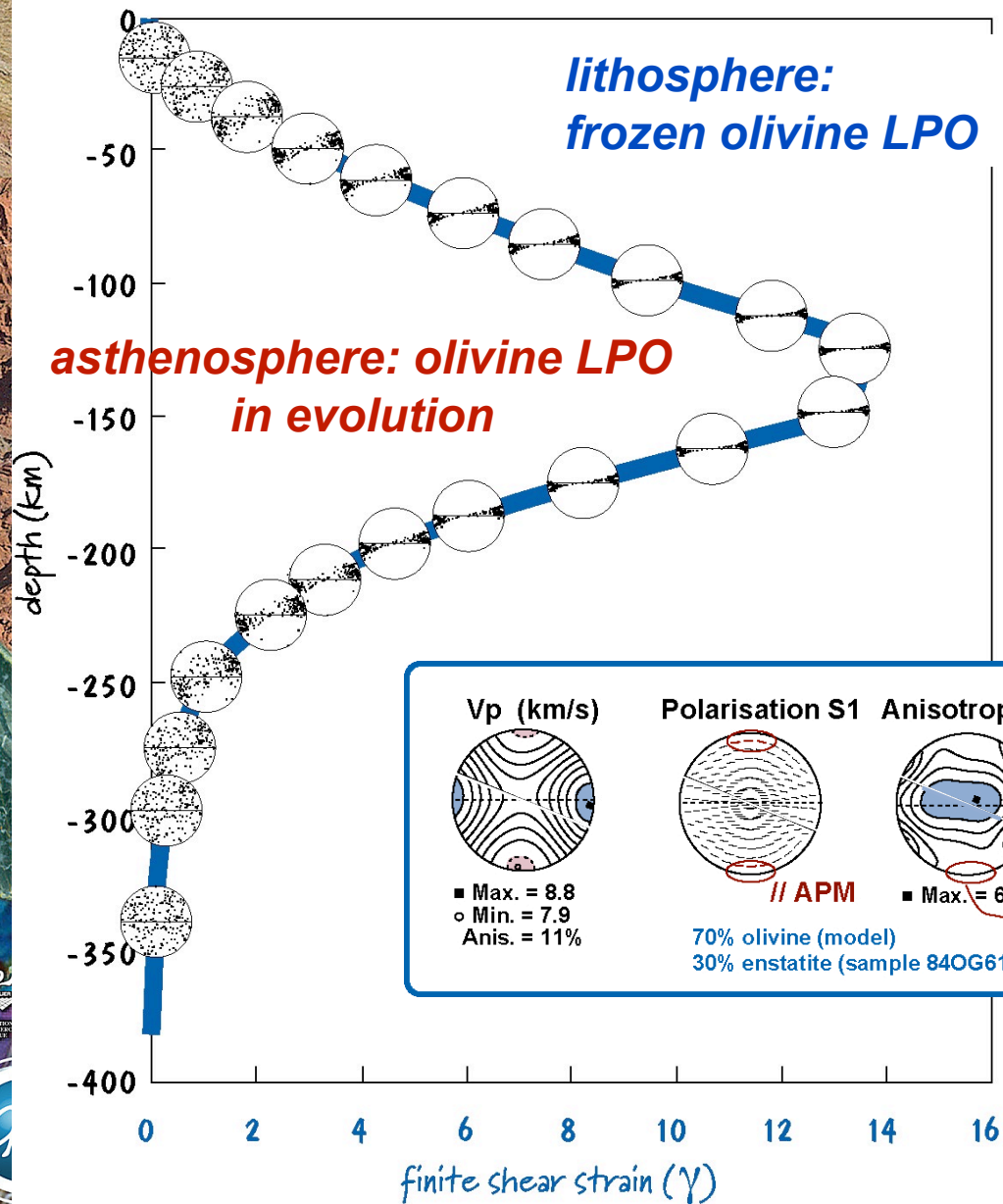
calculation of 3D elastic
properties &
seismic waves propagation

SEISMIC ANISOTROPY

seismological data:
SKS splitting



[100] PREFERRED ORIENTATIONS
 100 m.y. old plate ($dv = 1.5 \text{ cm/y}$)



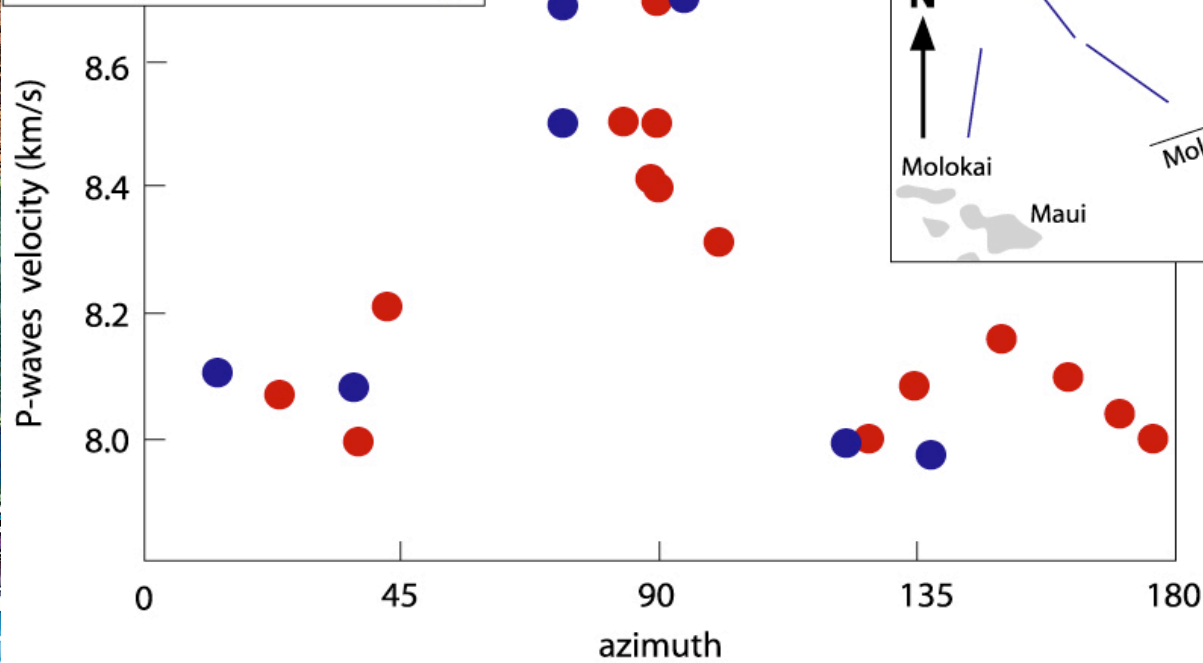
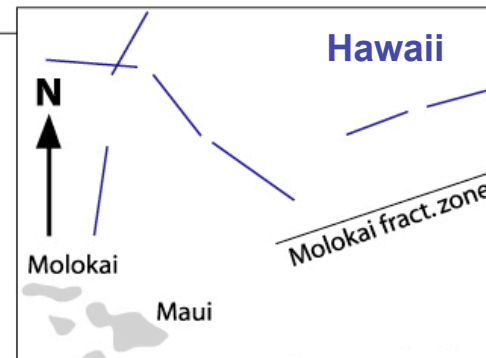
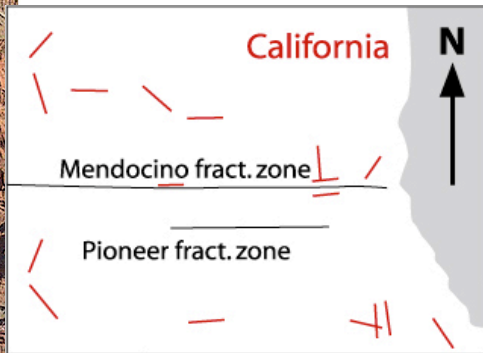
$dt = \int dt_i = 2.3s$



Seismic anisotropy: P waves

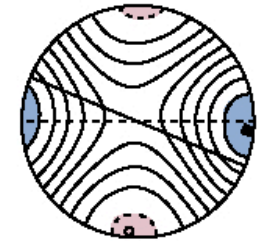
$v_P = F(\text{propagation direction})$

fast velocities // fractures zones
 ➤ *fossil spreading direction*



Hess (1964), Nature

Vp (km/s)

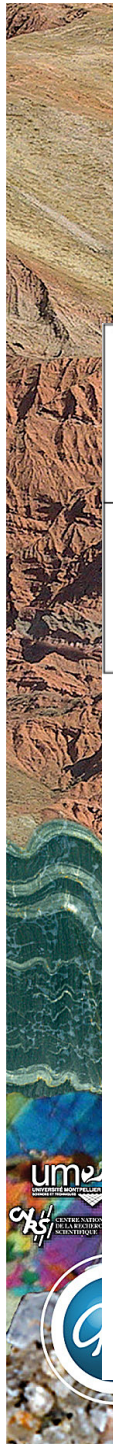


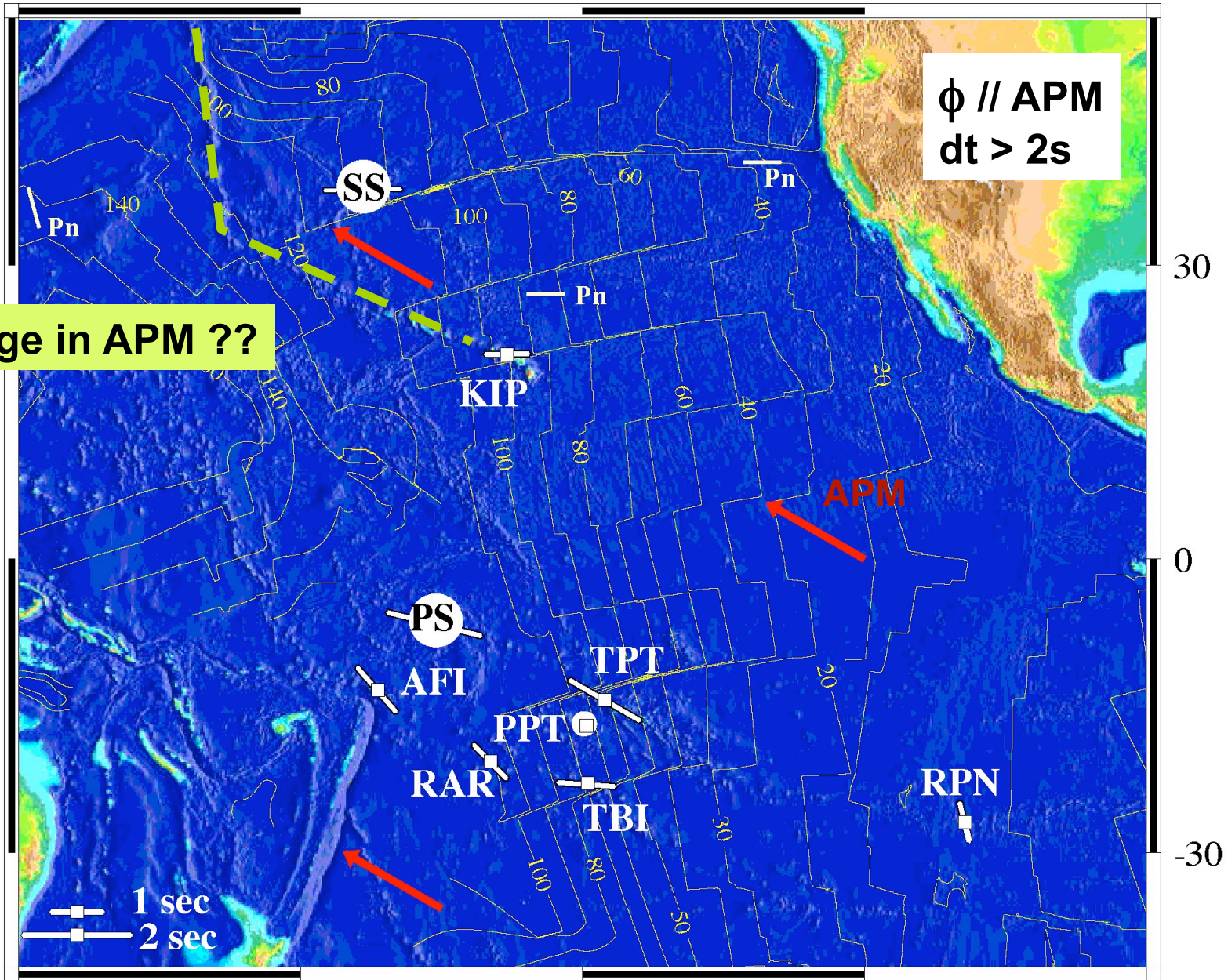
■ Max. = 8.8
 ○ Min. = 7.9
 Anis. = 11%

Polaris



70%
 30%



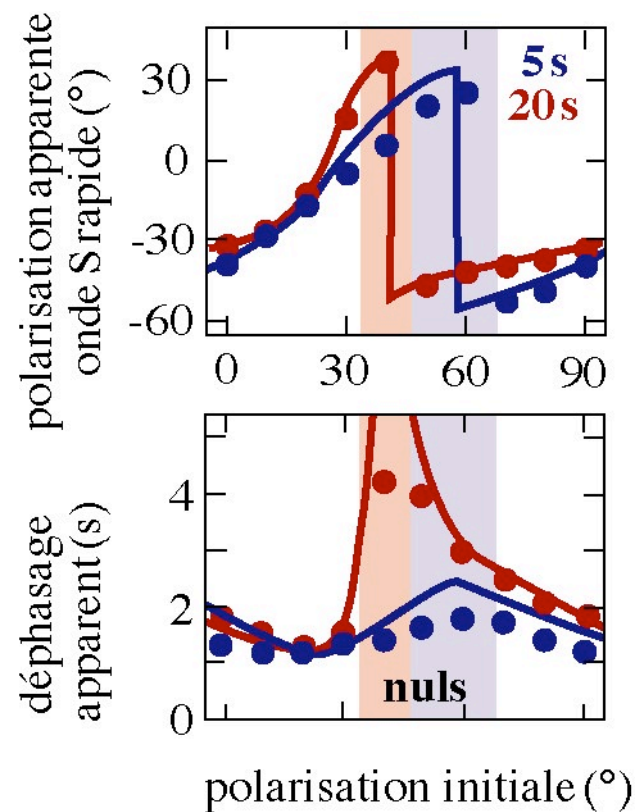
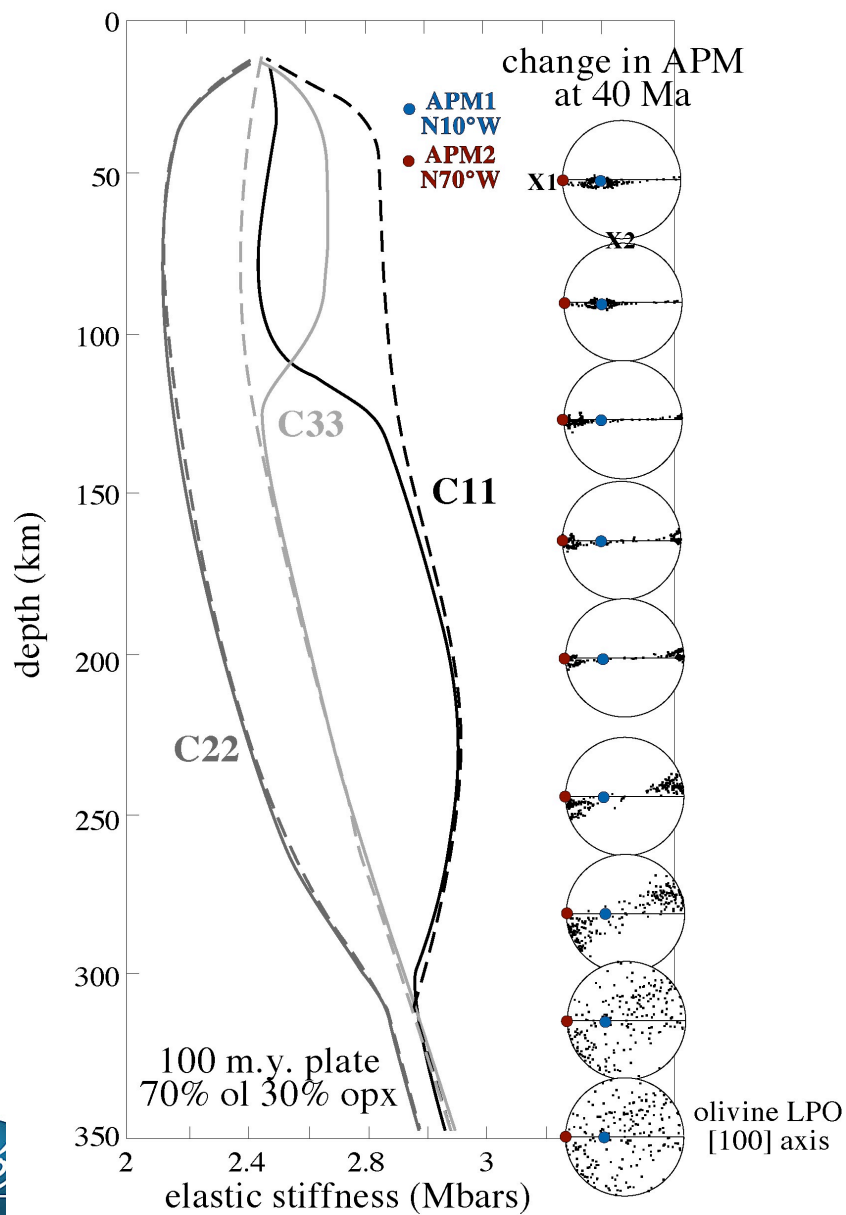


change in APM ??

150 180 210 240 270

Data from Okal & Russo 1997 GJI, Wolfe & Silver 1997 JGR; Su and Park, 1994 PEPI

APM variation = vertical variation of anisotropy



Hawaii (KIP)

SKS: $\phi = E-W$; $dt = 0.9s$

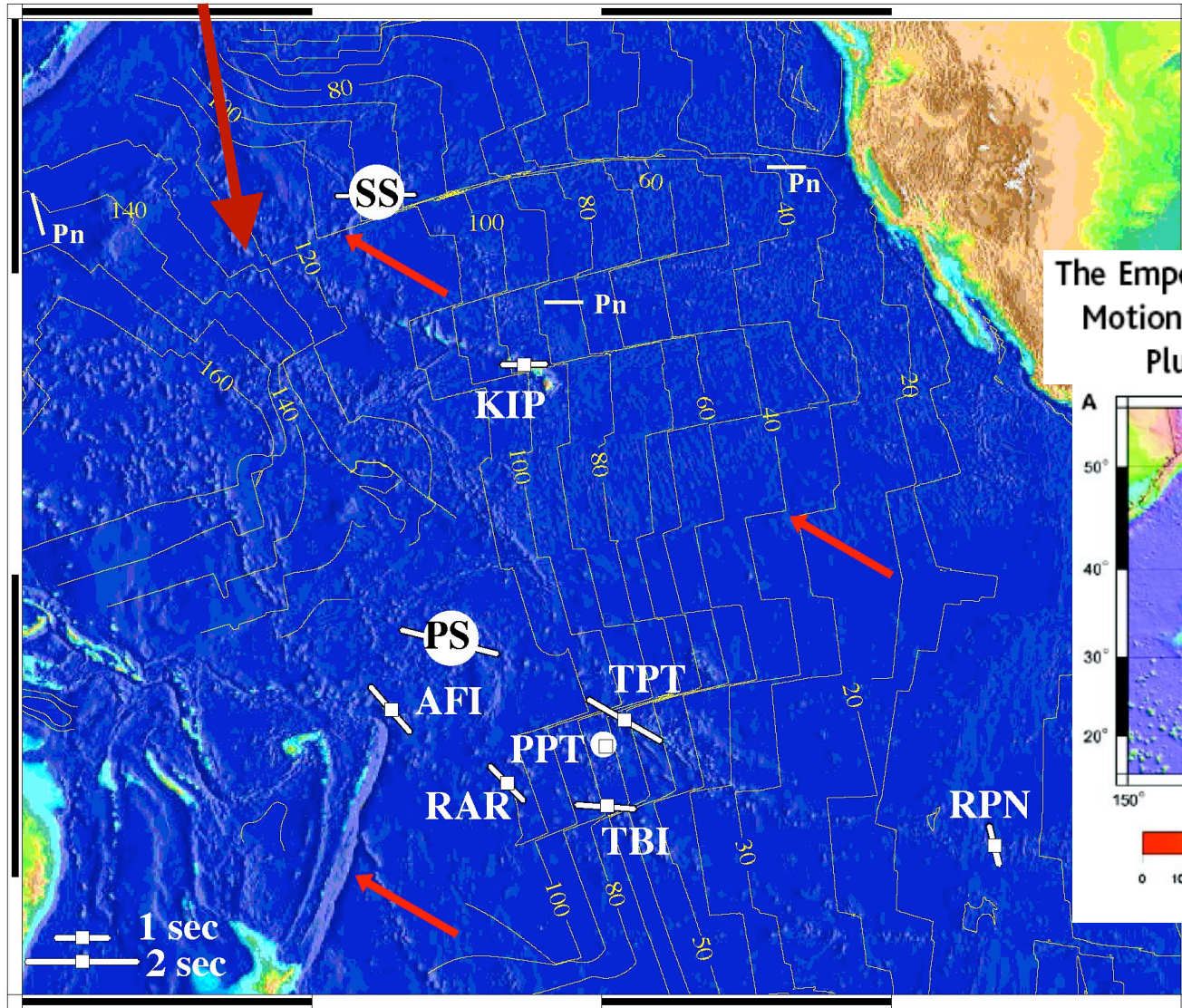
$\phi = 45^\circ$; $dt = 1s$

Pn: fast propagation = E-W

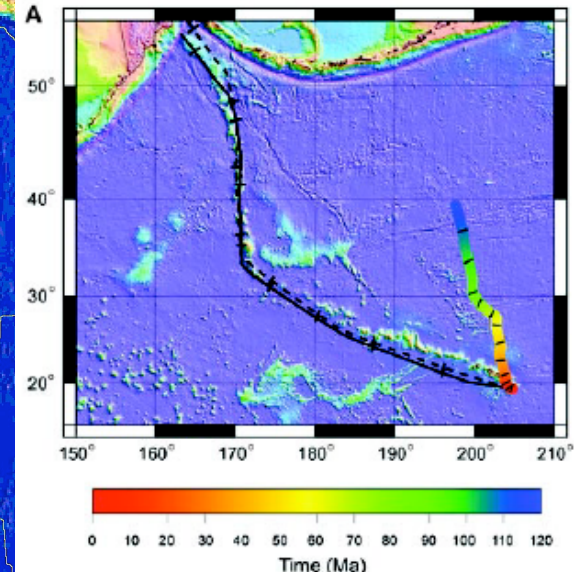
Tommasi 1998, Rumpker et al.. 1999



Emperor = displacement of the Hawaii plume pre-43Ma



The Emperor Seamounts: Southward Motion of the Hawaiian Hotspot Plume in Earth's Mantle



Tarduno et al. Science 2003

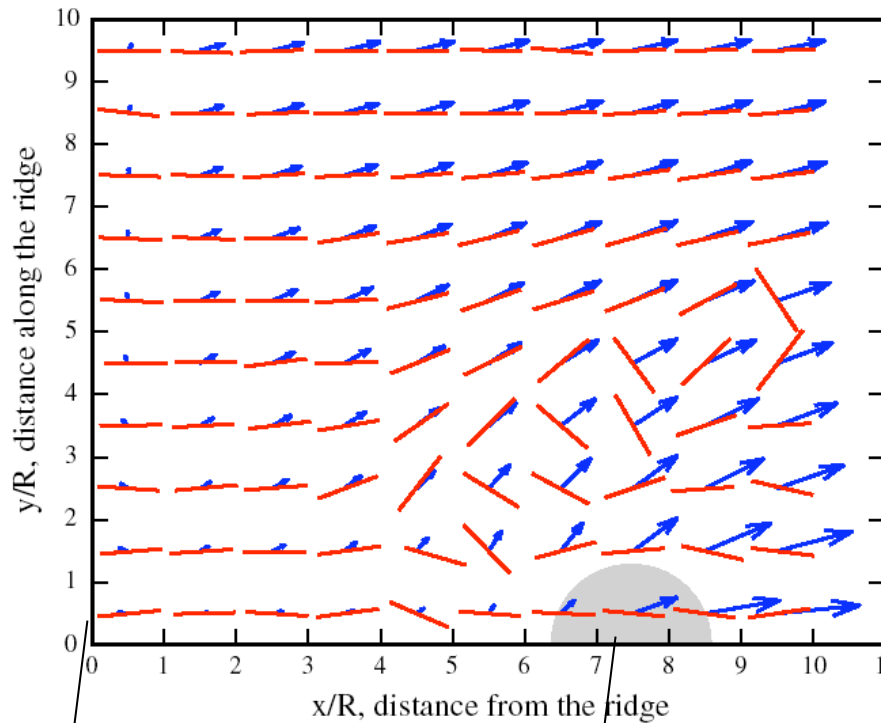
150 180 210 240 270
 Data from Okal & Russo 1997 GJI, Wolfe & Silver 1997 JGR; Su and Park, 1994 PEPI



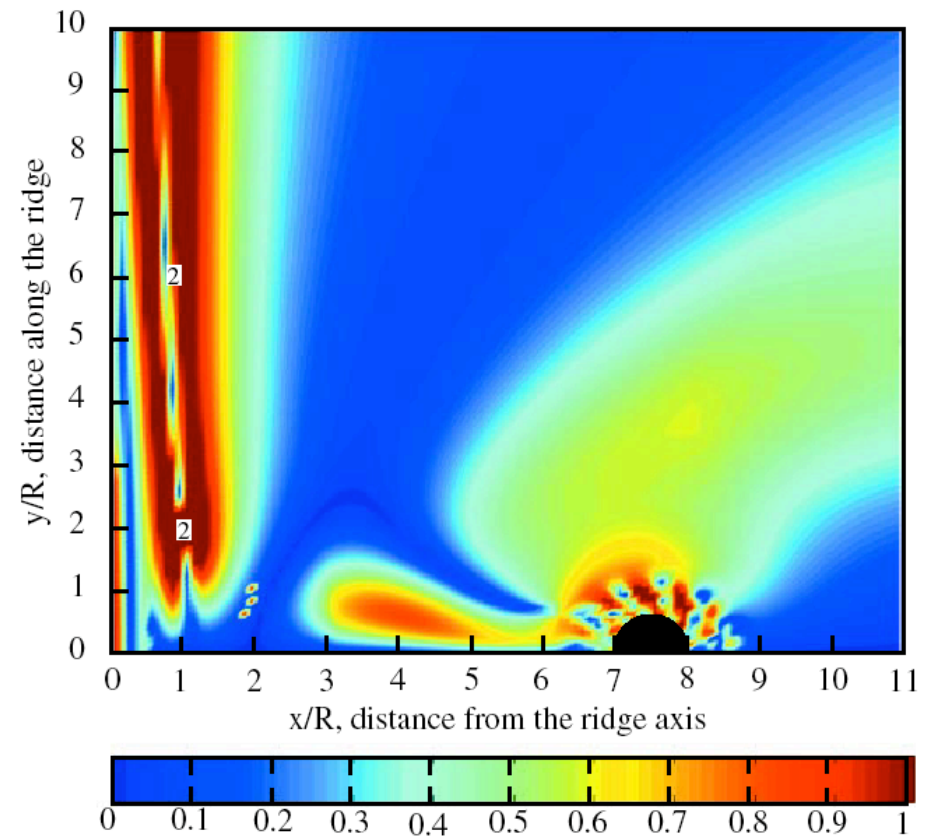
When is the full calculation of the CPO evolution needed?

- complex 3D strain field
- evolution of CPO slower than changes in strain pattern

ex: plume-ridge interaction



grain orientation lag parameter π





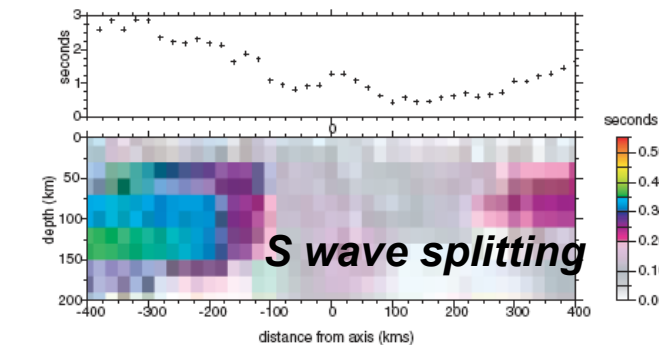
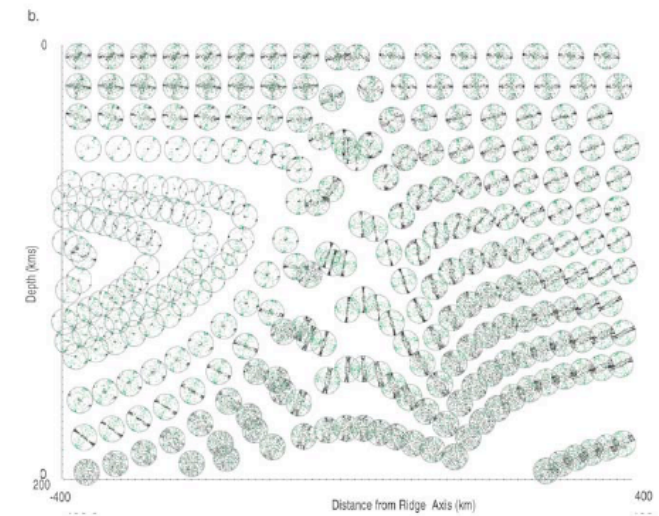
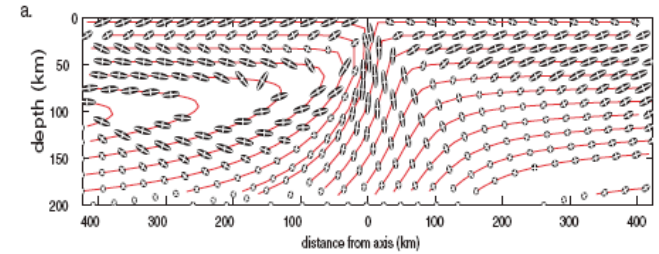
Seismic anisotropy in the upper mantle 2. Predictions for current plate boundary flow models

Donna K. Blackman and J.-Michael Kendall

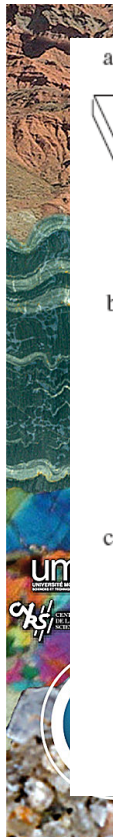
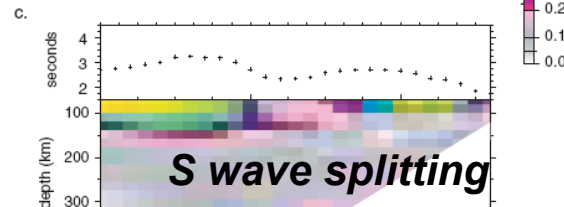
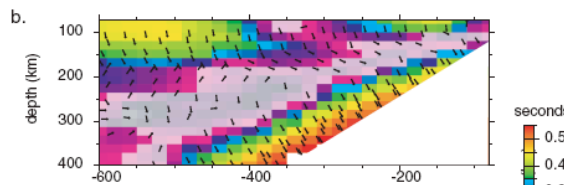
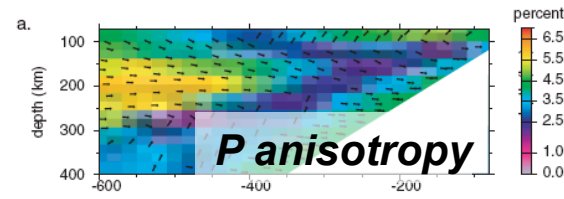
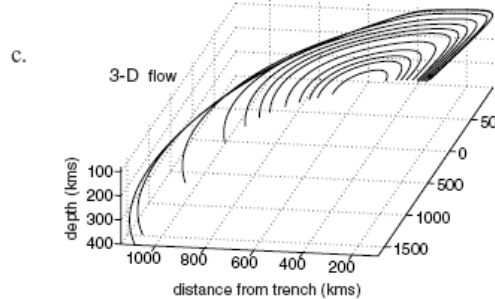
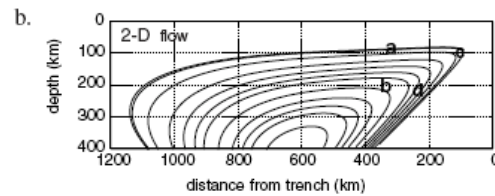
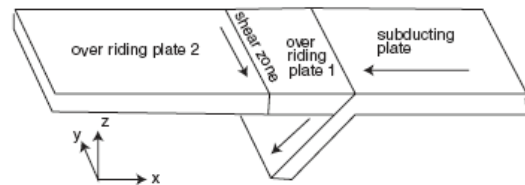
*Scripps Institution of Oceanography, 8602 La Jolla Shores Drive, La Jolla, California 92037, USA
(dblackman@ucsd.edu)*

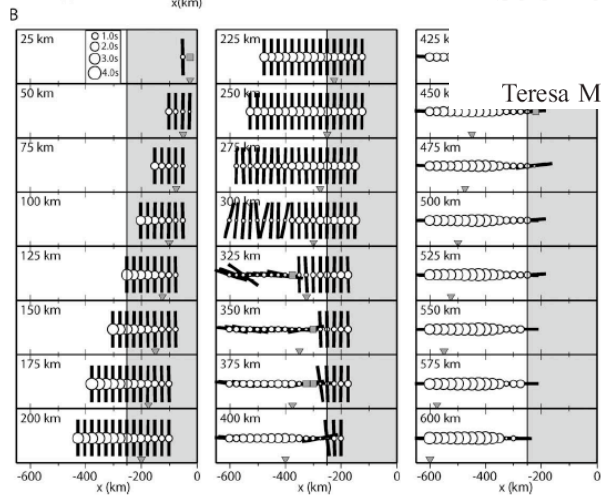
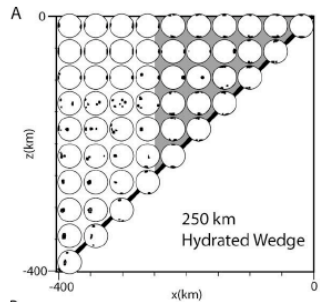
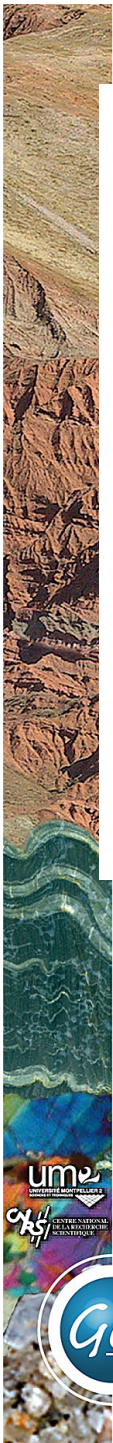
Department of Earth Sciences, University of Leeds, Leeds LS2 9JT, UK (kendall@earth.leeds.ac.uk)

ridge + shallow *T* anomaly



subduction zones





Available online at www.sciencedirect.com

SCIENCE @ DIRECT®

Earth and Planetary Science Letters 243 (2006) 632–649

EPSL

www.elsevier.com/locate/epsl

Seismic characterization of mantle flow in subduction systems:
Can we resolve a hydrated mantle wedge?

Teresa Mae Lassak^{a,*}, Matthew J. Fouch^a, Chad E. Hall^b, Édouard Kaminski^c

deformation mechanisms at crystal scale?



Available online at www.sciencedirect.com

SCIENCE @ DIRECT®

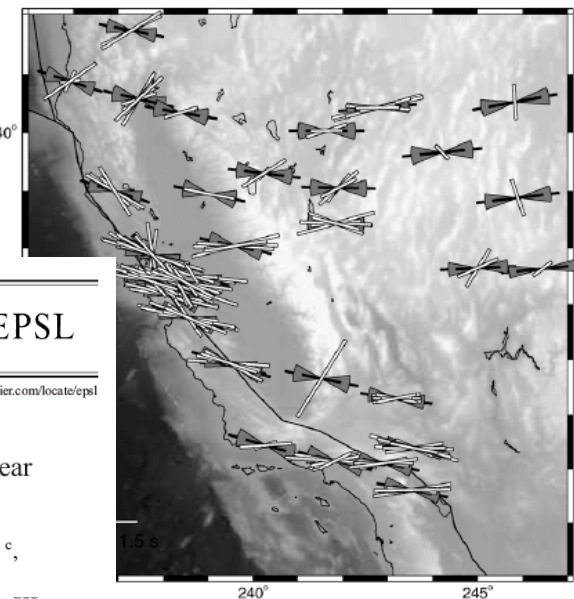
Earth and Planetary Science Letters 247 (2006) 235–251

EPSL

www.elsevier.com/locate/epsl

Mantle flow under the western United States from shear
wave splitting

Thorsten W. Becker^{a,*}, Vera Schulte-Pelkum^b, Donna K. Blackman^c,
James B. Kellogg^d, Richard J. O'Connell^e



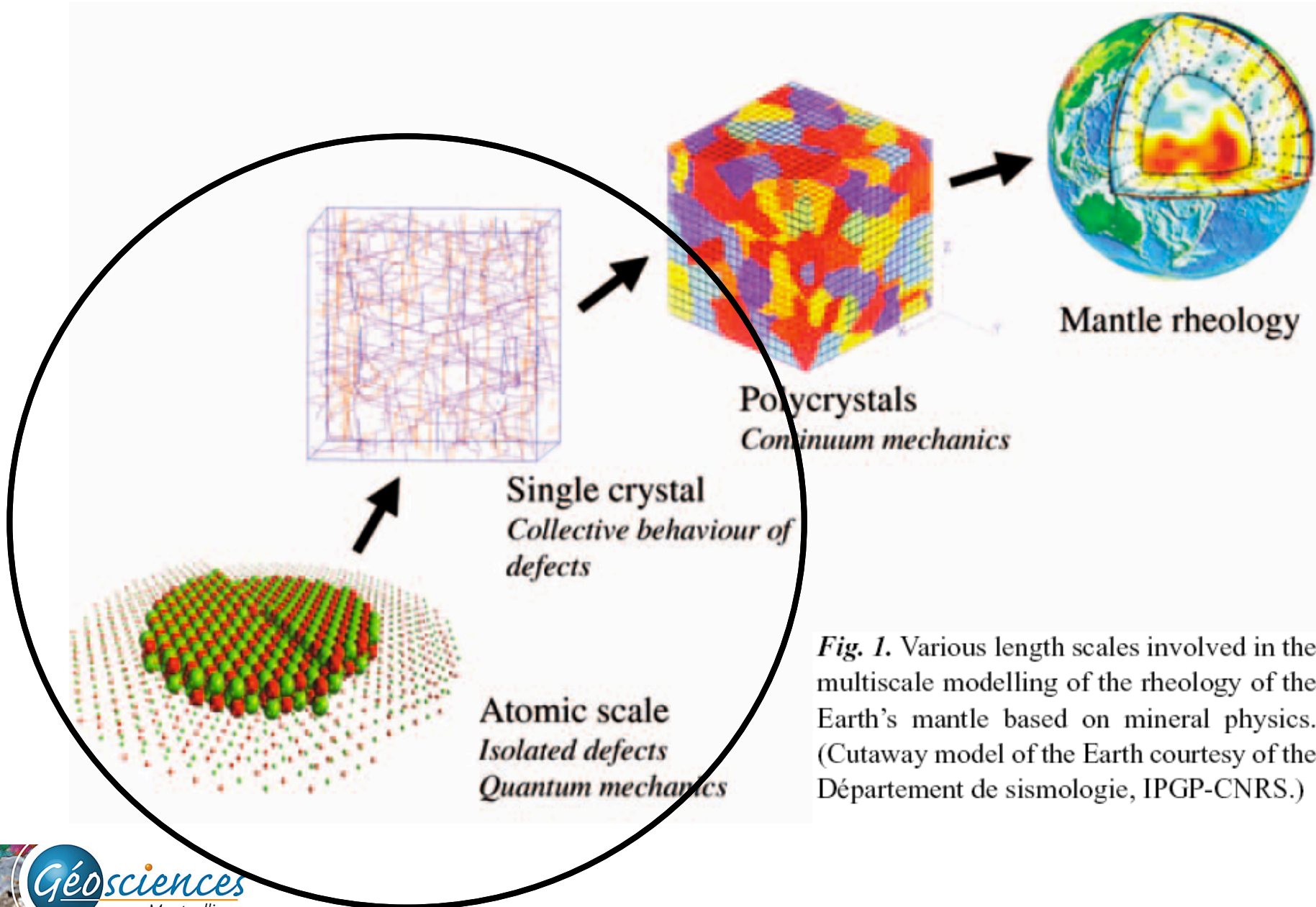
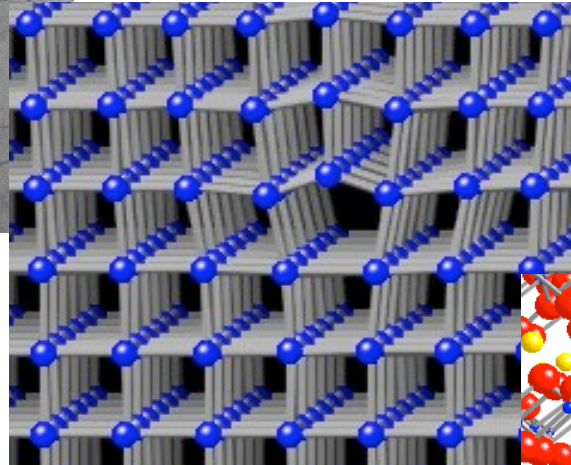
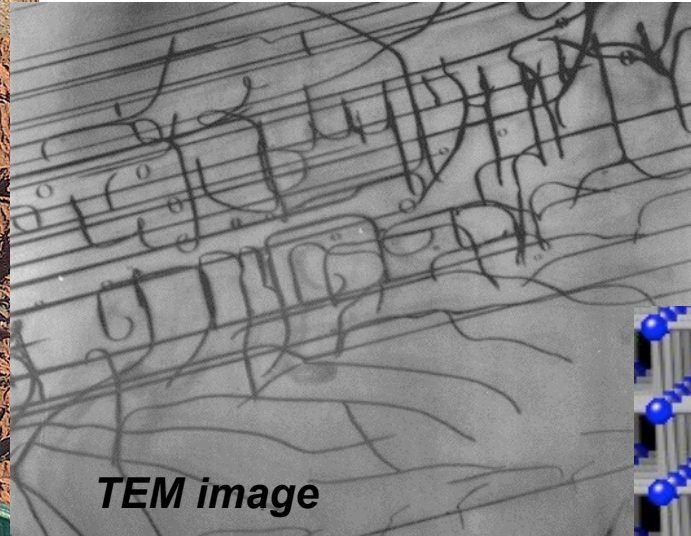


Fig. 1. Various length scales involved in the multiscale modelling of the rheology of the Earth's mantle based on mineral physics. (Cutaway model of the Earth courtesy of the Département de sismologie, IPGP-CNRS.)

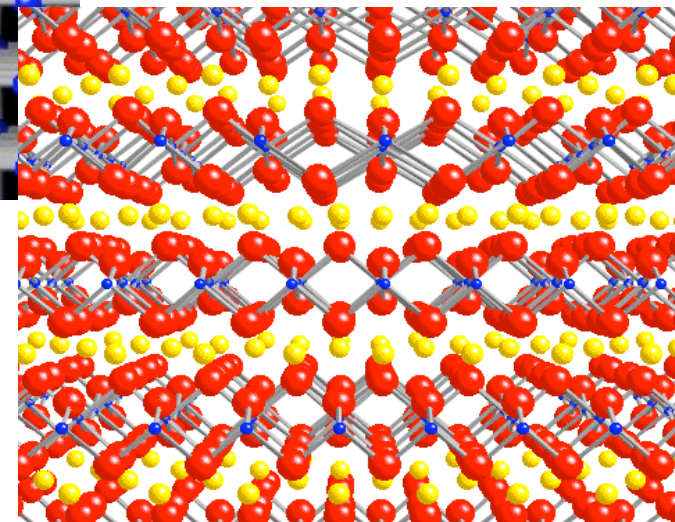
Ab-initio modeling of dislocation core properties: the Peierls-Nabarro model

P. Cordier, P. Carrez, D. Ferré (Lille)



*[100](010) edge
dislocation in PPV
(Carrez 2006)*

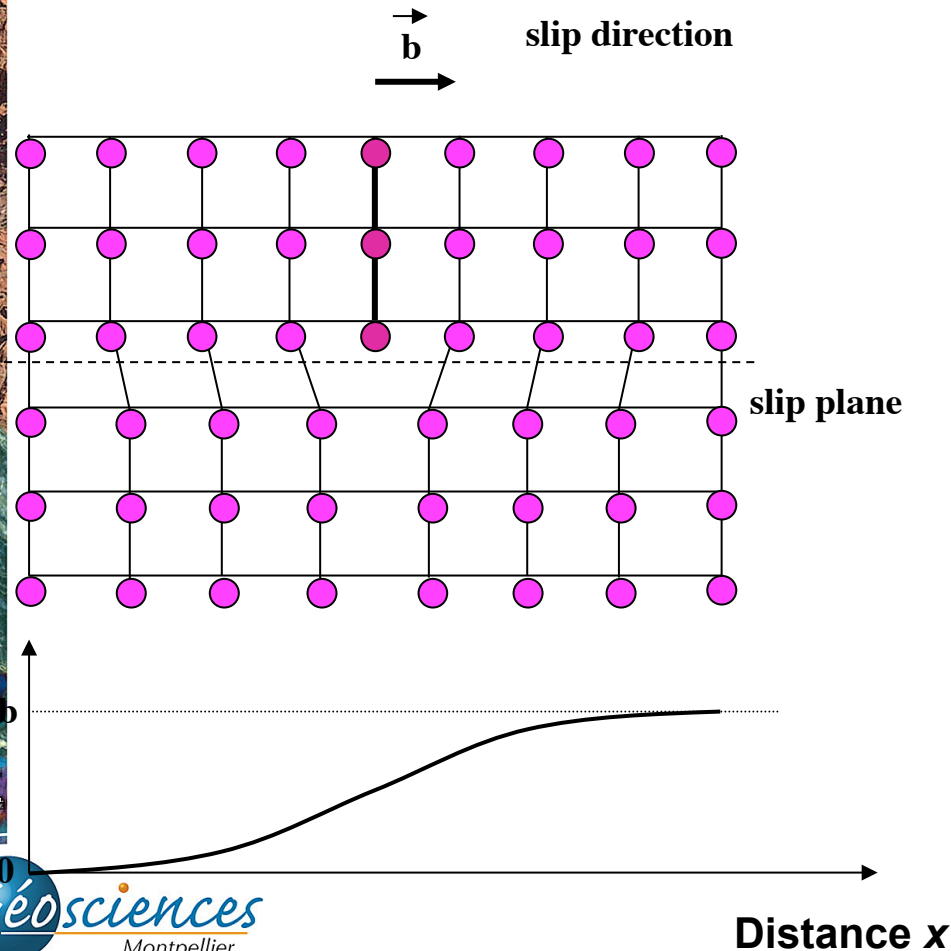
*"traditional"
dislocation model*



Ab-initio modeling of dislocation core properties: the Peierls-Nabarro model

P. Cordier, P. Carrez, D. Ferré (Lille)

shear strain in the vicinity of the dislocation core

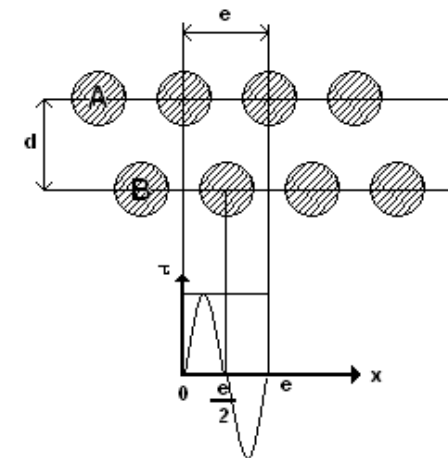


shear \Leftrightarrow dislocation density

$$\int_{-\infty}^{+\infty} \rho(x) dx = \int_{-\infty}^{+\infty} \frac{dS(x)}{dx} dx = b$$

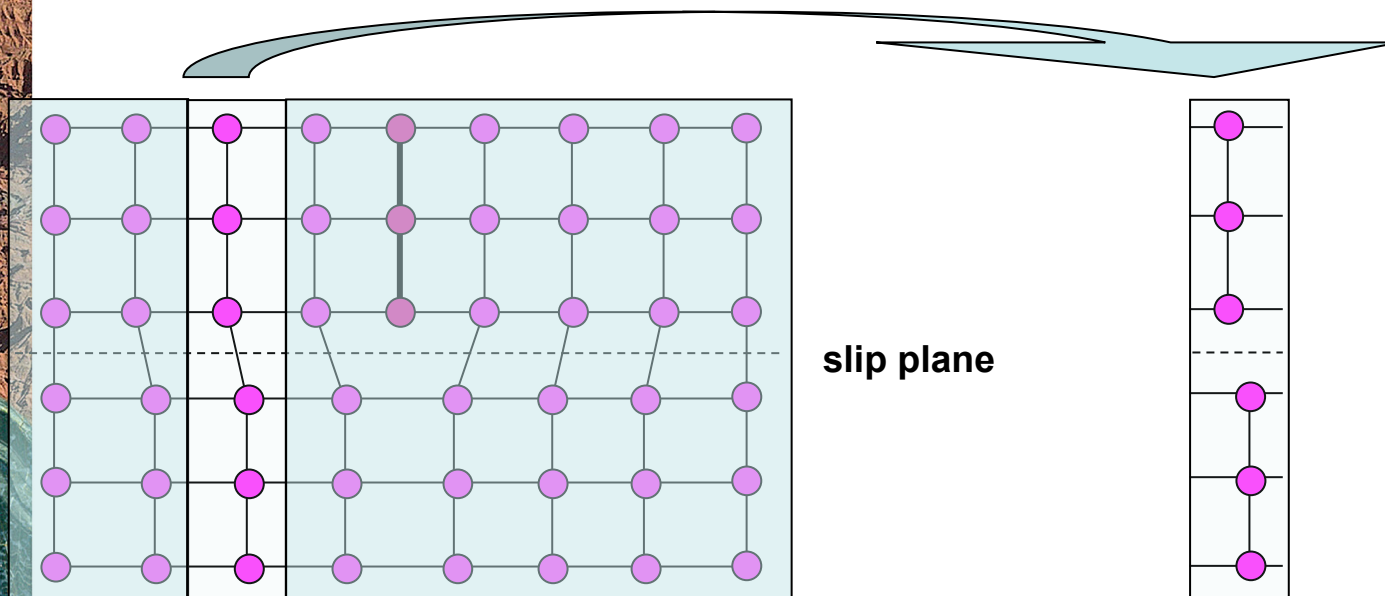
stress \Leftrightarrow misfit of crystal planes

$$F(S(x)) = \tau_{\max} \sin\left(\frac{2\pi S(x)}{b}\right)$$



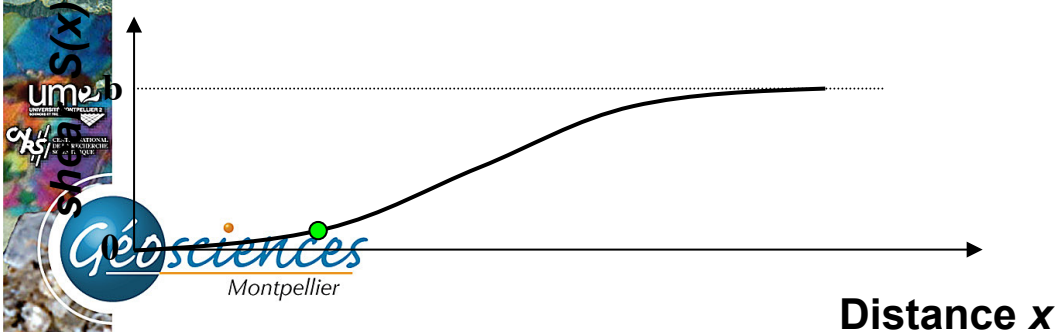
Ab-initio modeling of dislocation core properties: Generalised Stacking Fault (GSF) model

P. Cordier, P. Carrez, D. Ferré (Lille)



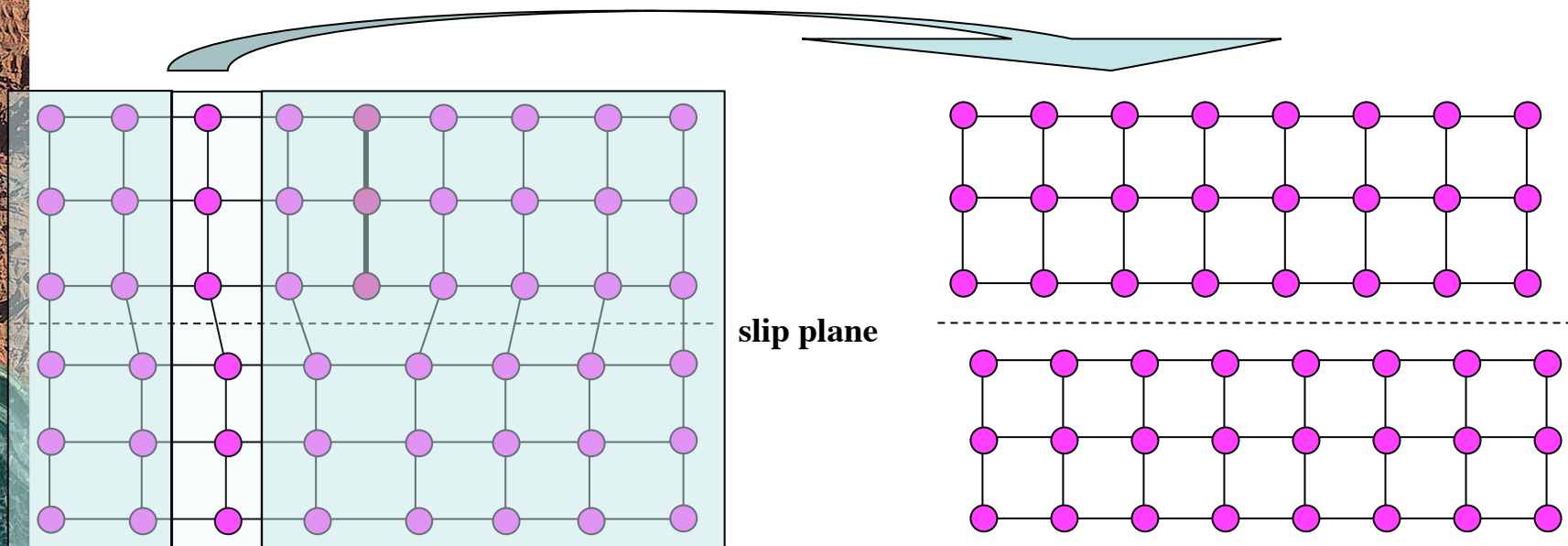
slip plane

isolate a piece of the crystal



Ab-initio modeling of dislocation core properties: Generalized Stacking Fault (GSF) model

P. Cordier, P. Carrez, D. Ferré (Lille)



slip plane

**Generalised Stacking Fault (GSF):
equivalent to a homogeneous
shear**

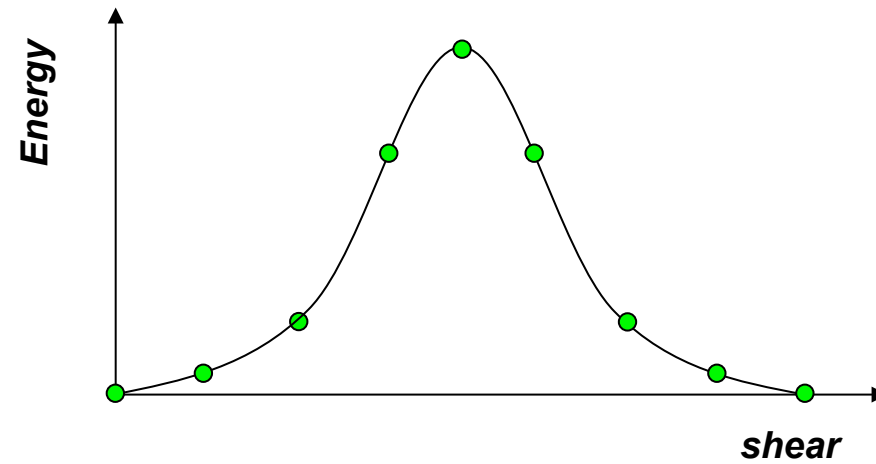
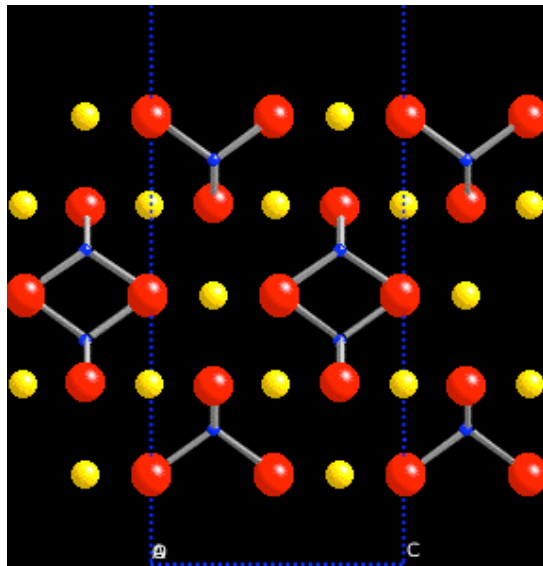
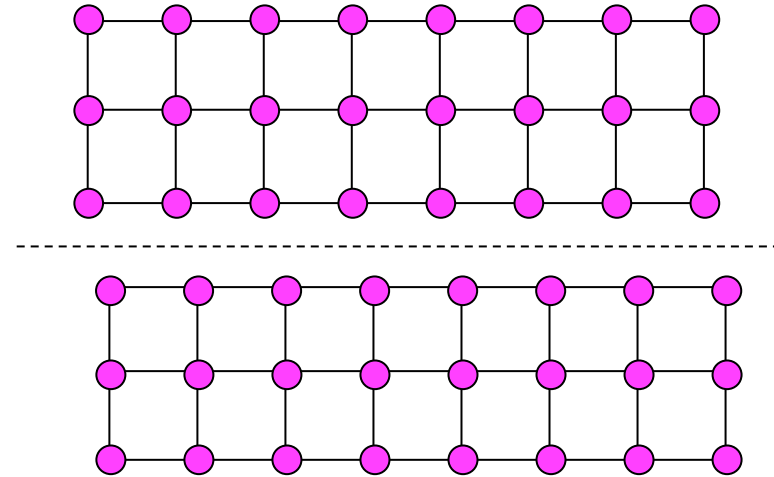
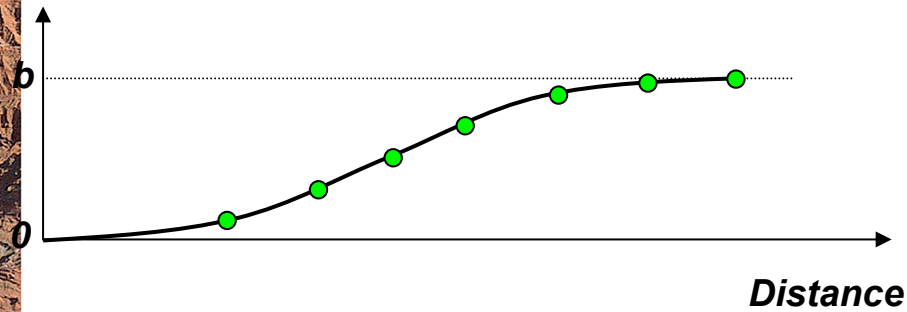


Montpellier

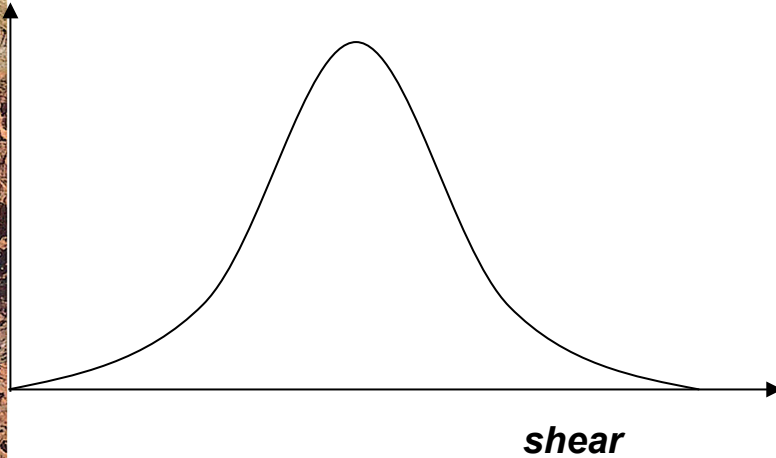
Distance x

Ab-initio calculation of GSF

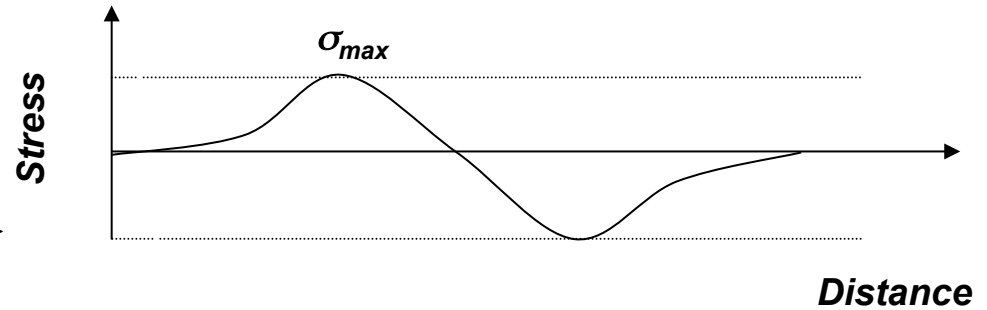
impose the shearing & for each position calculate the energy of the atomic configuration



Ideal Shear Stress: intrinsic resistance to shear



ISS : derivative of the energy barrier



first order approximation of the resolved shear stress of a given slip system = input for viscoplastic models (aggregate-scale deformation)

$$\frac{\dot{\gamma}^s}{\dot{\gamma}_0} = \left(\frac{\tau_r^s}{\tau_0^s} \right)^{n^s} = \left(\frac{R_{ij}^s \sigma_{ij}}{\tau_0^s} \right)^{n^s}$$

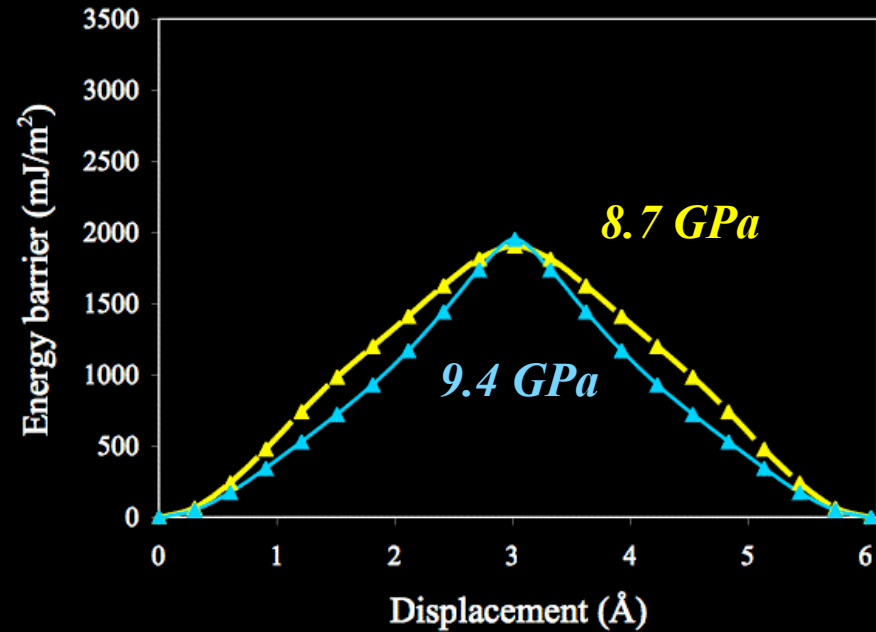
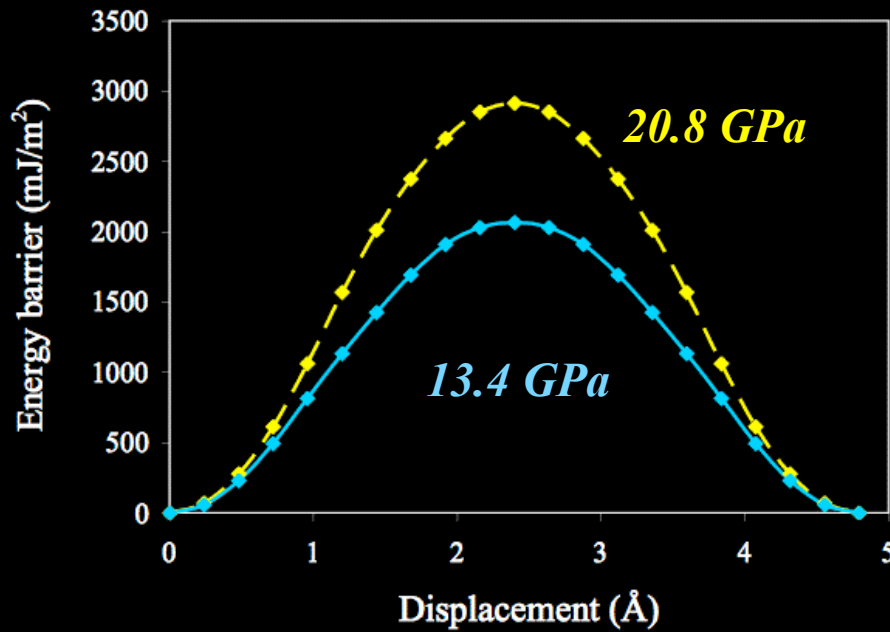
GSF + Crystal periodicity → Peierls-Nabarro model = Peierls stress (lattice friction)



Olivine: energy barriers for $[100](010)$ and $[001](010)$ dislocations at 0 GPa & 10 GPa

$[100](010)$

$[001](010)$



✓ easy slip on $[100](010)$ at high pressure

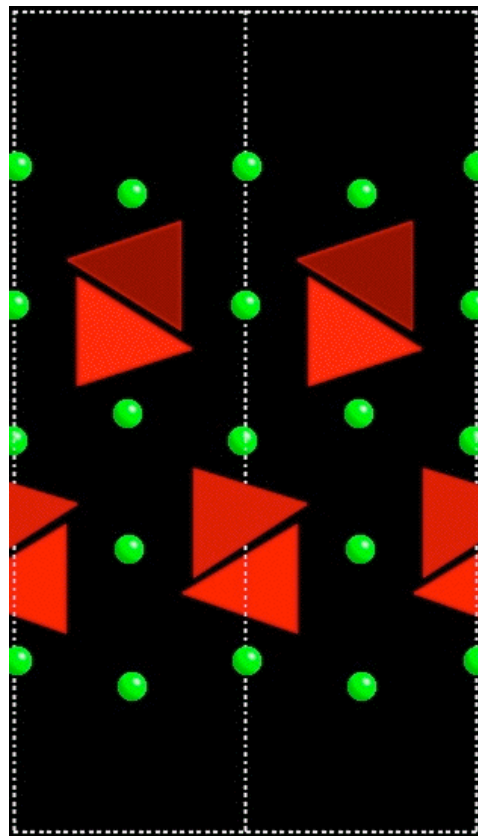
consequences to seismic anisotropy in the deep upper mantle?



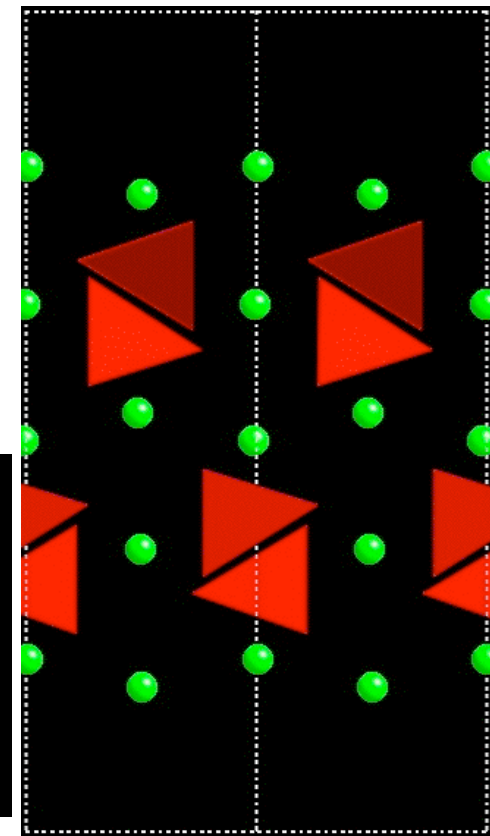
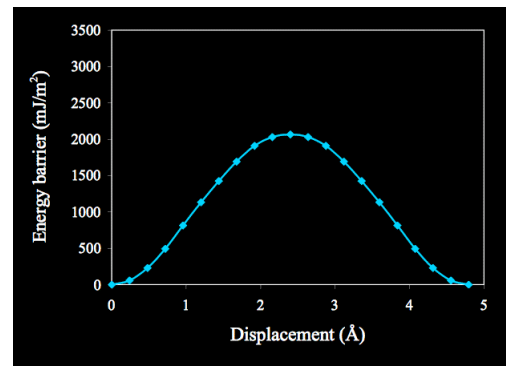
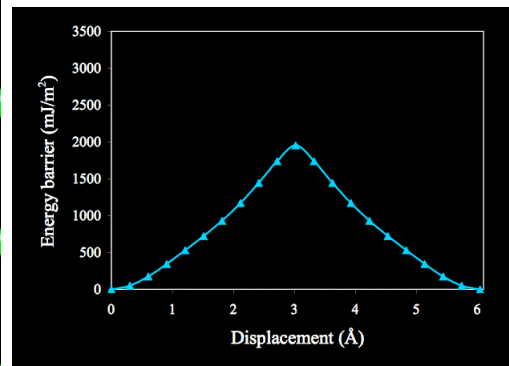
Ab-initio calculation of GSF



1. Construct crystal structure
2. Impose shear on various planes & directions & calculate energy barriers (fixed + relaxed structure)



[001](010)



[100] (010)

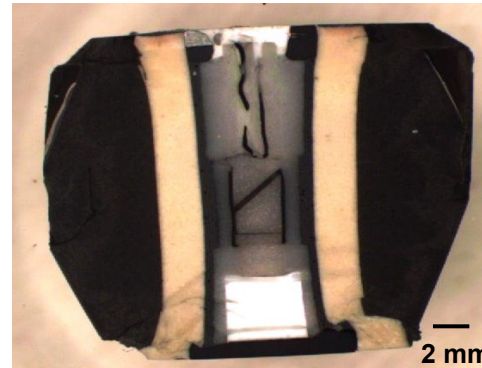


[100]



HP experimental deformation of olivine

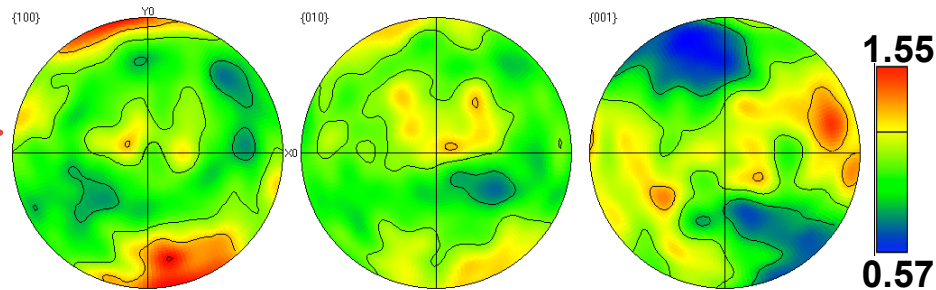
H. Couvy & P. Cordier
Bayreuth/Lille



simple shear

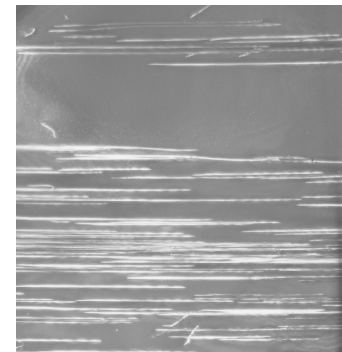
100% olivine aggregate
11 GPa e 1400°C

EBSD: olivine CPO



0.3

[001](010)
[001](100)



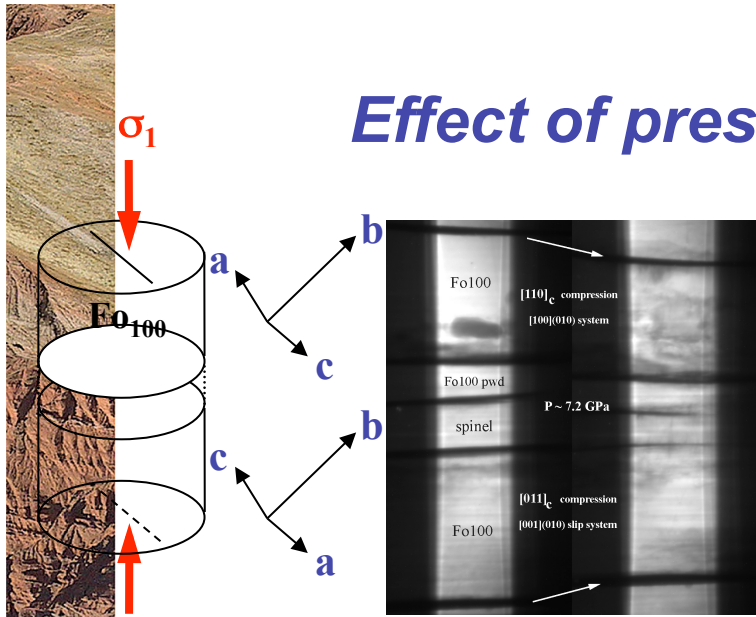
TEM: only [001] screw dislocations

um2
UMR 5073

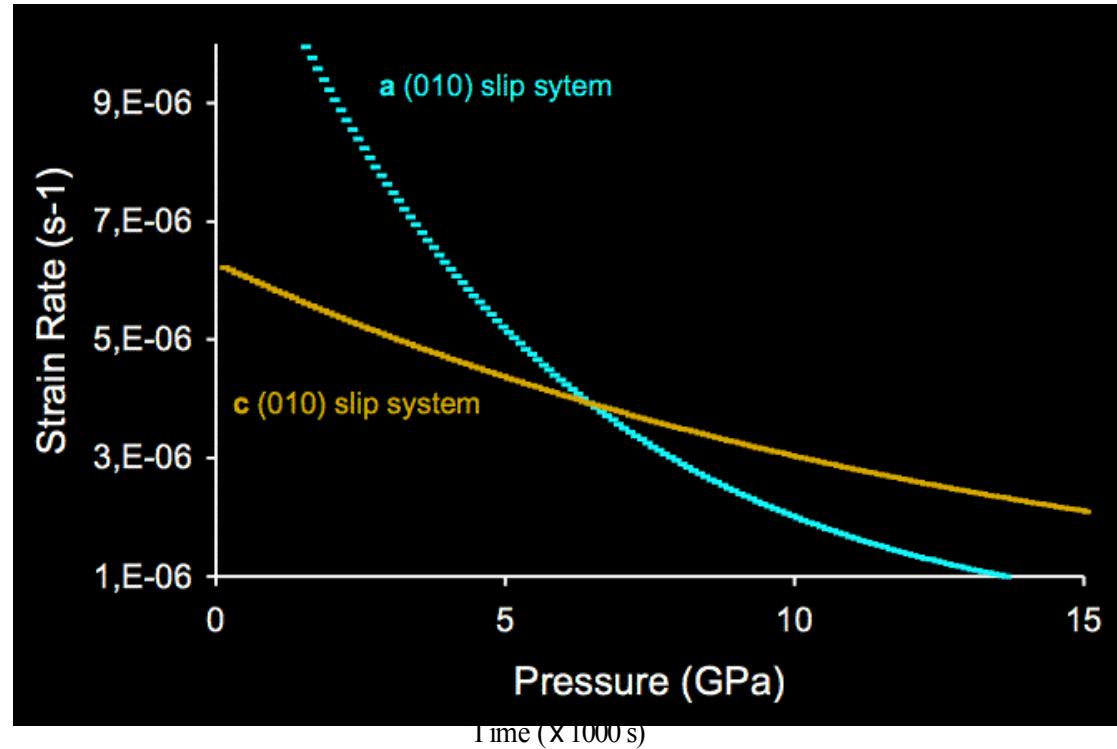
Géosciences
Montpellier

Couvy et al. *EJM* 2004

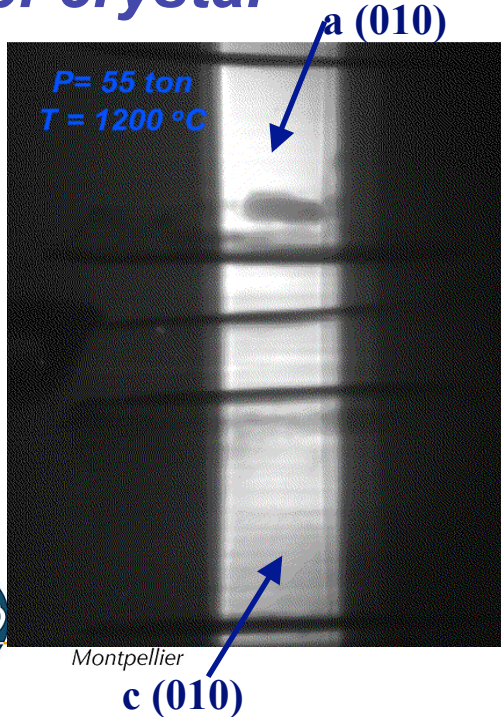
Effect of pressure on olivine deformation



P = 7.2 GPa



bi-crystal



- higher strain on c crystal
✓ [001](010) slip easier than [100](010)
- very low activation volume
✓ dislocation creep dominant

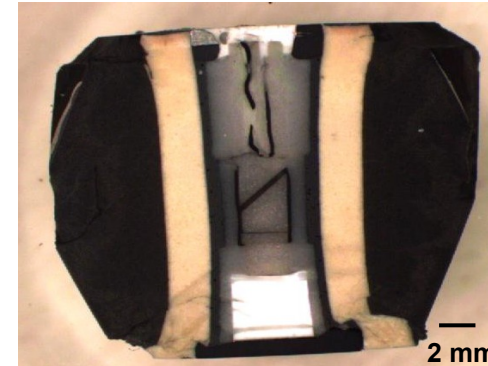
Paul Raterron, pers. commun.



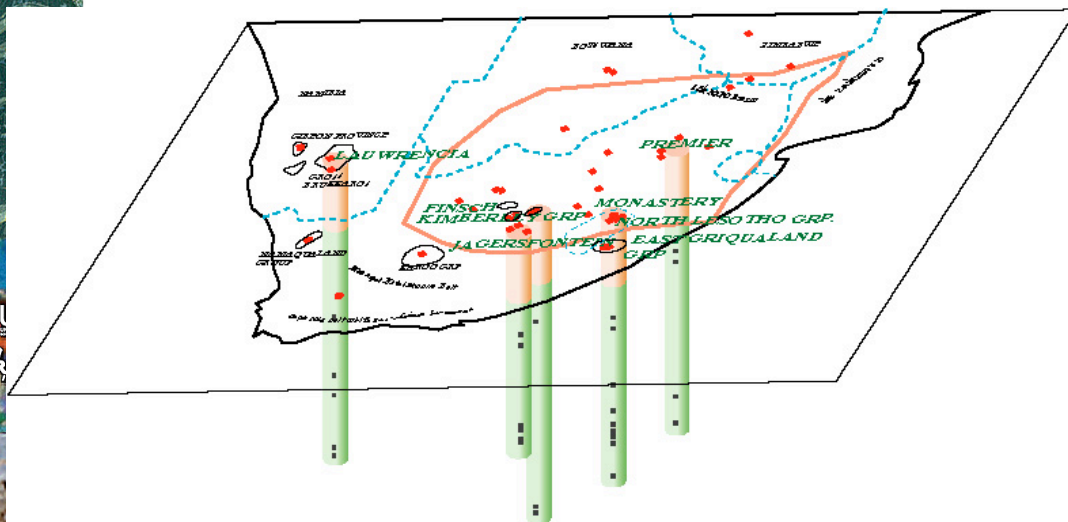
Depth of the transition from [100] slip to [001] slip?

HP-HT experiments (*Cordier, Couvy, Raterron...*)

- $P \leq 3\text{ GPa}$ (~90 km) : [100] slip dominant
- $P \geq 7\text{ GPa}$ (~215 km): [001] slip dominant
- ✓ transition stress-dependent?



CPO data on naturally deformed peridotites (depths ≤ 160 km)



sp- and garnet-bearing peridotites :

- ✓ [100] CPO only

[001] CPO only observed in :

high-pressure massifs (subduction)

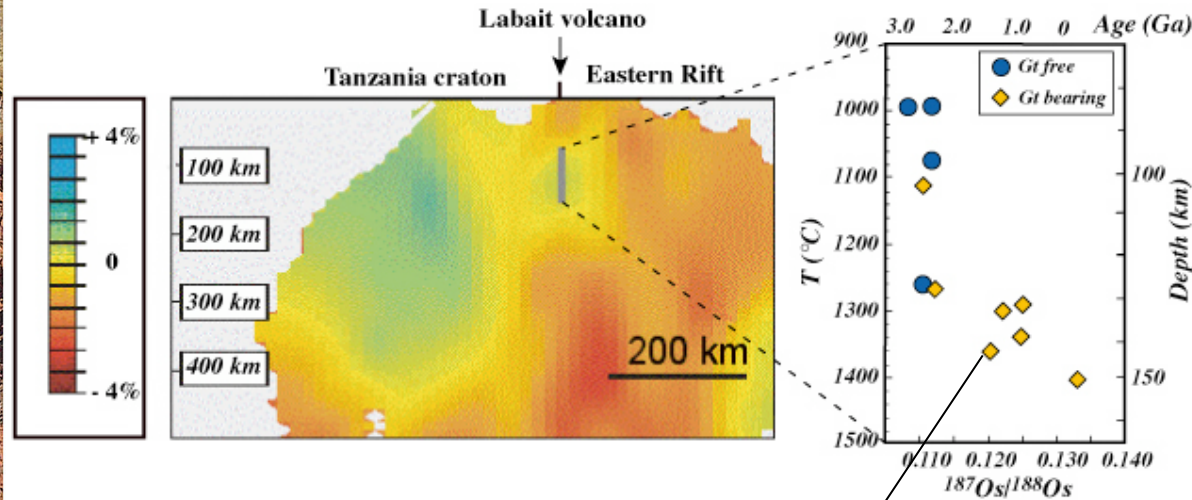
- ✓ effect of pressure or water ?

(*Jung and Karato Science 2001*)

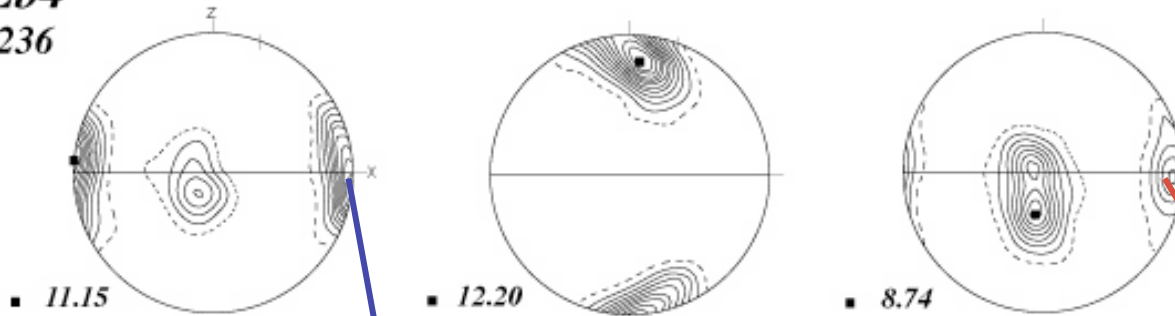
some deep cratonic xenoliths...

deep samples from the Tanzanian and South African craton

Vauchez et al, *EPSL*, in press



Lb4
236

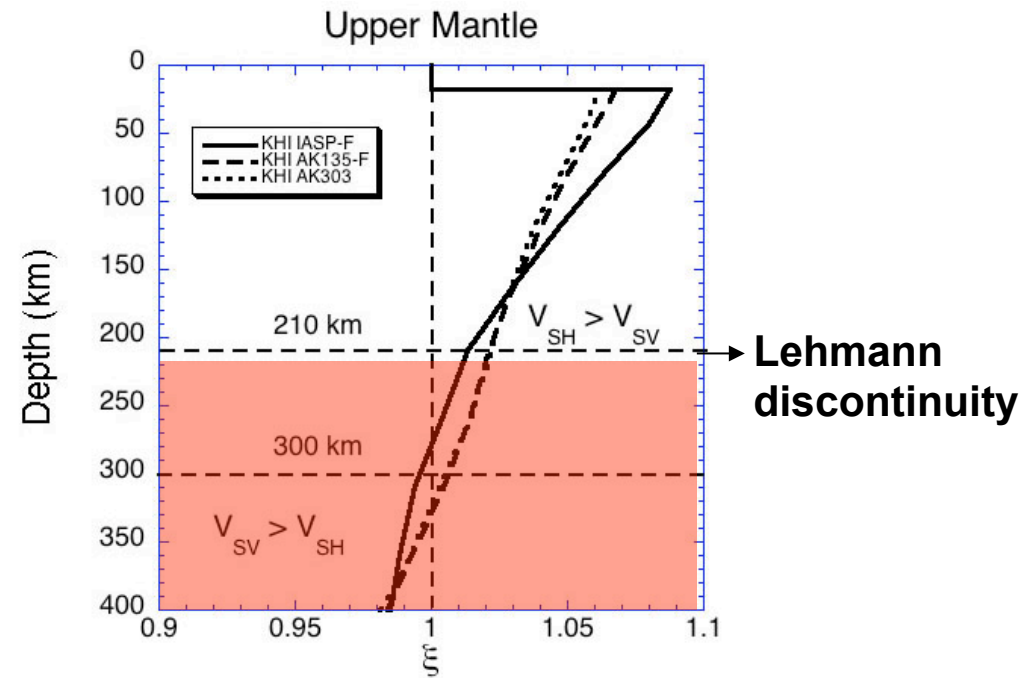
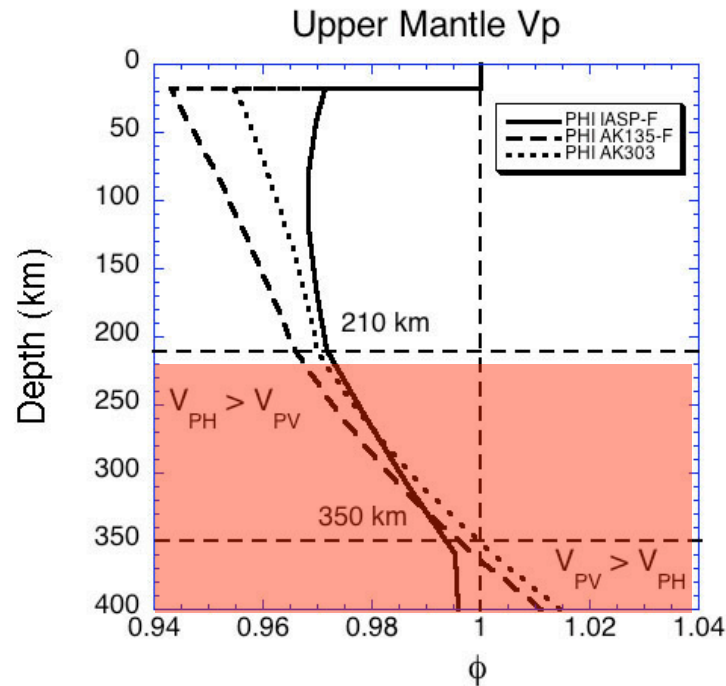


[100] slip

[001] slip

bimodal olivine CPO : activation of [100](010) and [001](010) slip systems?

Fast decrease in anisotropy at the bottom of the upper mantle - 200 to 400 km

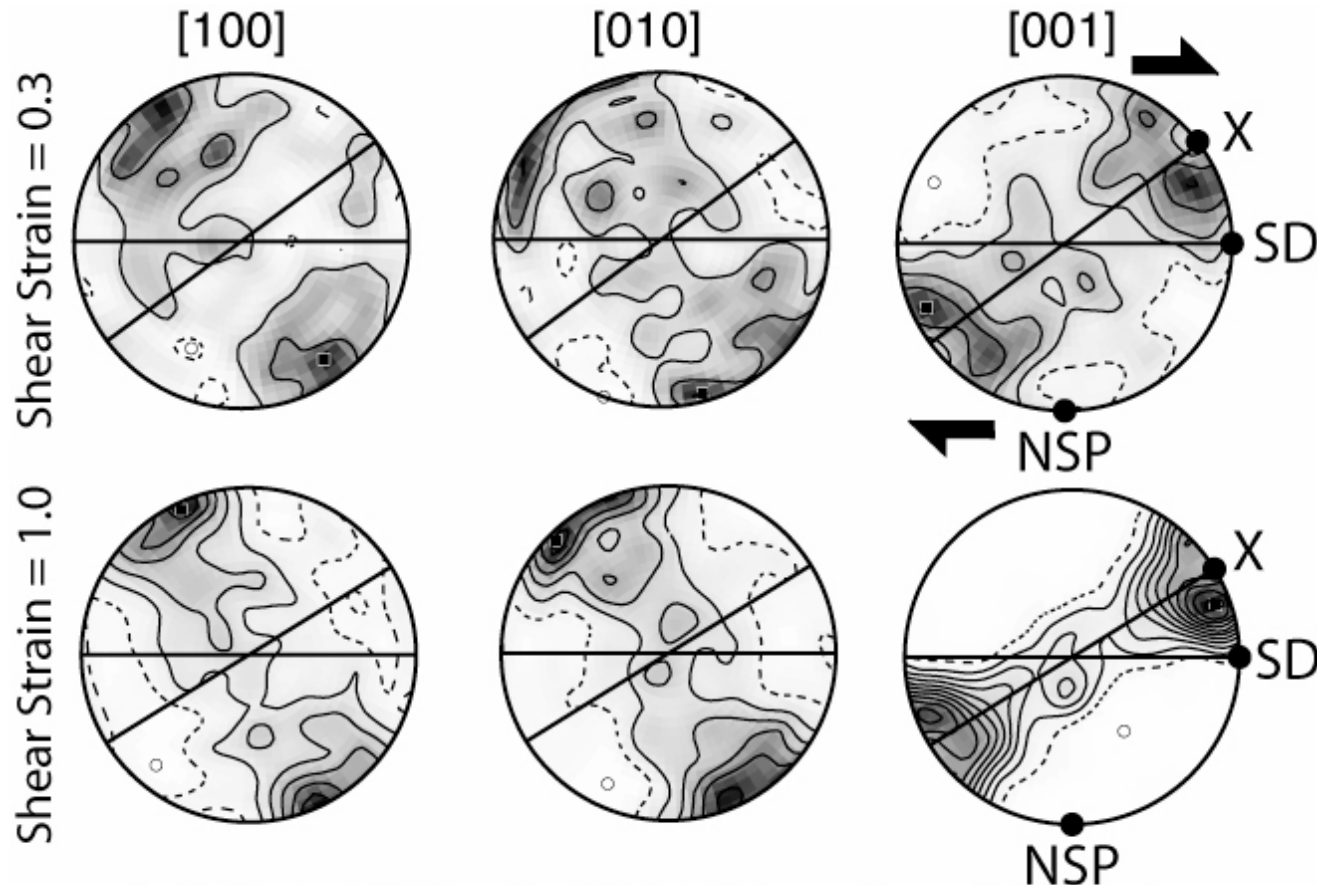
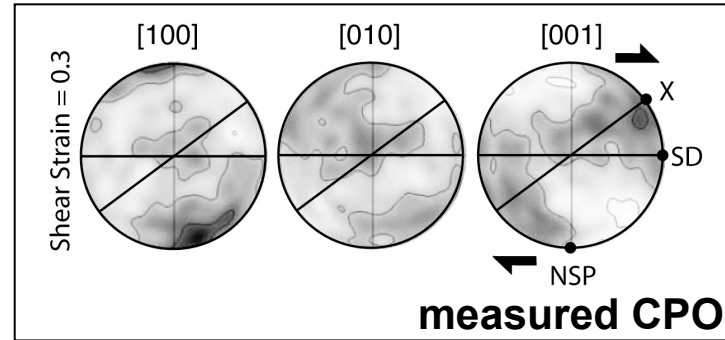


Transition from dislocation to diffusion creep
(no CPO -> no seismic anisotropy)

yet ... recent experimental data:
olivine at high pressure deforms by dislocation creep,
but with a change in slip direction from [100] to [001]



Texture evolution as function of strain: crystal plasticity modeling



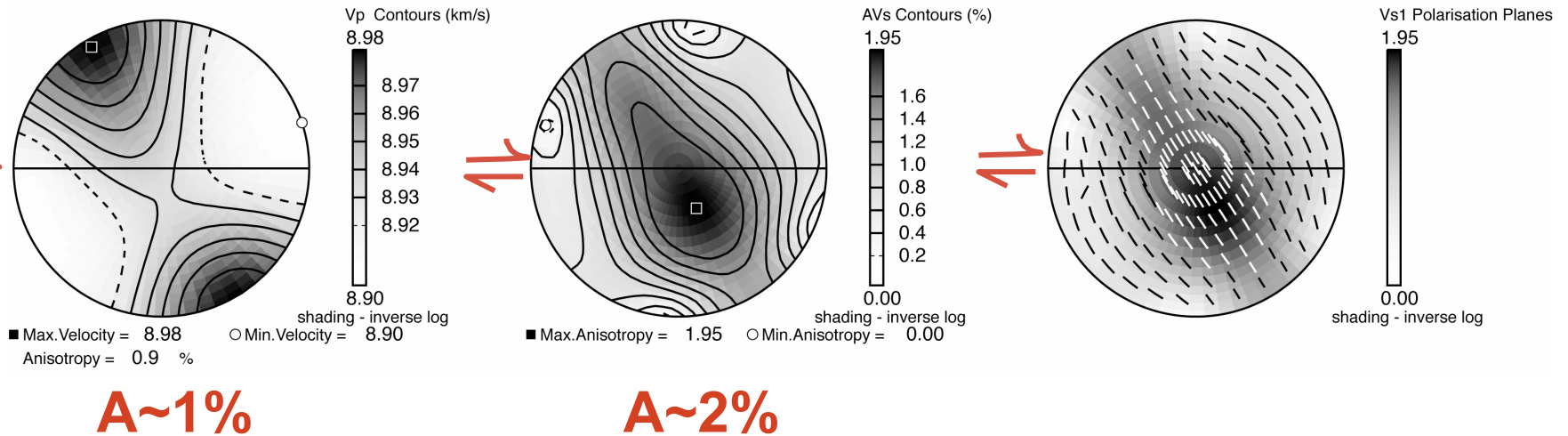
CRSS all [001] = 1 ; [100]=3(basal) or 6 (prism)



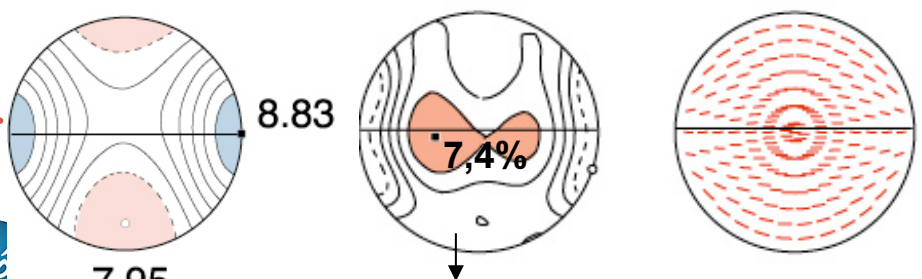
Seismic anisotropy

high-pressure olivine LPO : [001] glide

Model at 355 km depth for a composition of 63% olivine, 17% garnet and 20% diopside at shear strain of one



Vp (km/s) AVs polarisation S1

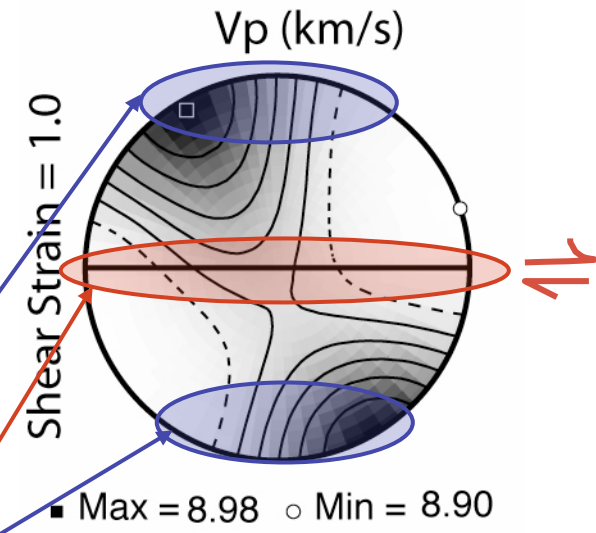
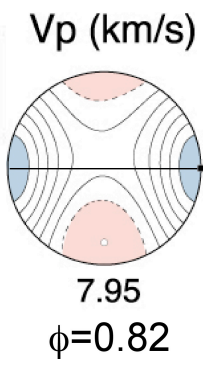
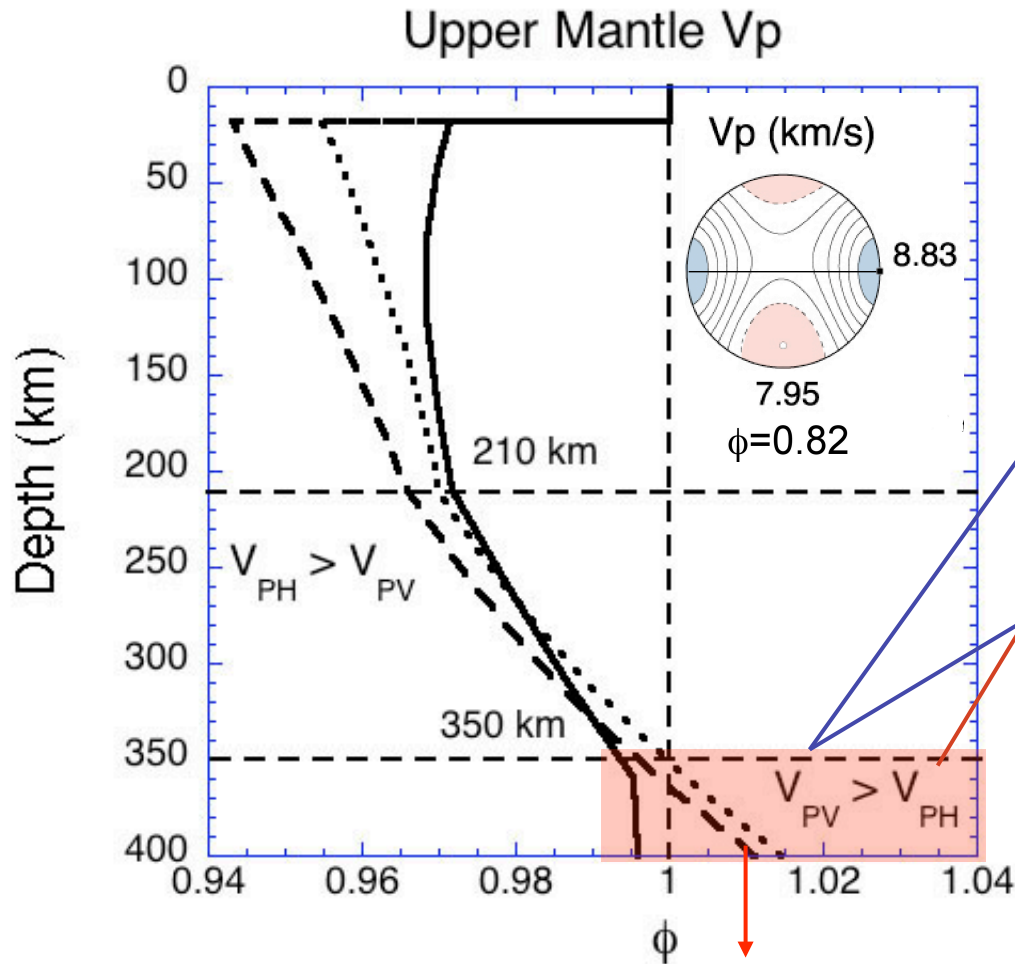


« typical upper mantle peridotite seismic anisotropy »
 low-pressure olivine LPO
 [100] glide





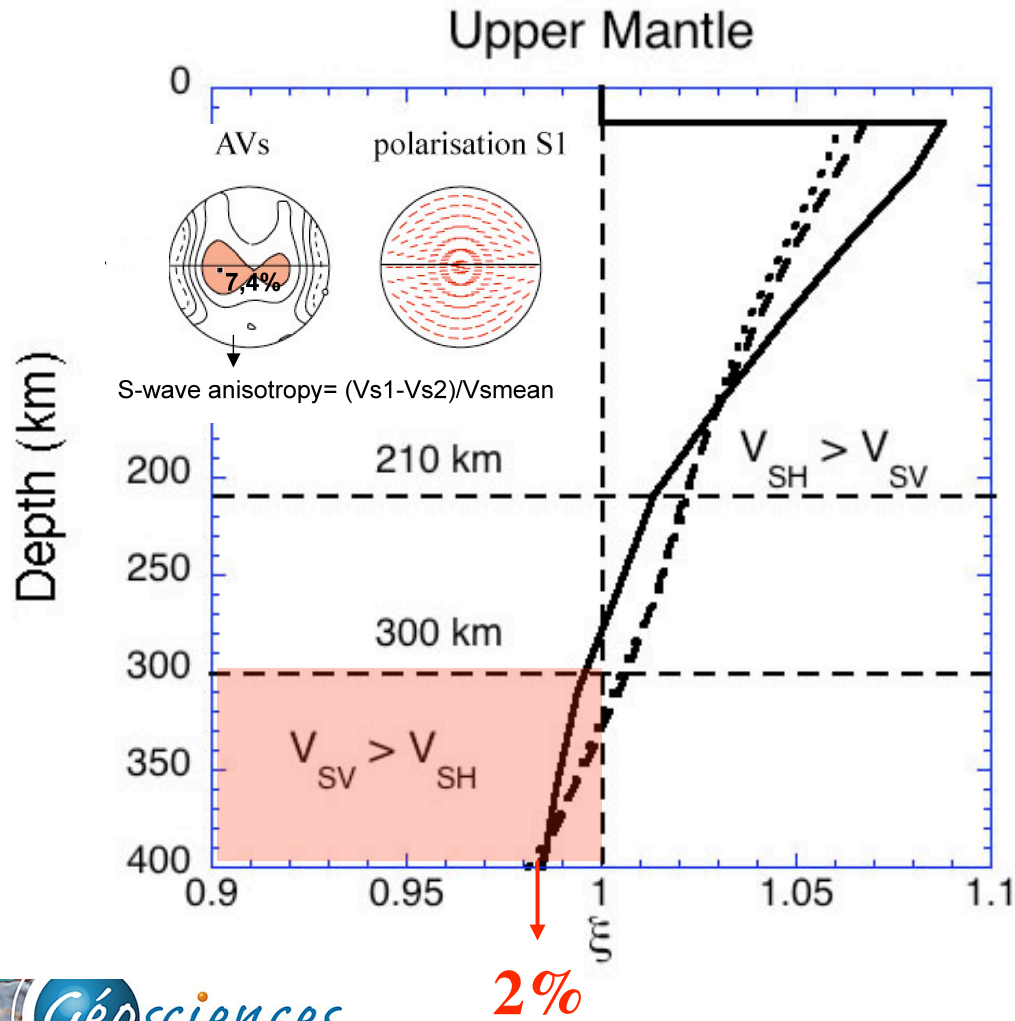
Global P-wave anisotropy in the deep upper mantle



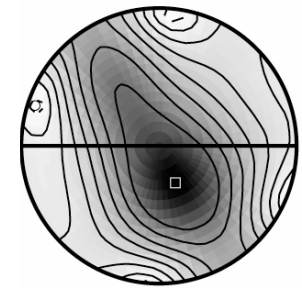
- Model prediction for horizontal flow:**
1. $V_{PV} > V_{PH}$
 2. V_p anisotropy about 1%



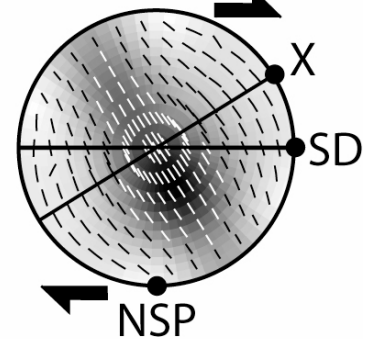
Global S-wave anisotropy in the deep upper mantle



dVs anisotropy (%)



Fastest Vs polarisation



Model prediction for horizontal flow:

1. $V_{SV} > V_{SH}$
2. Vs anisotropy $\leq 2\%$



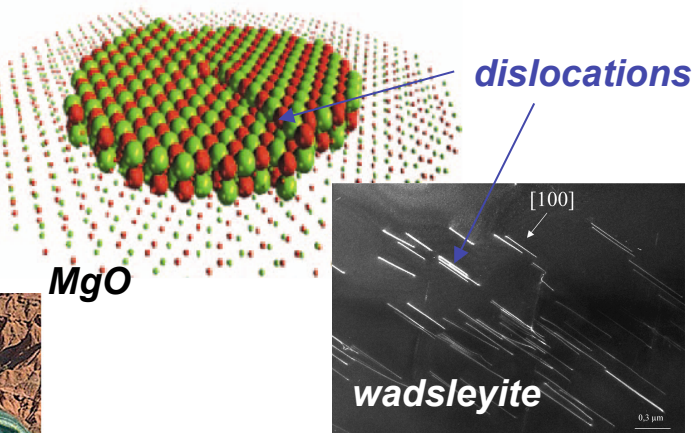
olivine deformation = $f(P)$
change in dominant slip direction
from [100] to [001]

- **strong decrease in seismic anisotropy with depth**
 - **fast P-wave propagation direction & fast S-wave polarisation direction in the deep upper mantle normal to shallow ones**
 - **seismic anisotropy data :**
dislocation creep in the entire upper mantle
horizontal shearing dominant

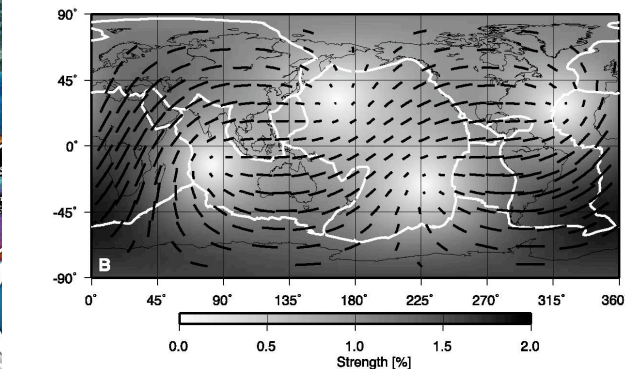
Déformation & anisotropy in the deep mantle

coll. P. Cordier, P. Carrez, D. Ferré (Lille),
D. Mainprice et C. Thoraval (Montpellier)

deformation of HP mantle minerals
HP-HT experiments + ab initio models

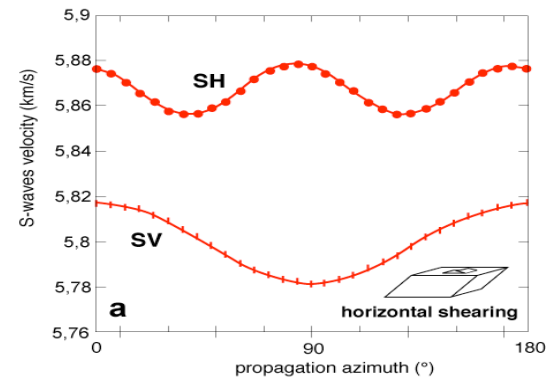
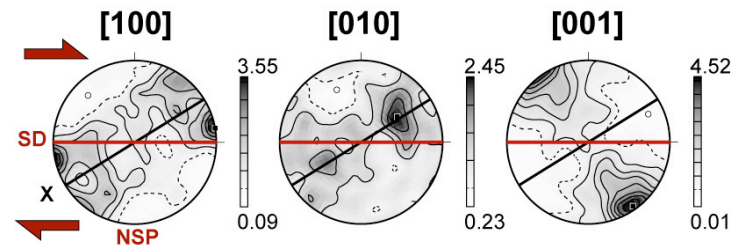


seismic anisotropy data
transition zone



Trampert & VanHeijst Science 2002

VPSC + seismic properties models (rock-scale)
+ mantle flow models



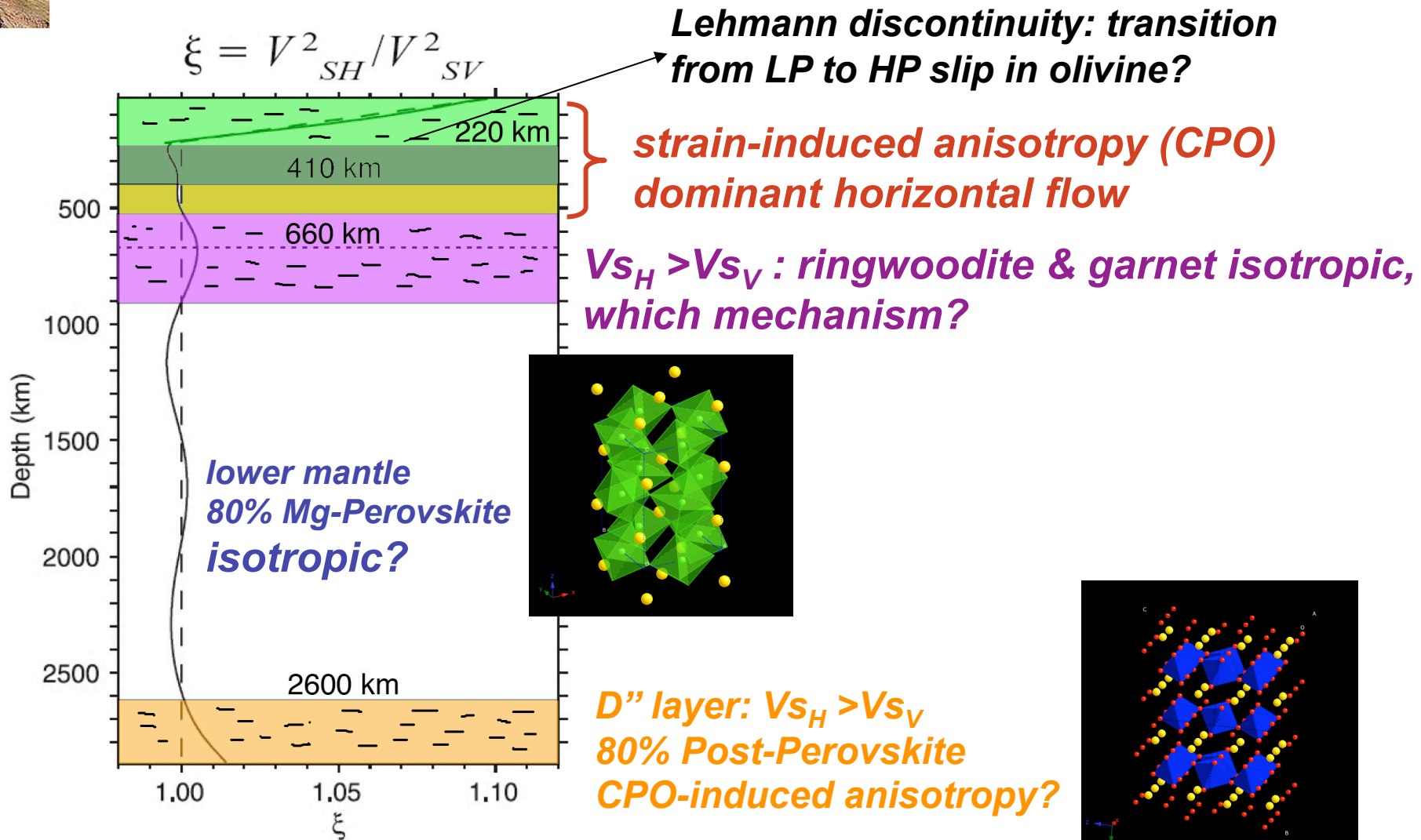
horizontal flow dominant in TZ
except in the vicinity of subduction

Tommasi et al., JGR, 2004

Carrez et al., Eur.J.Miner. 2006 (ringwoodite)
Cordier et al. 2005 EMU Notes

Anisotropy & deformation in the deep mantle?

Ab-initio dislocation models + HT-HP experiments + CPO modeling



Panning & Romanowicz 2004 Science

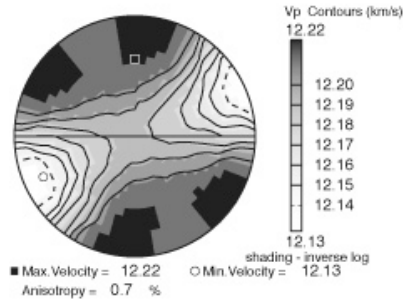


Lower mantle and D" anisotropy: work in progress...

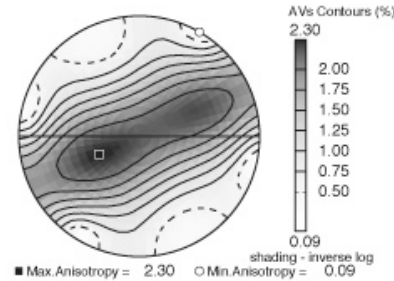
Perovskite 30 GPa

[100](001) dominant

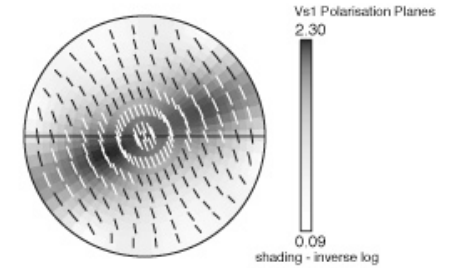
Vp (km/s)



dVs (%)



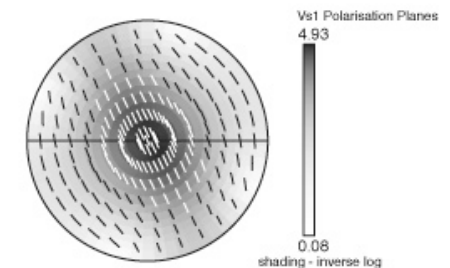
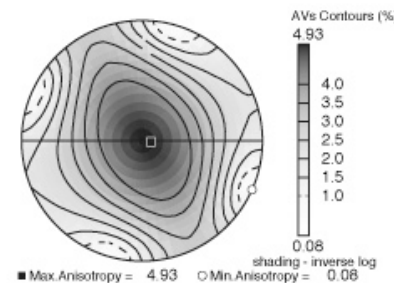
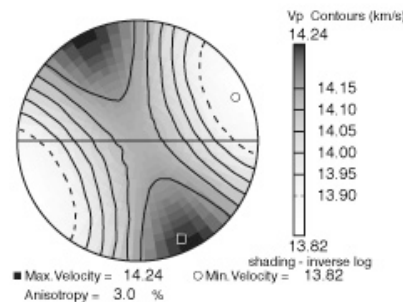
Vs1 polarisation



PV>PH OK
SV>SH OK
SKS isotropic OK

Perovskite 100 GPa

**[010](001), [100]
(001)
& [100](010)**



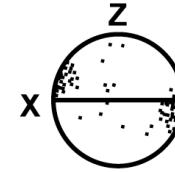
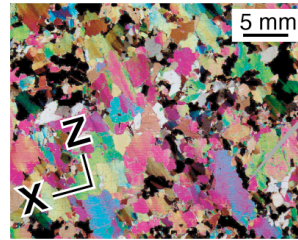
anisotropy increases!

PV>PH OK
SV>SH OK
2% SKS
anisotropy?

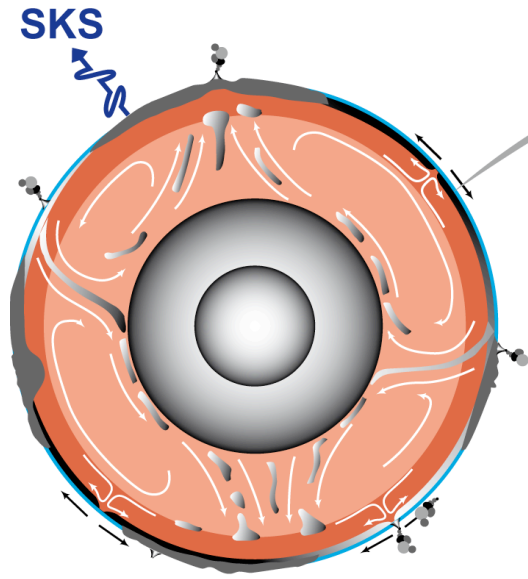


Other anisotropic properties..

dislocation creep

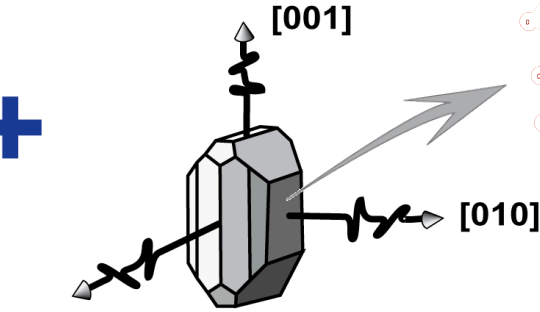


olivine crystal preferred orientation

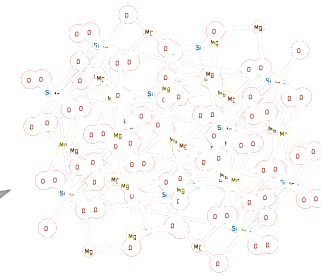


mantle flow

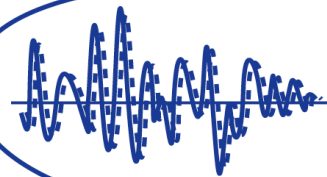
+



olivine crystal anisotropy



=



large-scale seismic, mechanical thermal & electrical anisotropy in the upper mantle

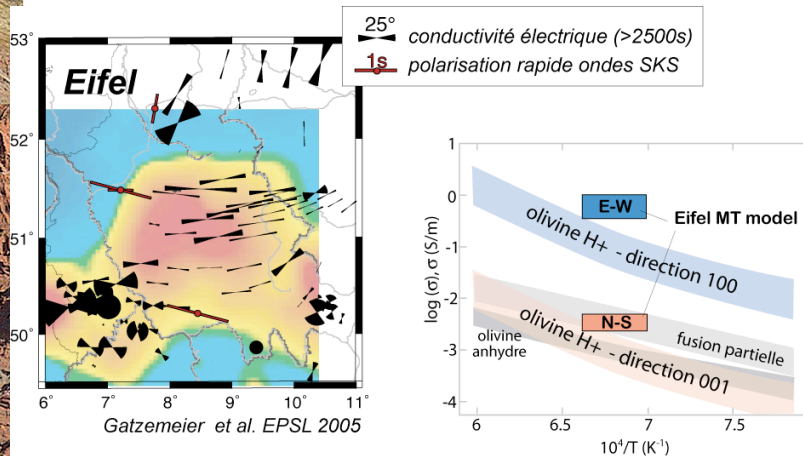


Anisotropie de conductivité électrique (données MT longue période): un outil complémentaire pour cartographier la déformation mantellique?

groupe de travail:

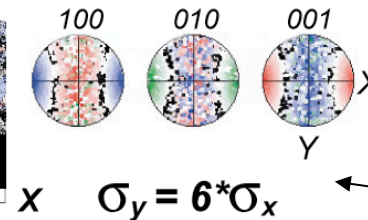
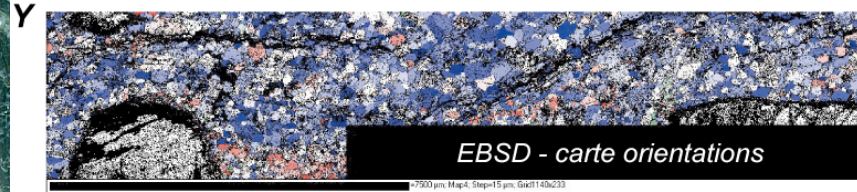
- B. Gibert, D. Mainprice, moi (Montpellier)
- A. Gatzemeier, F. Simpson, K. Bahr (Goettingen)
- J. Ingrin, M. Bystricky, M. Jessel (Toulouse)
- I. Vittorello, A. Padilha (Brésil)

- anisotropies électrique MT // sismique
- mais anisotropie électrique MT = cristal !!



Causes physiques de l'anisotropie électrique dans le manteau?

- modélisation numérique de l'anisotropie d'une roche mantellique



Conduction = diffusion intracristalline H⁺


Réseau resistances 2D: Simpson & Tommasi GJI 2005

EF 2,5D: Gatzemeier & Tommasi PEPI sous presse

→ modélisation conduction intracristalline en 3D et aux joints de grains en 2D

mesure en laboratoire de l'anisotropie de conductivité

électrique dans une roche mantellique à HT et fH₂O contrôlée (DyETI Gibert 2006)



Structural reactivation in plate tectonics controlled by olivine crystal anisotropy

***Andréa Tommasi, Mickael Knoll,
Alain Vauchez, Catherine Thoraval,
Javier W. Signorelli,
Roland Logé***

um2
UNIVERSITÉ MONTPELLIÈRE
CNRS
CENTRE NATIONAL
DE RECHERCHES
SCIENTIFIQUES

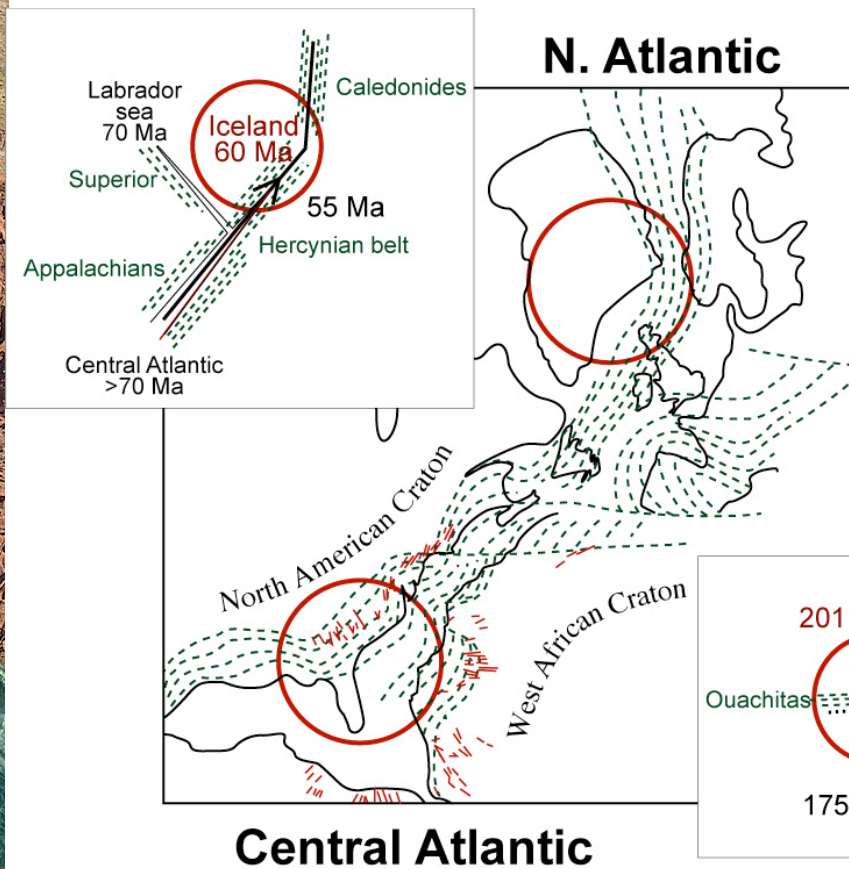
Géosciences
Montpellier

I F I R
CONICET
U N R

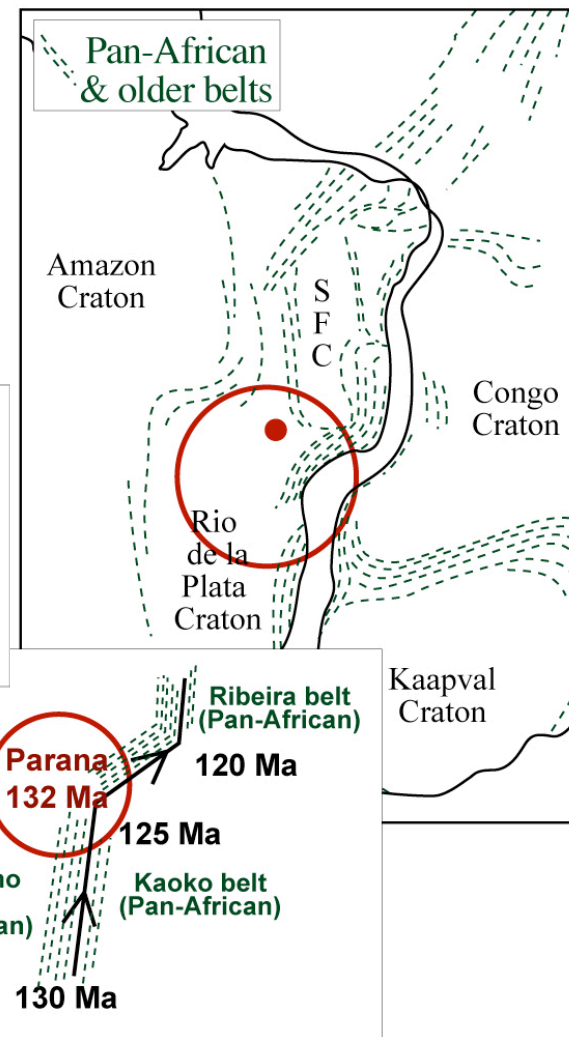
MINES
ParisTech

Fall AGU 2009

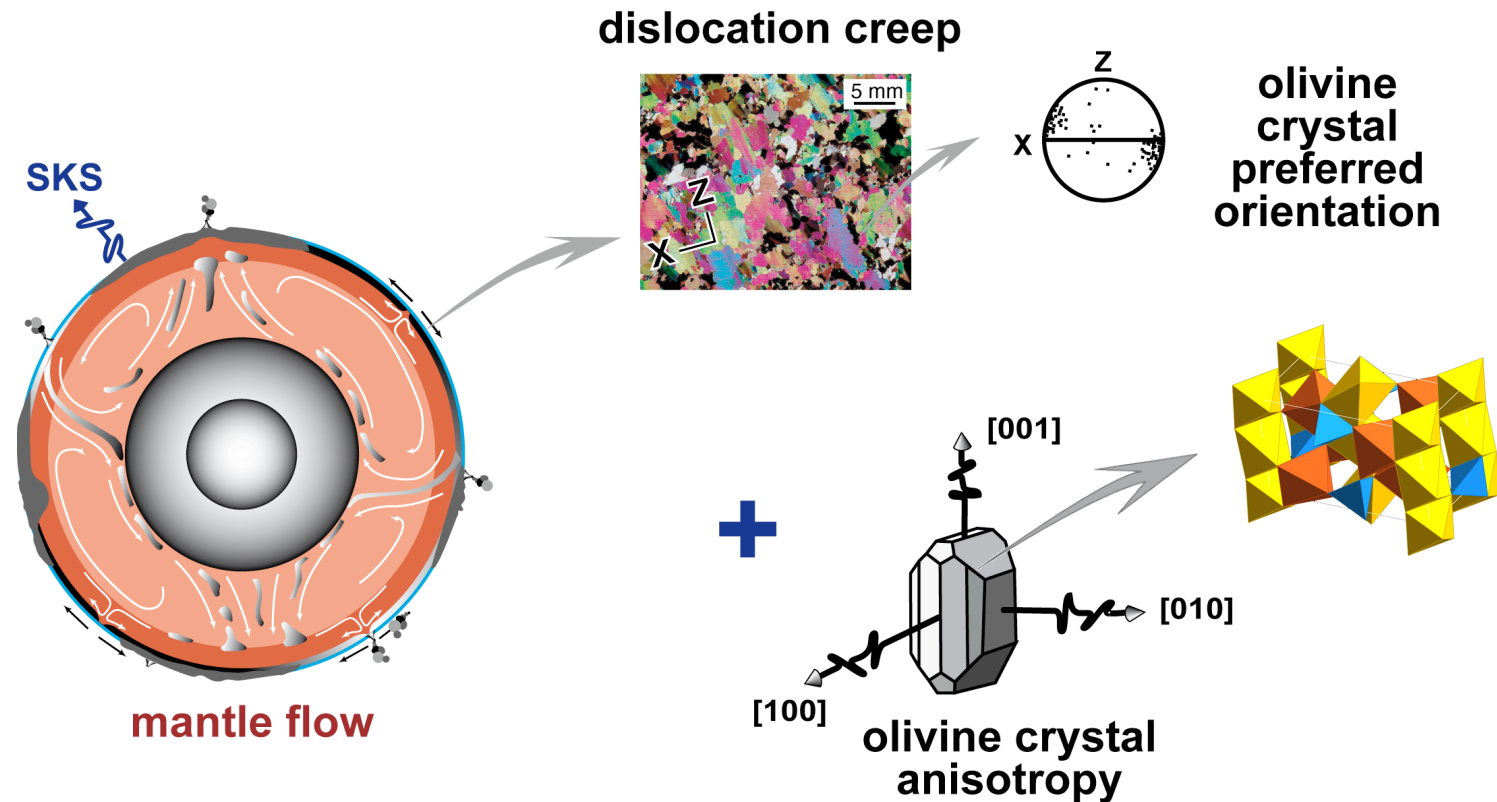
Structural reactivation: Continental breakup parallel to ancient collisional belts

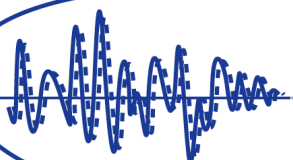


South Atlantic



Why? → mechanical anisotropy of the lithospheric mantle due to preferred orientation of anisotropic olivine crystals

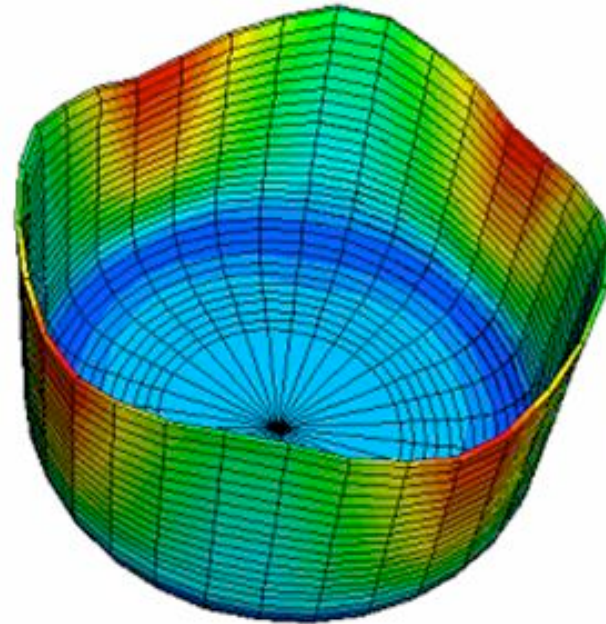
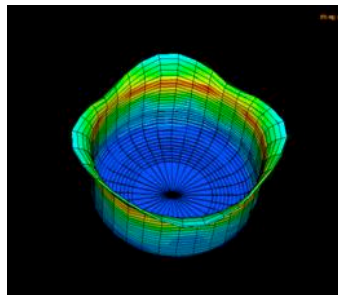
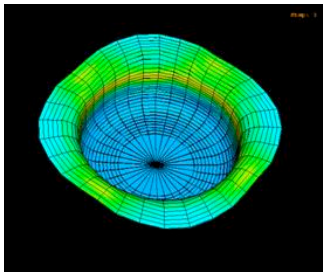
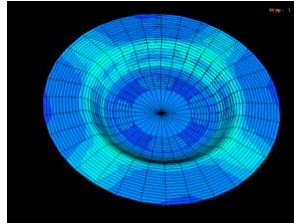
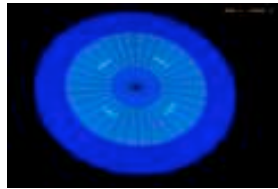


=  **large-scale seismic, mechanical thermal & electrical anisotropy in the upper mantle**



In metallurgy:

*CPO-induced mechanical anisotropy
= 1st order parameter*

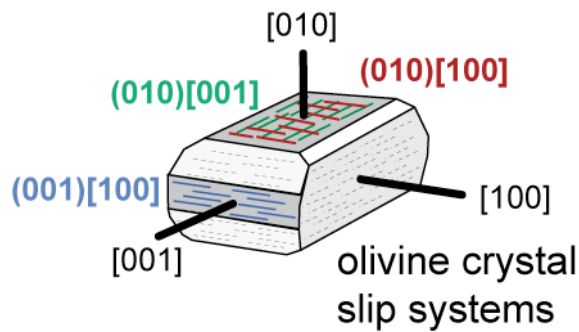
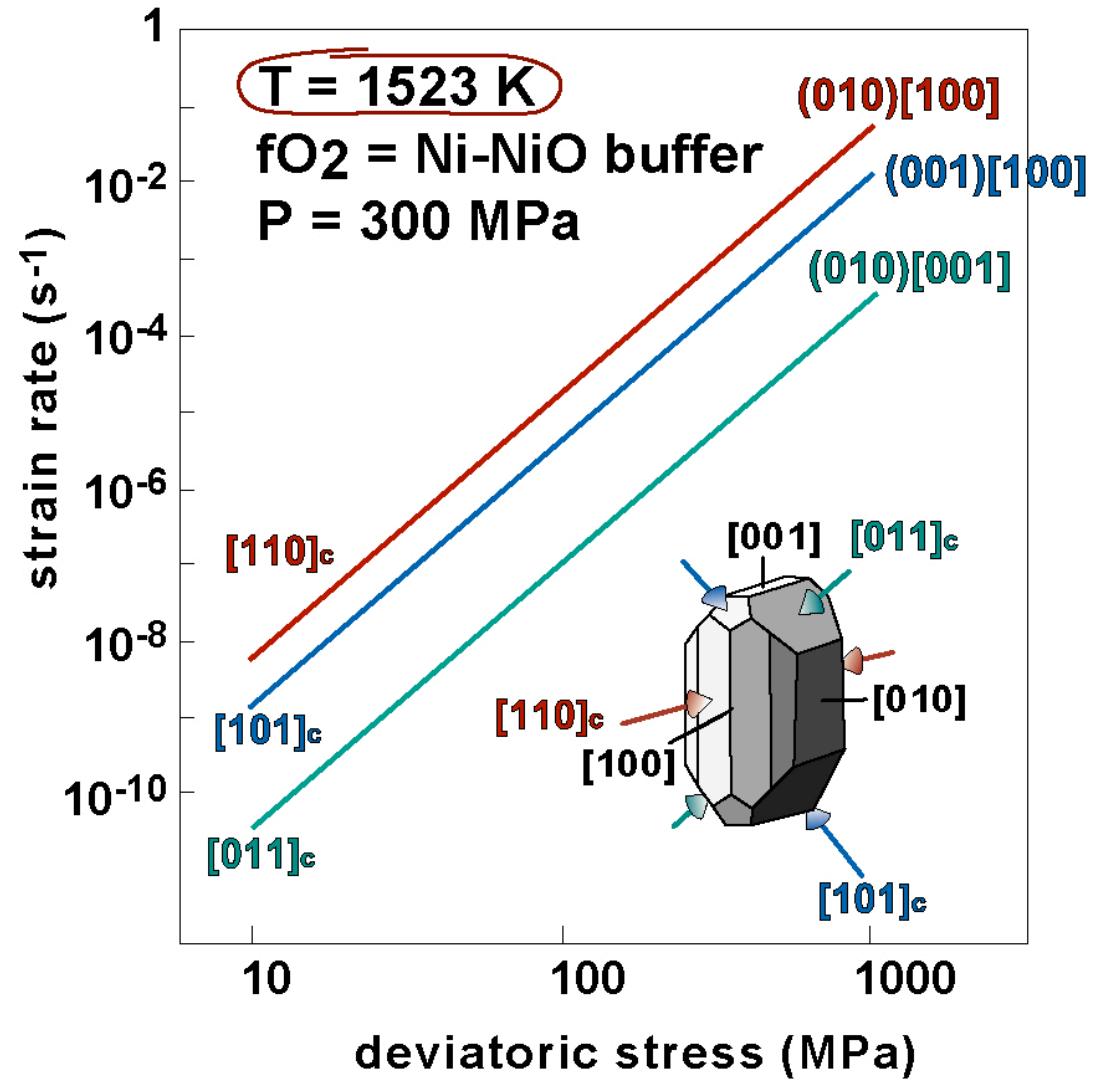


D.Raabe, Max Planck Institut

***Earing of Al cans → mechanical anisotropy Al crystal
+ preferred orientation of crystals developed during
the production of the sheet (rolling)***



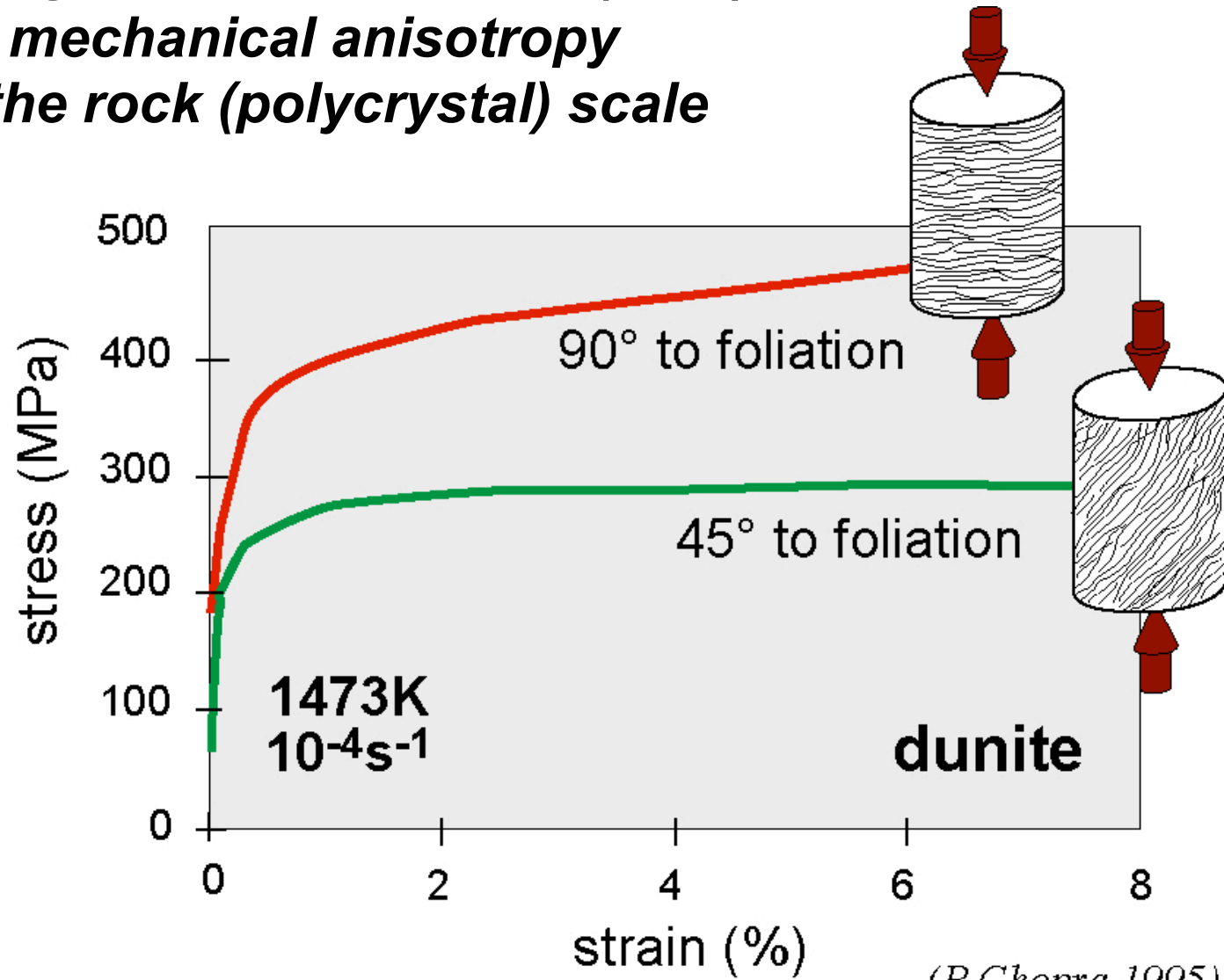
**ductile deformation of an olivine crystal is anisotropic:
few slip systems with highly \neq strenghts**



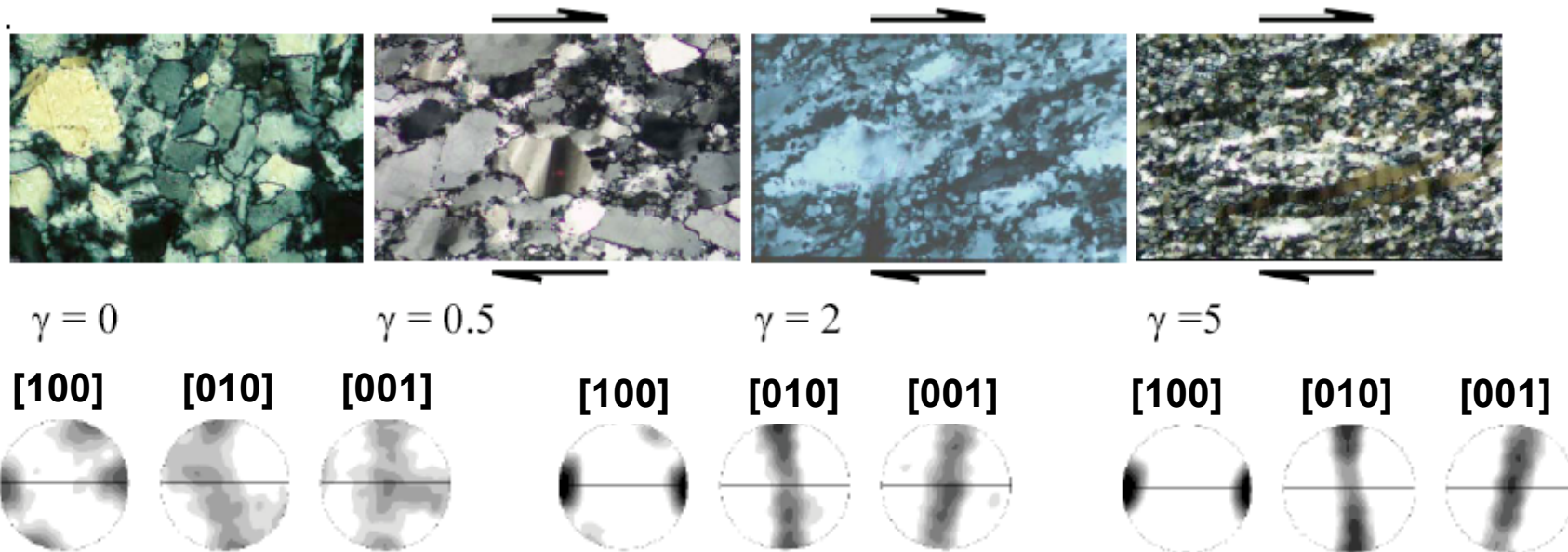
Bai et al. 1990-JGR



***olivine crystal anisotropy +
crystallographic orientations (CPO) =
mechanical anisotropy
at the rock (polycrystal) scale***



Strain weakening in torsion experiments \Leftrightarrow olivine CPO evolution ?



$\gamma = 0$

$\gamma = 0.5$

$\gamma = 2$

$\gamma = 5$

[100]

[010]

[001]

[100]

[010]

[001]

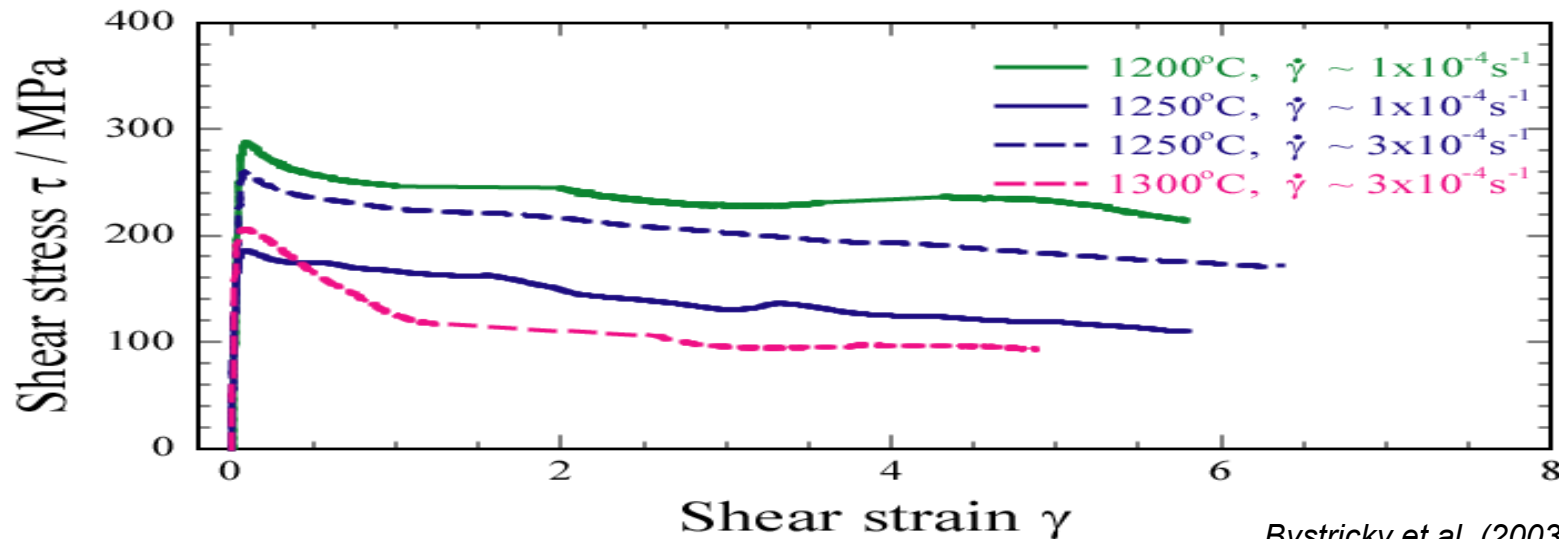
[100]

[010]

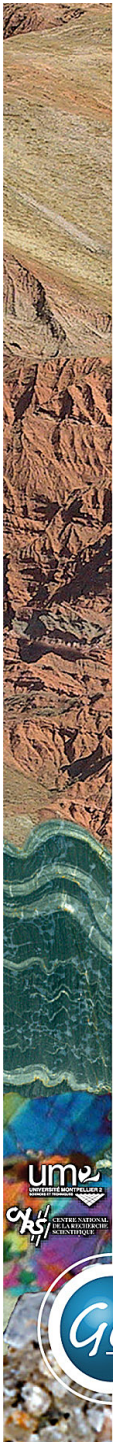
[001]

γ

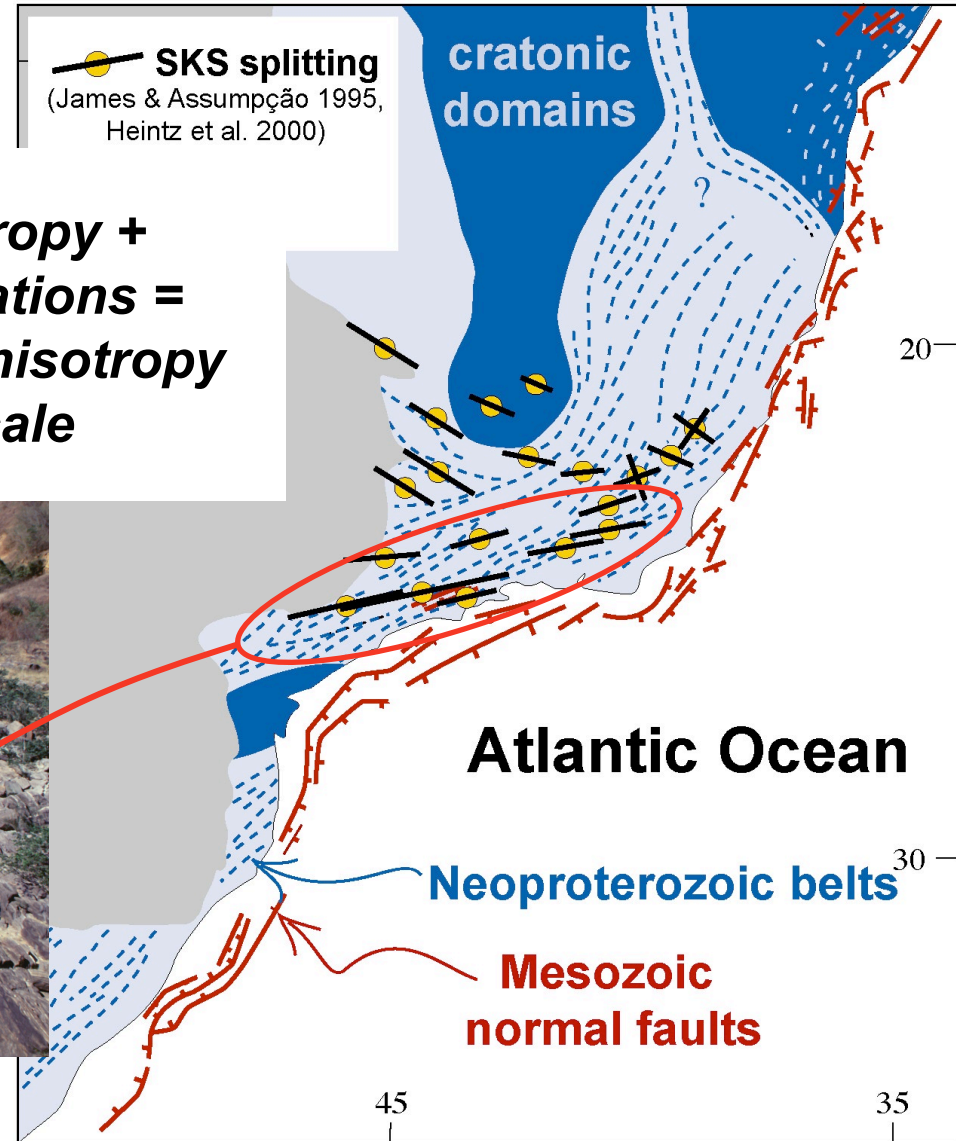
Dry Olivine FeFeO



Bystricky et al. (2003) Science
M. Bystricky, pers. commun.



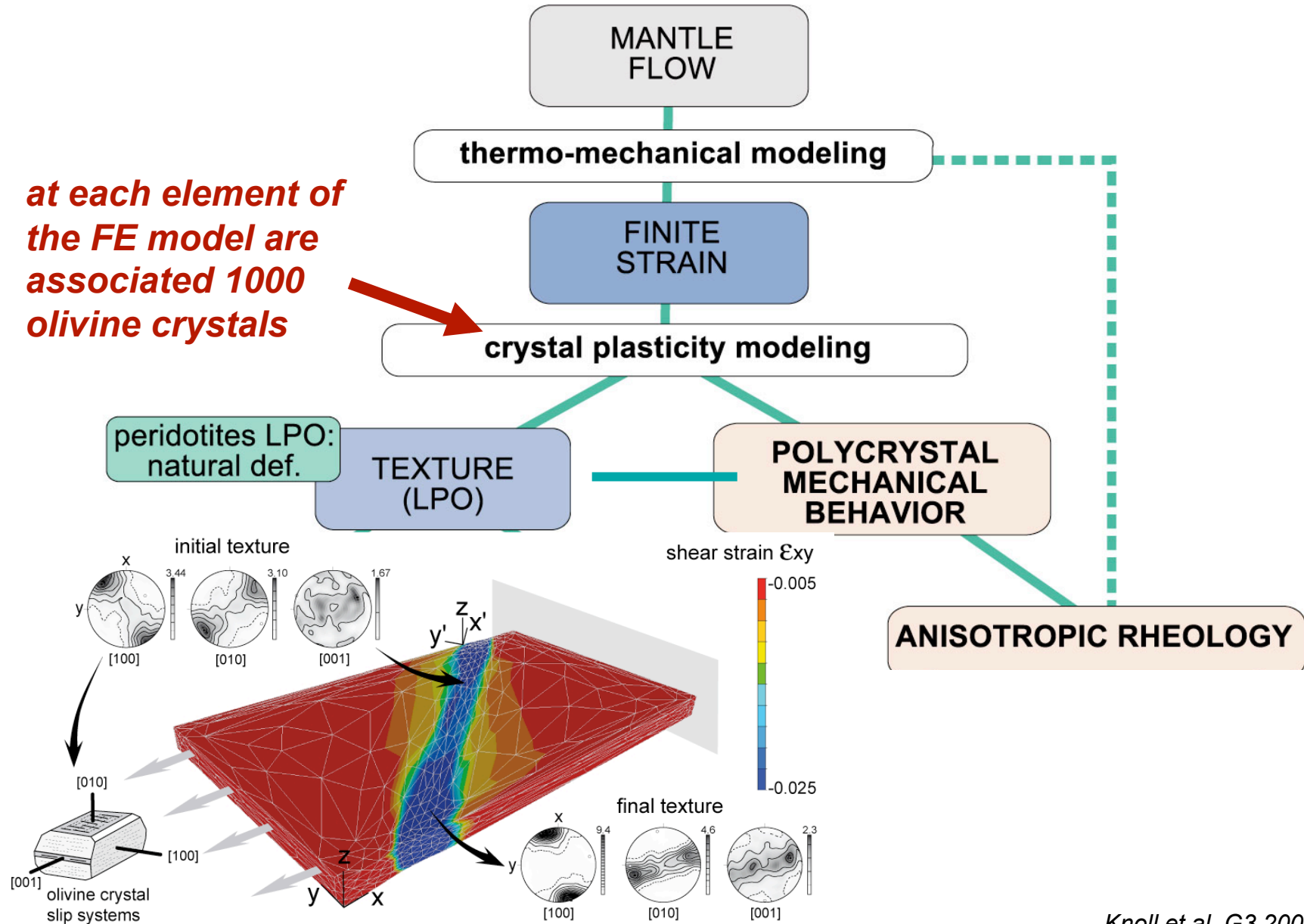
***olivine crystal anisotropy +
crystallographic orientations =
seismic & mechanical anisotropy
at the continent scale***



Control the formation of new plate boundaries: rifting?

coupled 3D geodynamic & crystal plasticity models: evolution of olivine orientations and anisotropy

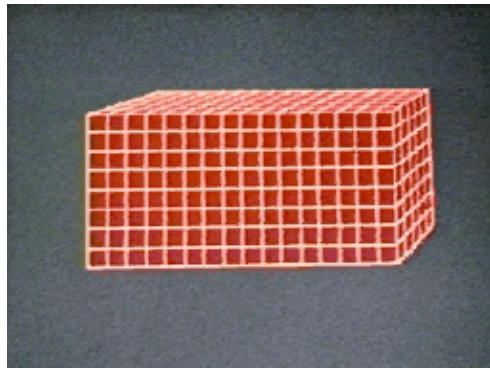
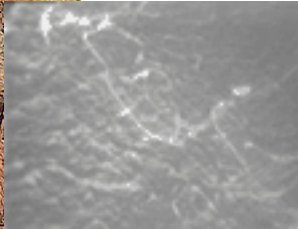
at each element of the FE model are associated 1000 olivine crystals



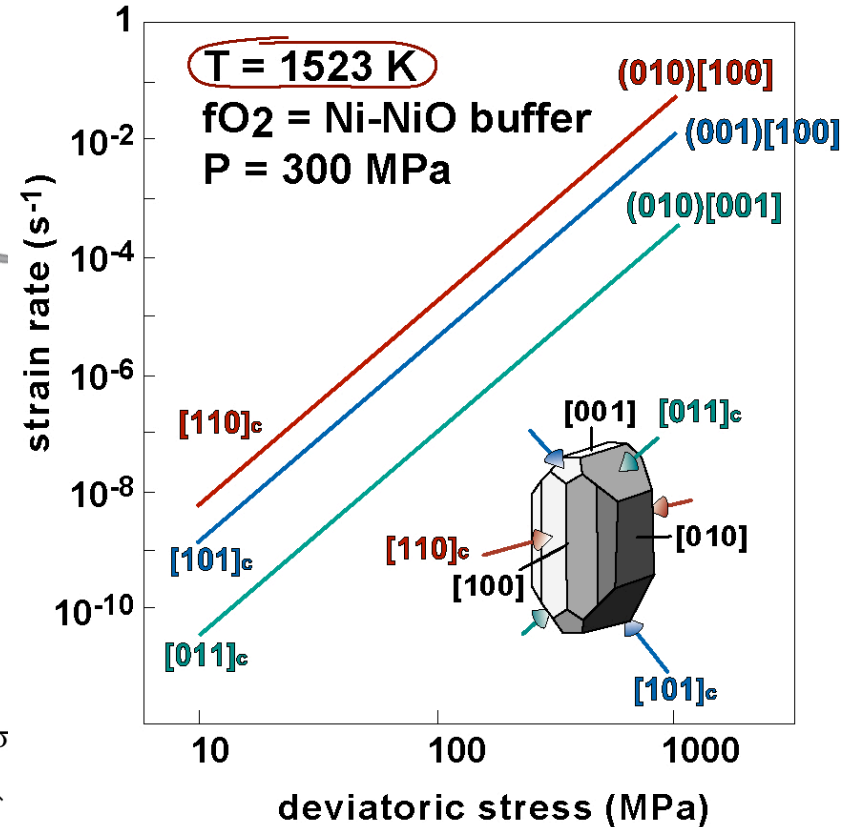
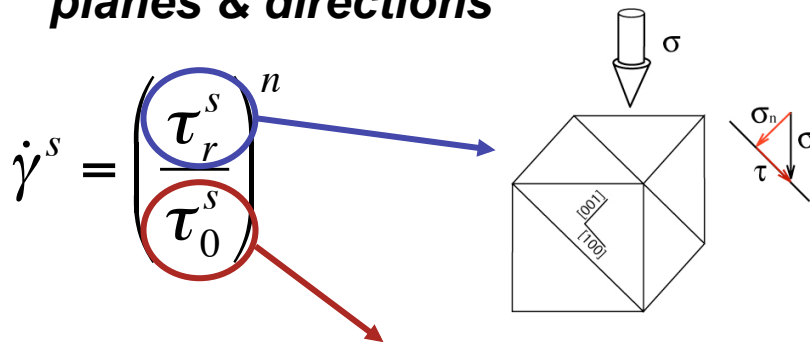
Modeling the deformation of a polycrystalline aggregate

VPSC: Molinari et al. 1987, Lebensohn & Tomé 1993

within a grain (crystal):



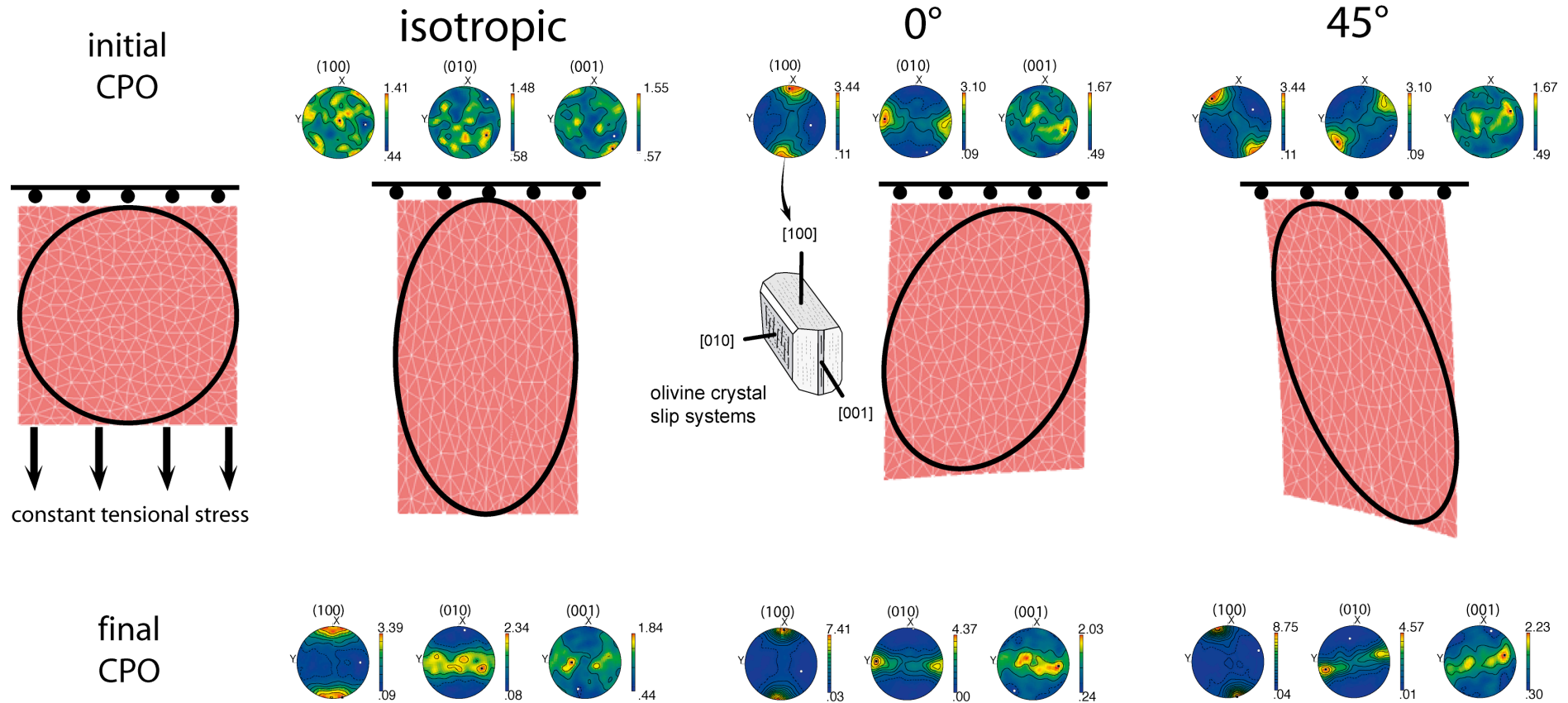
strain = motion of dislocations
on well-defined crystal
planes & directions



Bai et al. 1990 - JGR

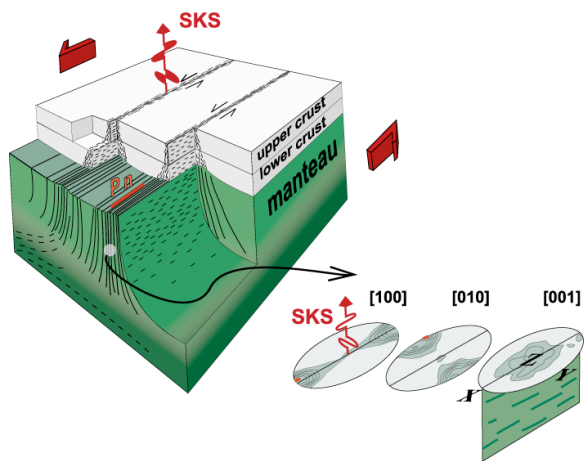
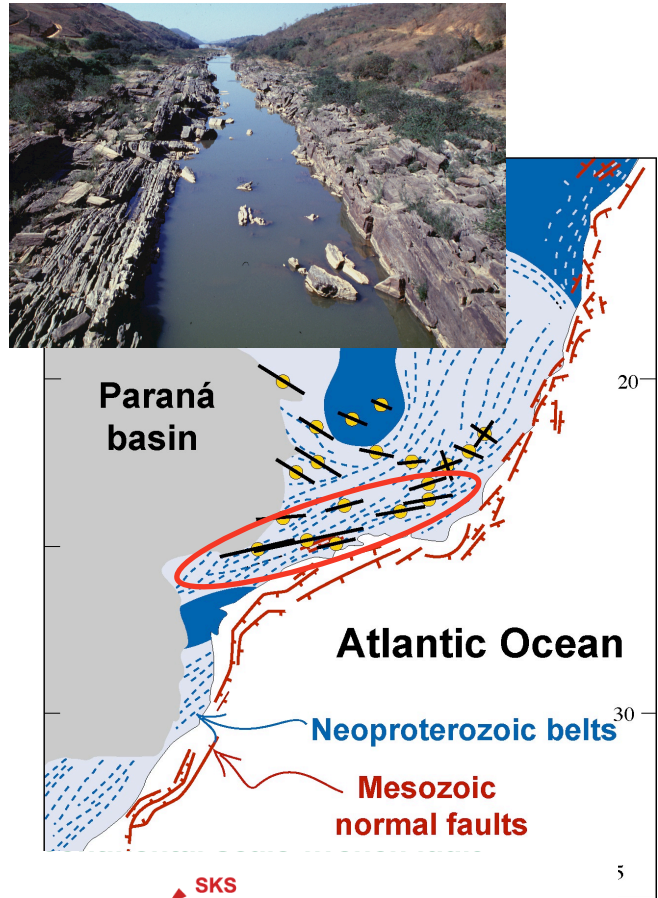
Input : slip systems' strength, initial texture &
mechanical sollicitation (**stress** or **velocity gradient tensor**)
output: evolution of crystallographic orientations &
mechanical response (**strain rate** or **stress tensor**)

Deformation of a homogeneous, BUT textured plate is strongly anisotropic

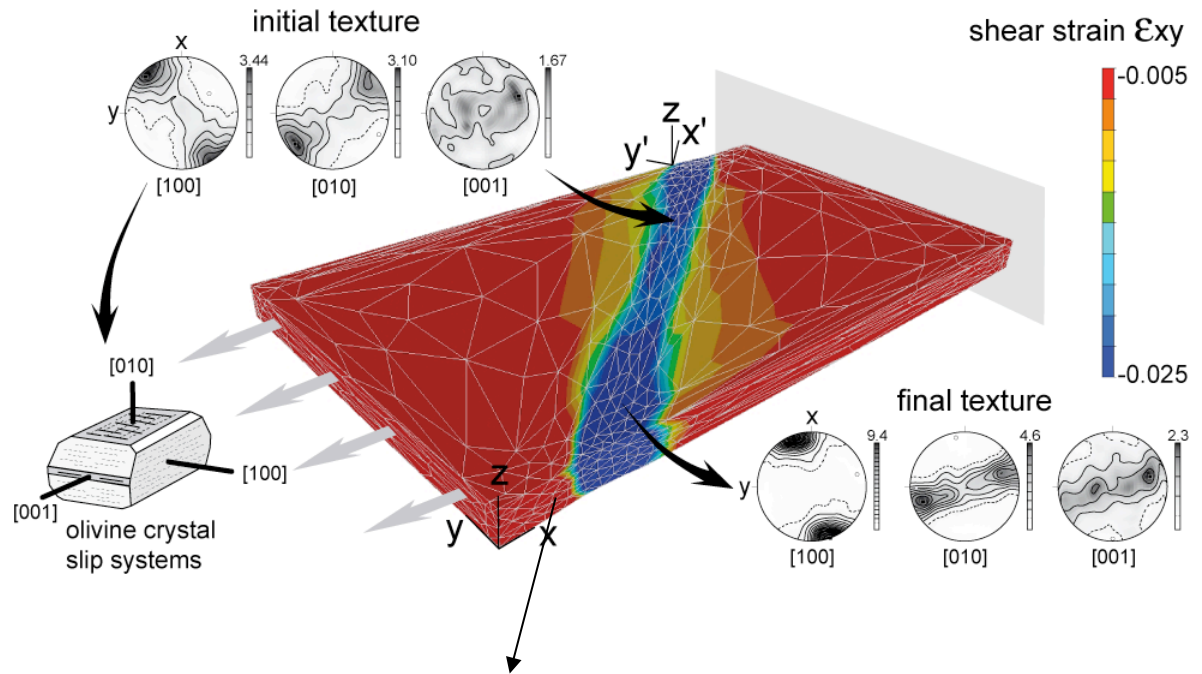


- strength & final deformation depend on the initial CPO
- finite strain ellipsoid axes are not parallel to stress ones
 - shearing // to average orientation of main olivine slip systems

Multi-domain models: Reactivation of a transpressional belt (lithospheric-scale strike-slip faults)

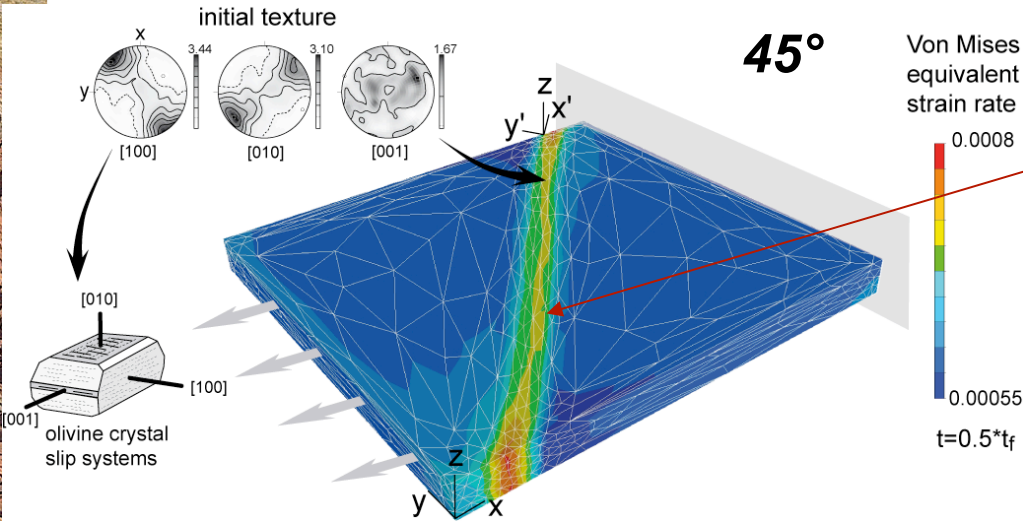


within the "old" strike-slip domain



outside = CPO initially random

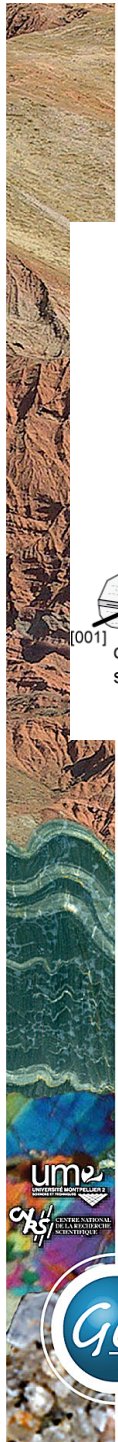
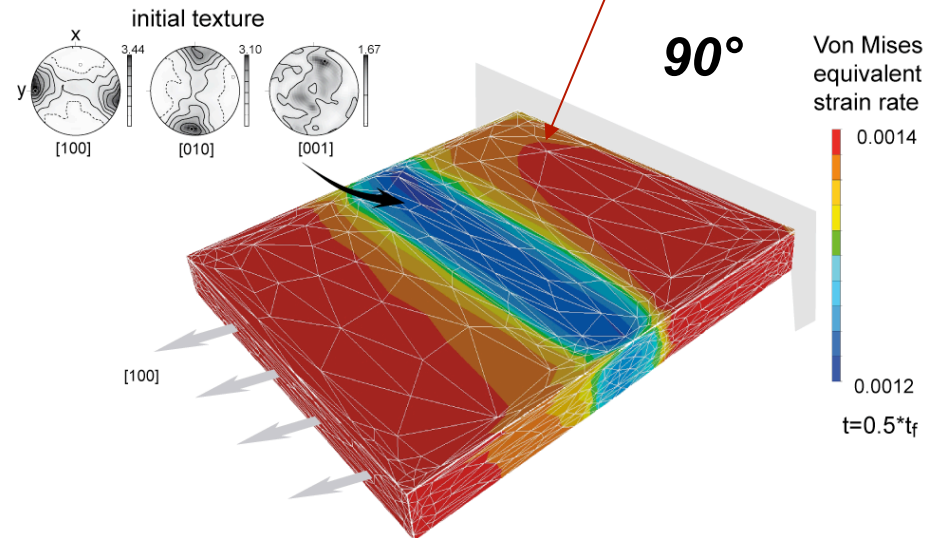
Mechanical anisotropy of the lithospheric mantle (frozen-in olivine crystal preferred orientations):



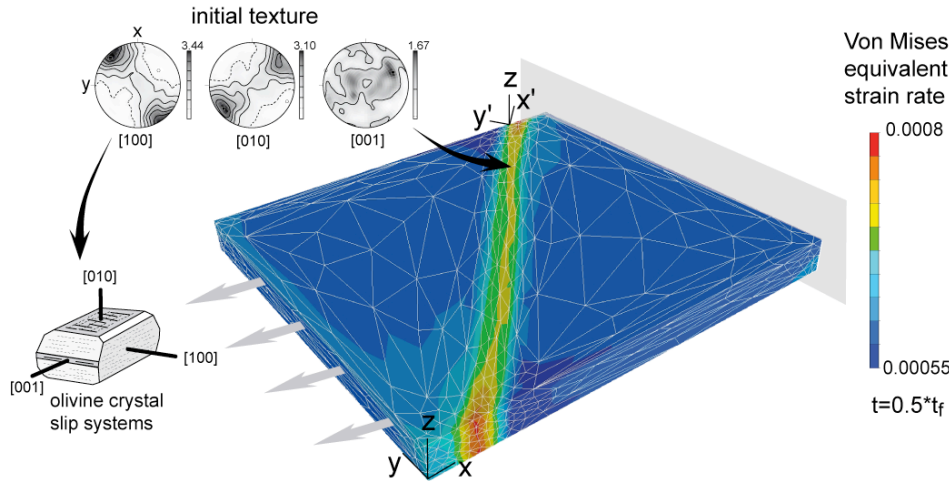
**strain localization
in the inherited SZ**

**higher strain rates
outside the inherited SZ**

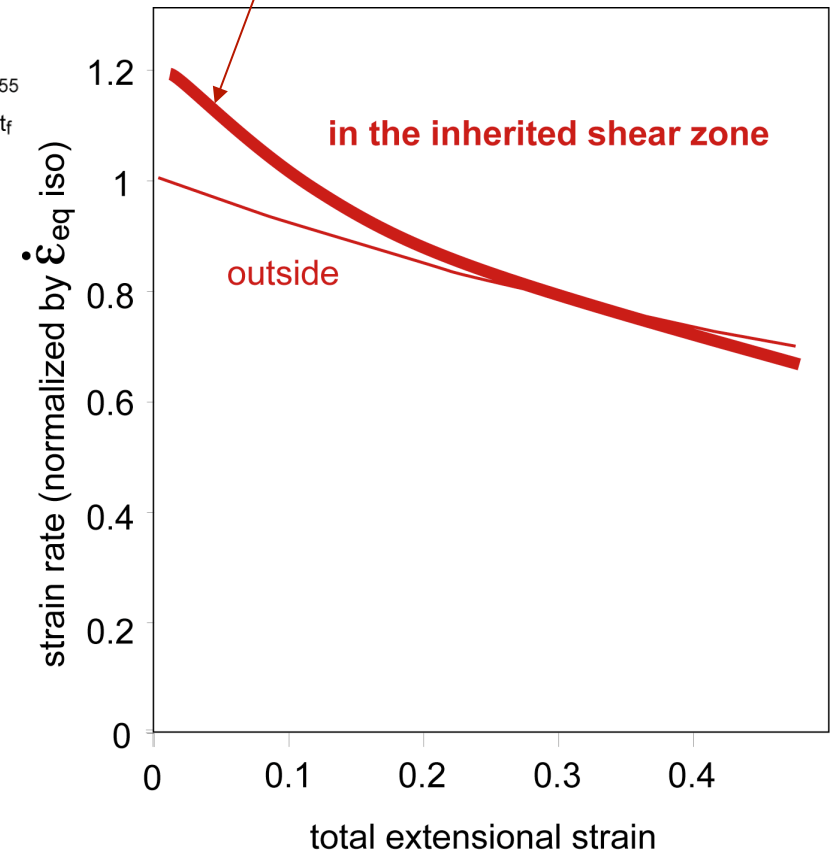
*Strain distribution depends
on the orientation of
the preexisting mantle fabric
relative to
the imposed stress field*



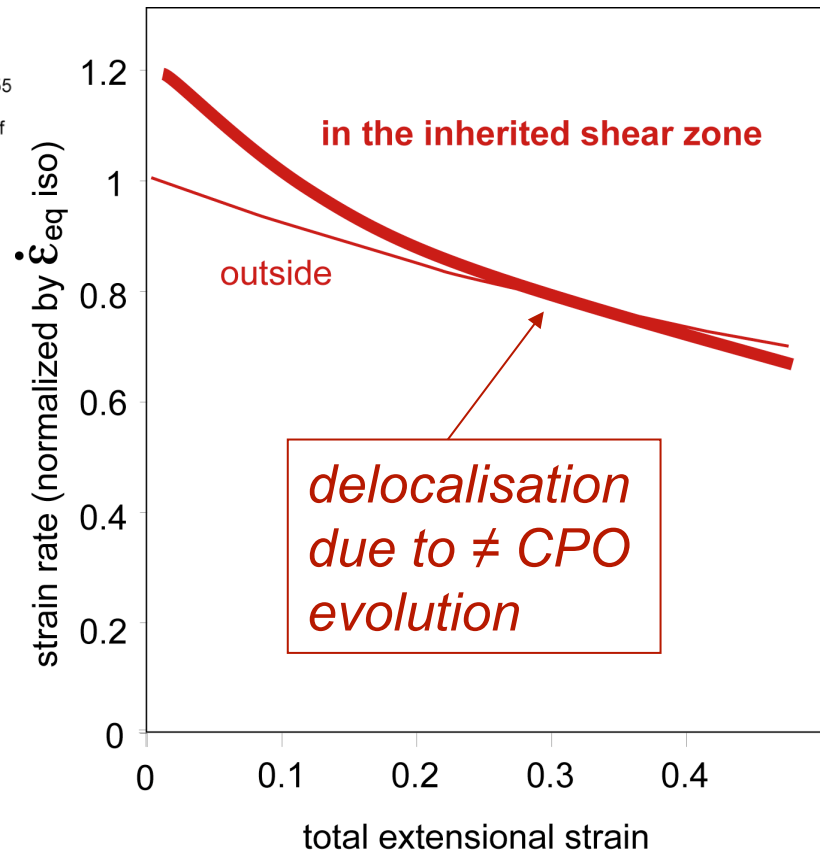
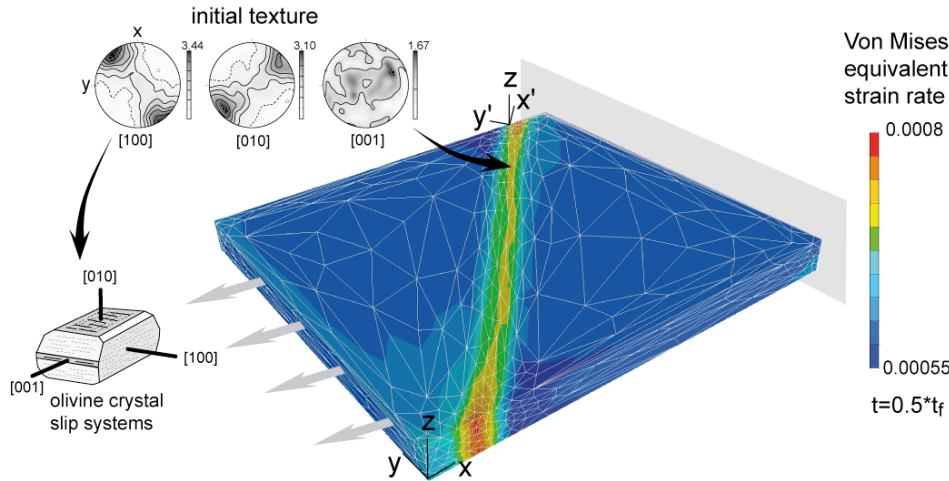
Reactivation of a lithospheric-scale strike-slip zone due to mechanical anisotropy of the lithospheric mantle (frozen-in olivine crystal preferred orientations)



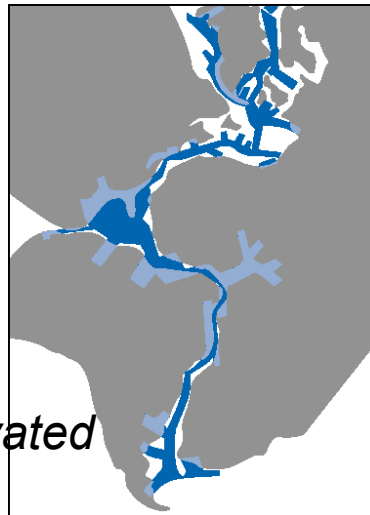
strain localization in the inherited SZ



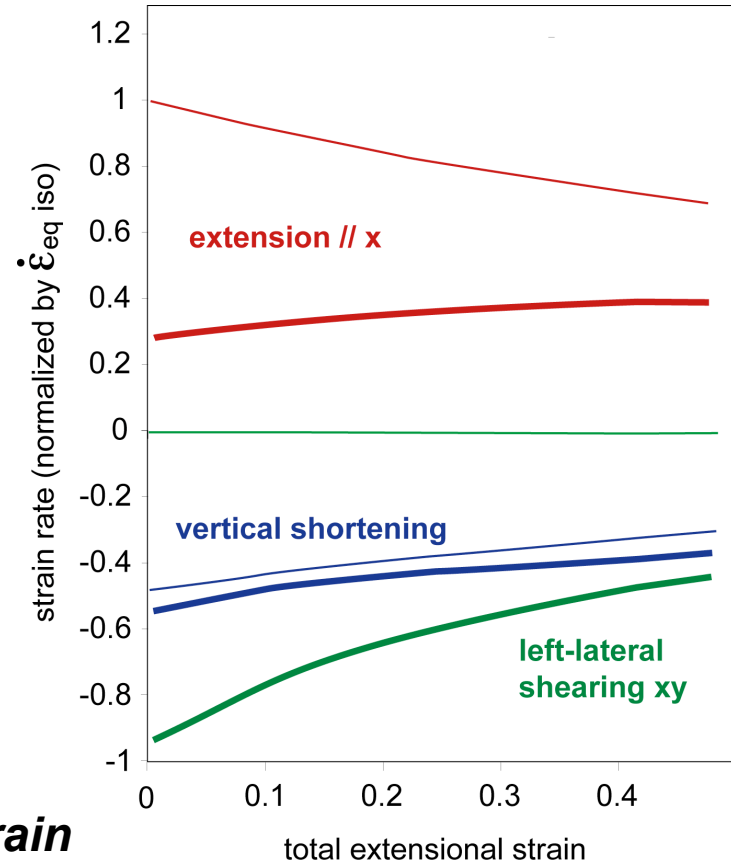
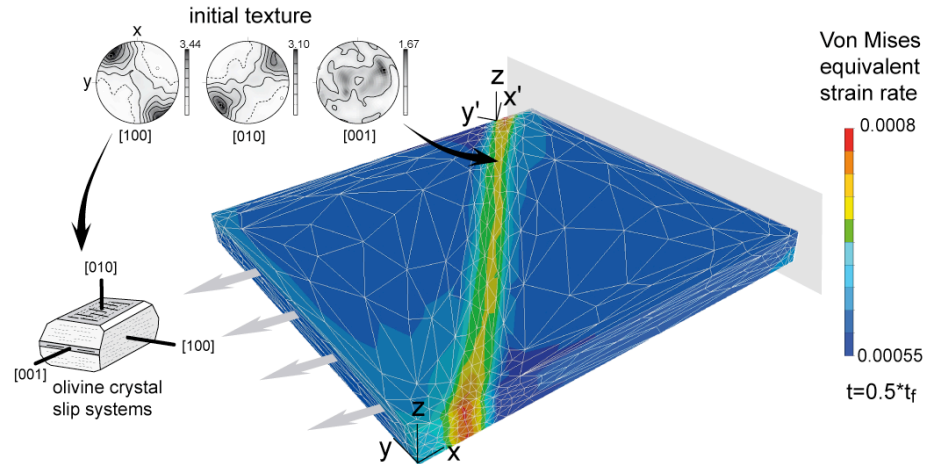
Reactivation of a lithospheric-scale strike-slip zone due to mechanical anisotropy of the lithospheric mantle (frozen-in olivine crystal preferred orientations)



rift avorts if another strain localisation mechanism is not activated



Reactivation of a lithospheric-scale strike-slip zone due to mechanical anisotropy of the lithospheric mantle (frozen-in olivine crystal preferred orientations)

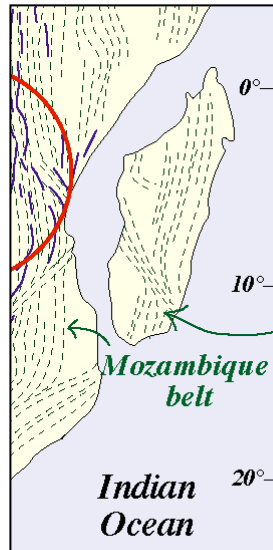


transtension in the inherited shear zone,
but **shearing** decreases with increasing strain

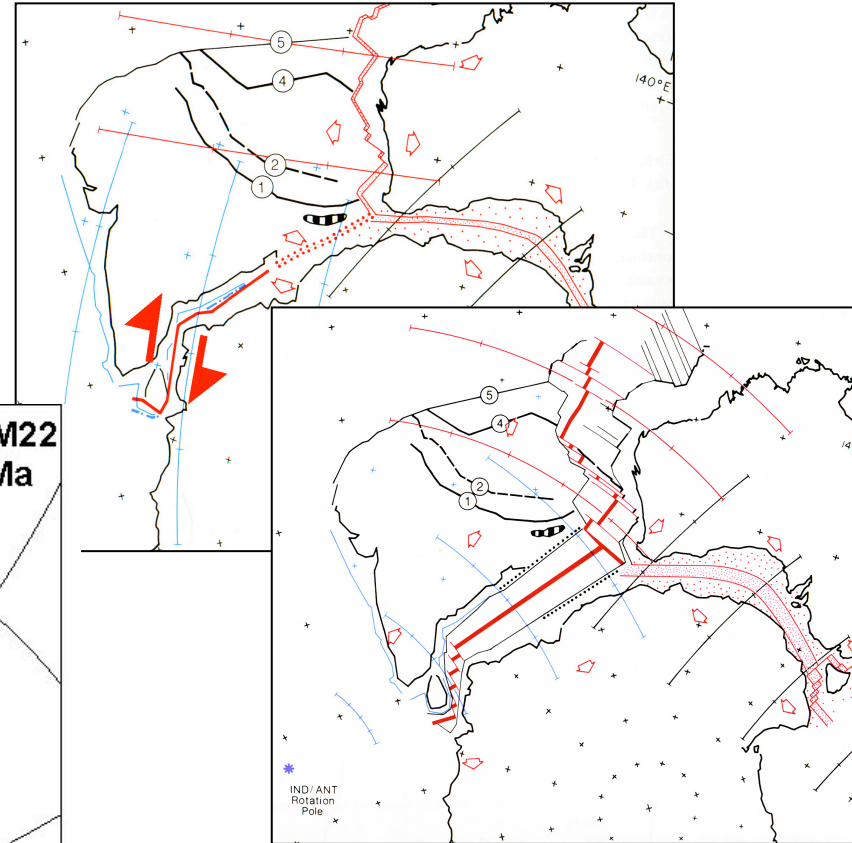
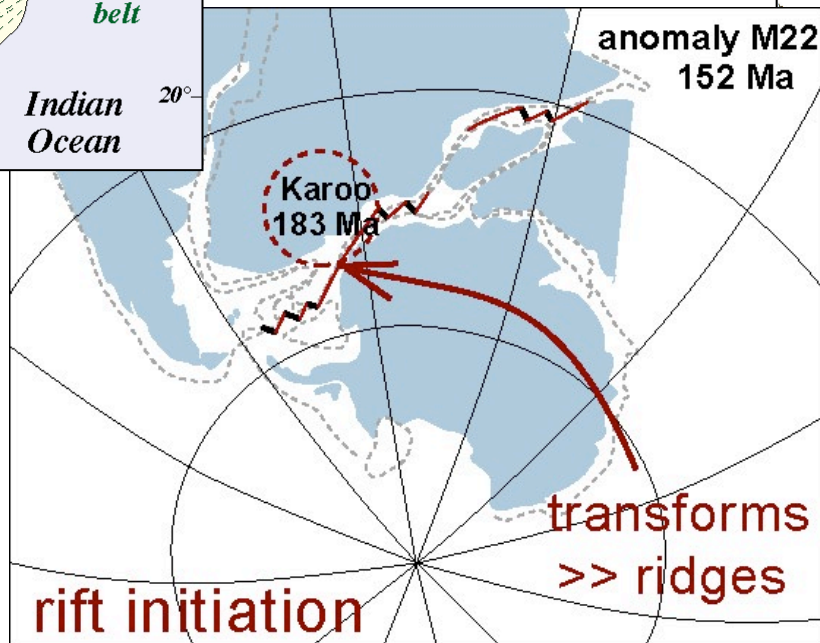
normal extension & thinning outside



Model predictions : reactivation of preexisting faults in transtension in the initial stages of rifting followed by normal extension



E Gondwana breakup

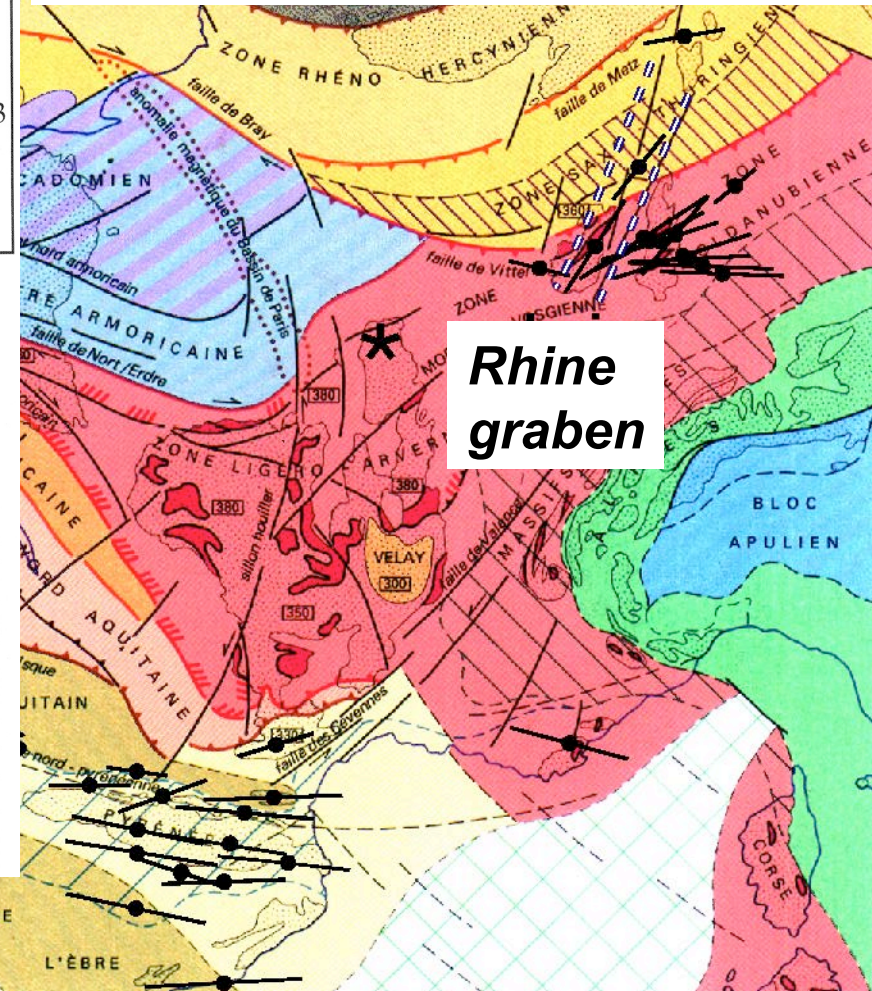
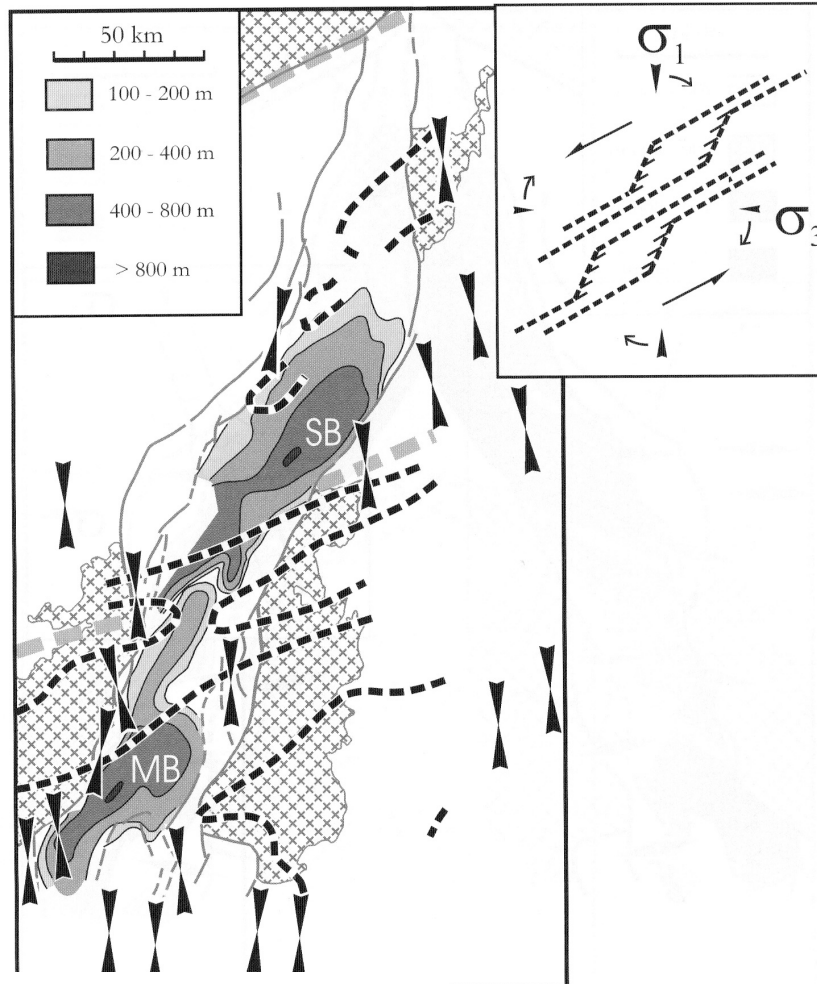


Powell et al., *Tectonophysics*, 1988

Lawer et al., *Tectonophysics*, 1985

Model predictions : reactivation of preexisting faults in transtension in the initial stages of rifting followed by normal extension

Eocene : pull apart basins shearing // to Hercynian structures

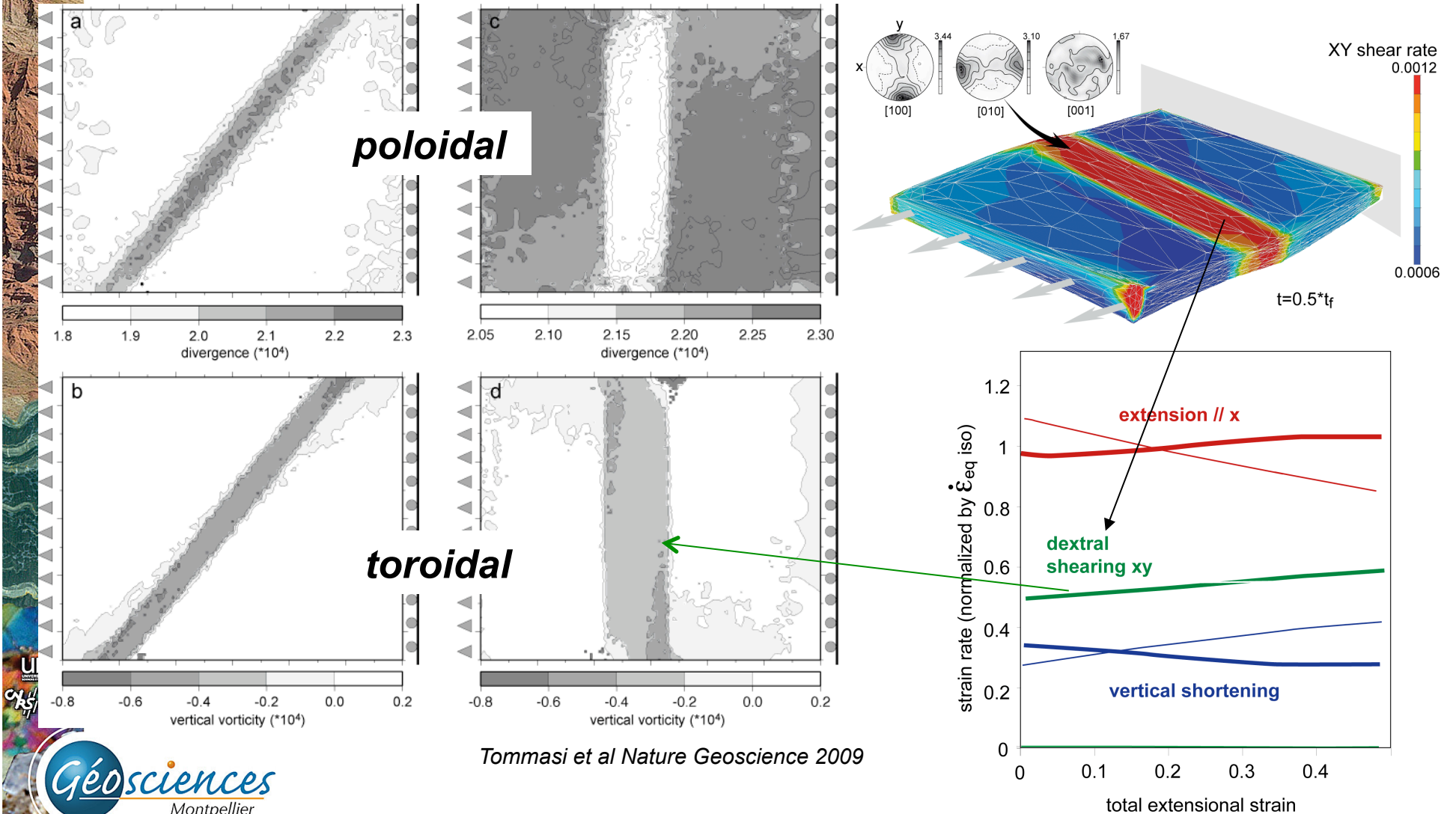


Schumacher Tectonics 2002



CPO-induced mechanical anisotropy = shearing // to preexisting mantle fabric

*Reactivation of preexisting strike-slip faults:
transforms convection-induced poloidal solicitations
(plate convergence or divergence) into toroidal (strike-slip) flow*





- **Mechanical anisotropy of the lithospheric mantle**
(frozen-in olivine crystal preferred orientations)

- *Intrinsic characteristic of the plates: olivine CPO are preserved in the lithospheric mantle until a new deformation occurs*

- *1st order parameter in plate tectonics :
together with rheological heterogeneity, anisotropy leads to intraplate strain localization:*

- *initiation of rifting*

- *linear belts of intraplate seismicity + volcanism?*

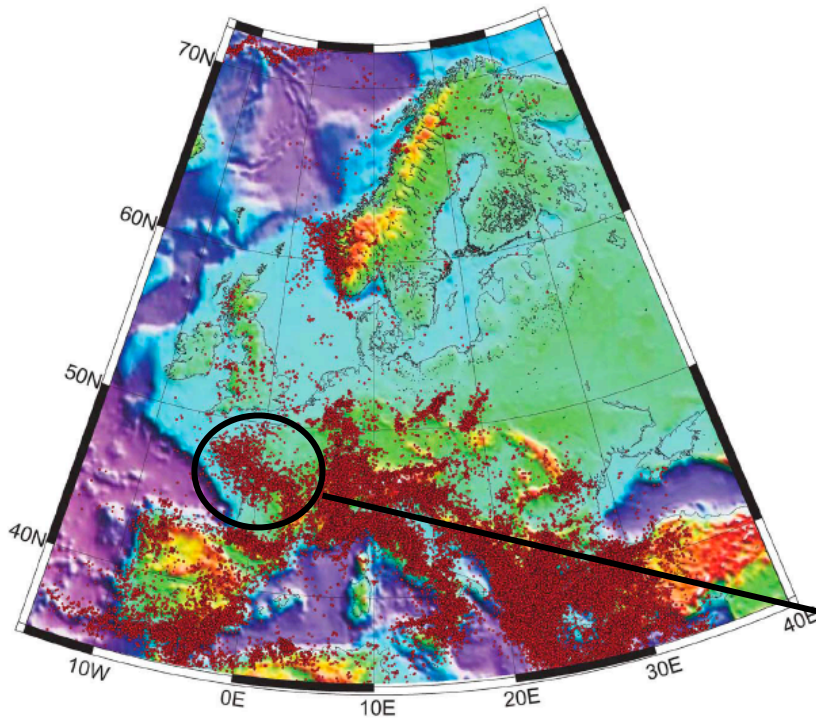
- // to ancient lithospheric faults*

- *highly effective in transforming convection-related poloidal flow into toroidal (strike-slip) motions*

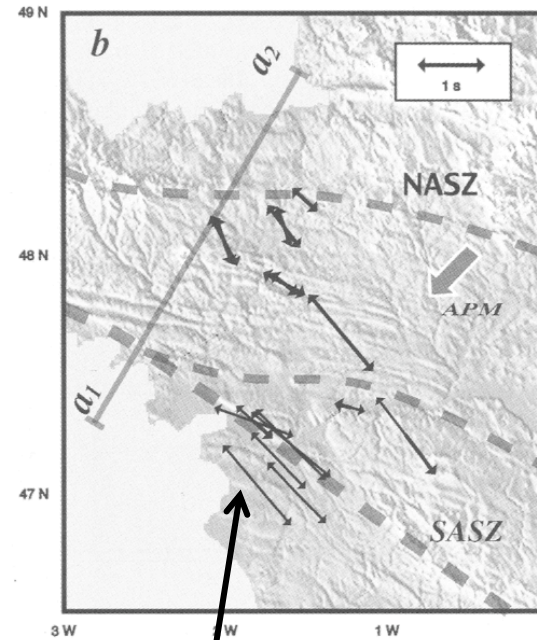
- *except for shearing // to preexisting faults, olivine CPO evolution results in hardening → delocalization unless other strain softening mechanisms are activated*

Intraplate seismicity

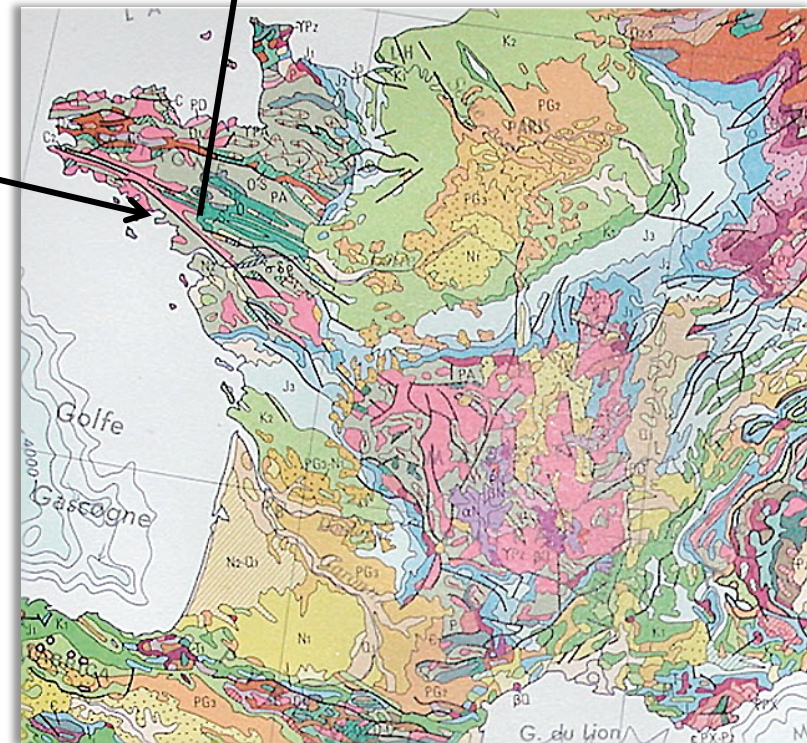
S. Cloetingh et al. / Quaternary Science Reviews 24 (2005) 241–304



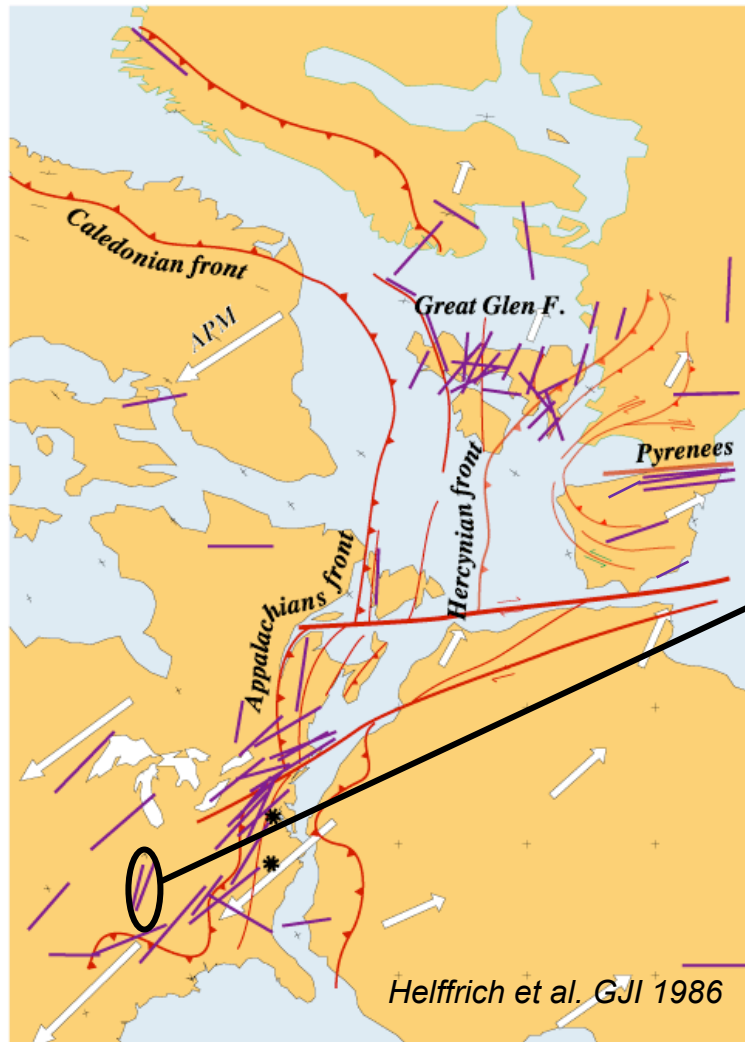
**Reactivation of
Hercynian shear zones
in France**



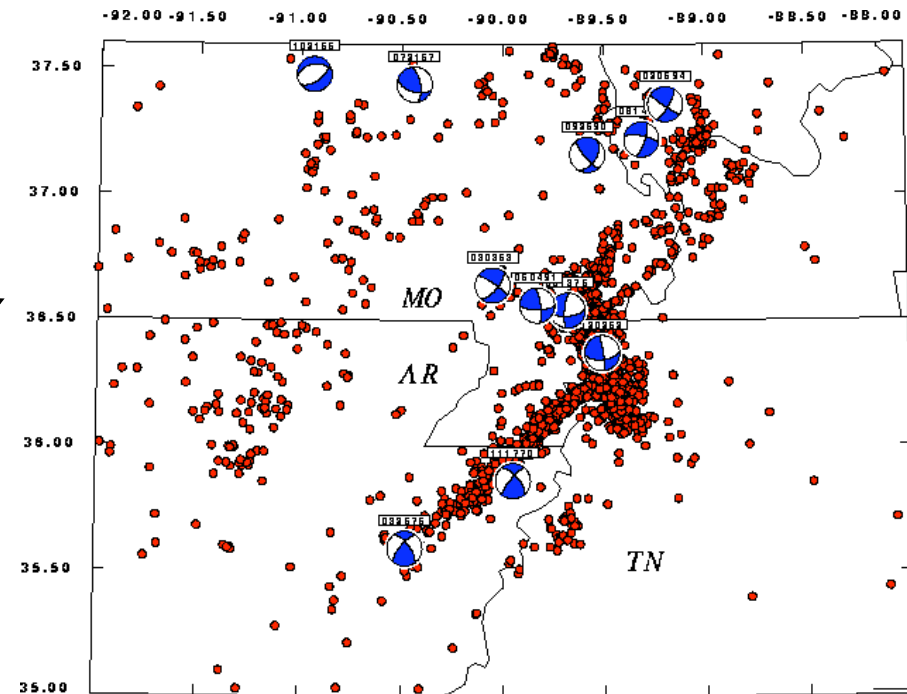
**SKS splitting,
Judenherc et al.
BSGF 2003**



Structural reactivation: Linear belts of intraplate seismicity



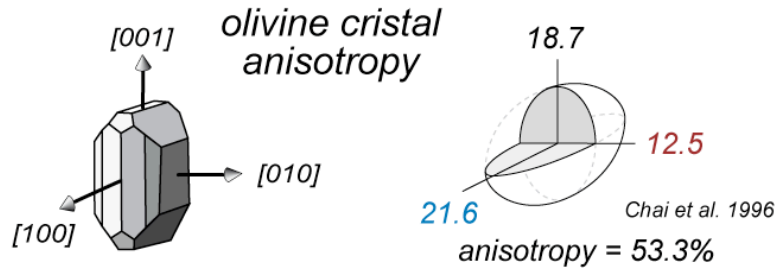
*New Madrid Seismic Zone, US
reactivation of Precambrian Reelfoot rift:*



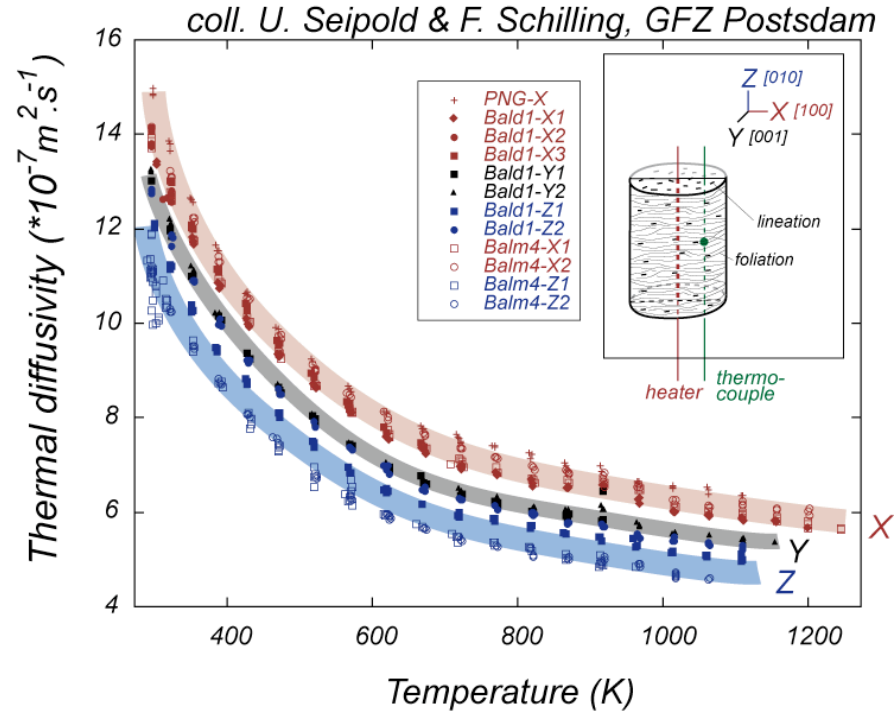
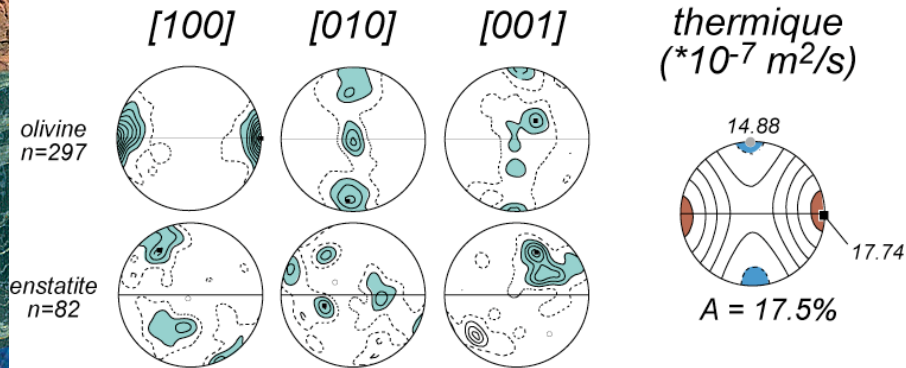
http://www.eas.slu.edu/Earthquake_Center/SEISMICITY/focalmech.html

predominance of strike-slip focal mechanisms

Anisotropic thermal diffusivity in the upper mantle



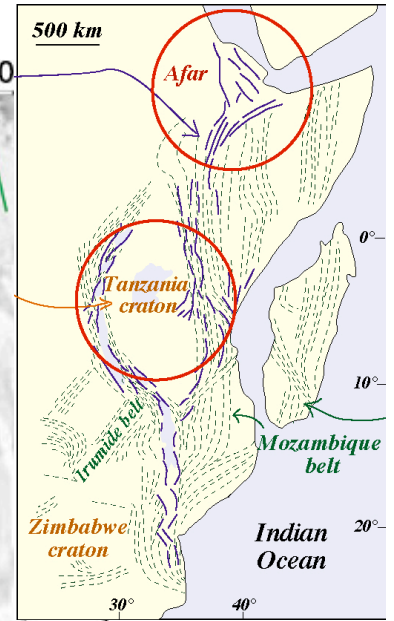
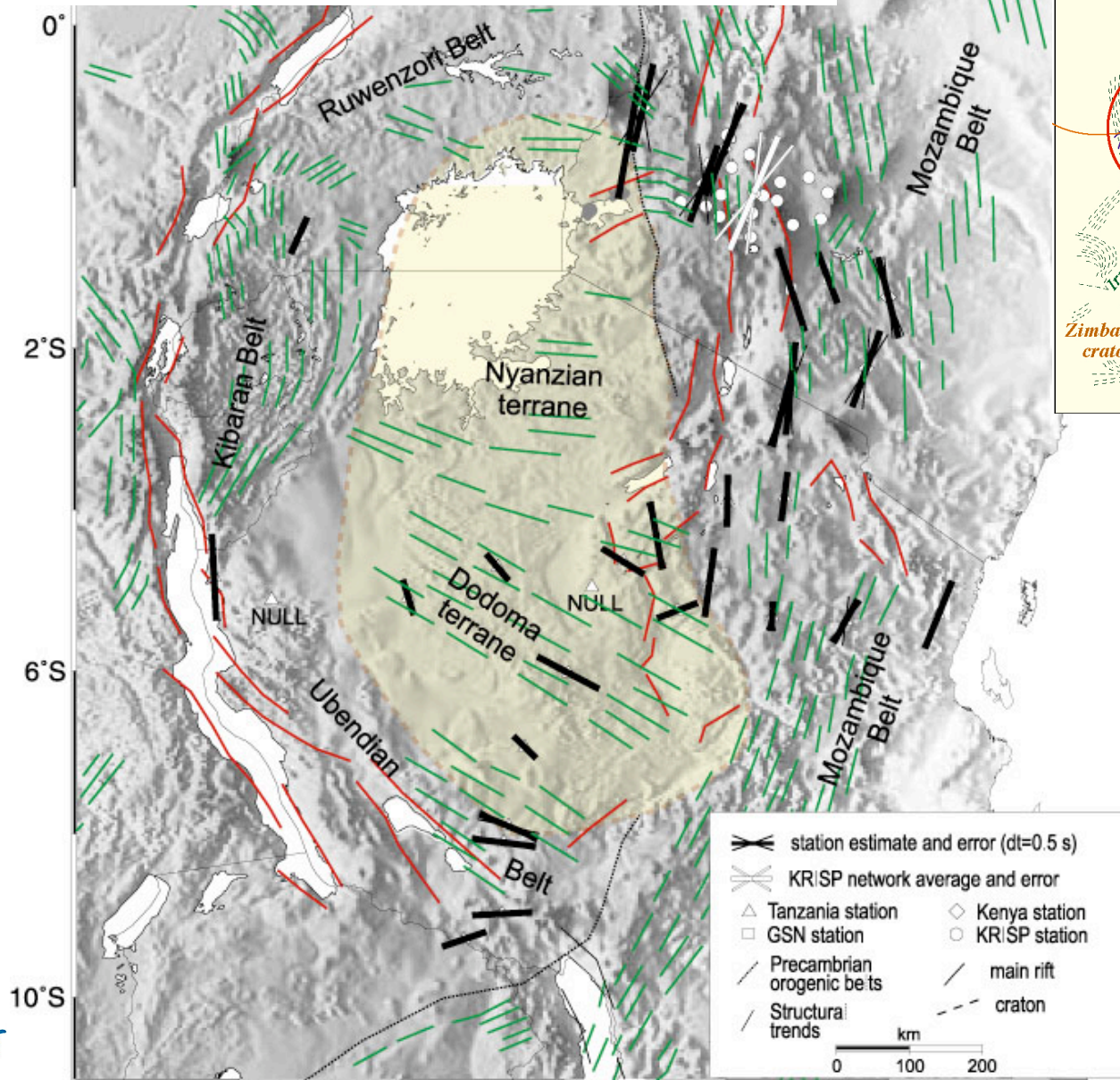
Voigt-Reuss-Hill averaging



Tommasi, Gibert, Seipold & Mainprice, Nature 2001
 Gibert, Seipold, Tommasi & Mainprice, JGR 2003
 Gibert, Schilling, Tommasi & Mainprice, GRL 2003
 Gibert, Schilling, Gratz & Tommasi, PEPI 2005

fastest heat conduction // [100] // to flow direction
slowest heat conduction // [010] normal to flow plane
 • channelling of heat along preexisting faults

**ripping : heterogeneity (lateral variation of geotherm)
& anisotropy of the plate often work together!**



Walker et al JGR 2004



Géosciences
Montpellier

Heterogeneity vs. anisotropy

Rheological heterogeneity

= lateral variations in the **thermal structure** (tectonic age or enhanced **heat production** in the lithospheric mantle due to metasomatism) or lateral variations of the **Moho depth**

Mechanical & thermal anisotropy

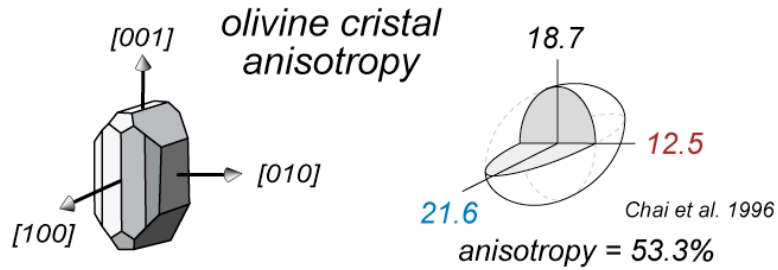
= preferred orientation of olivine crystals in the lithospheric mantle

= **intrinsic features of continental plates**

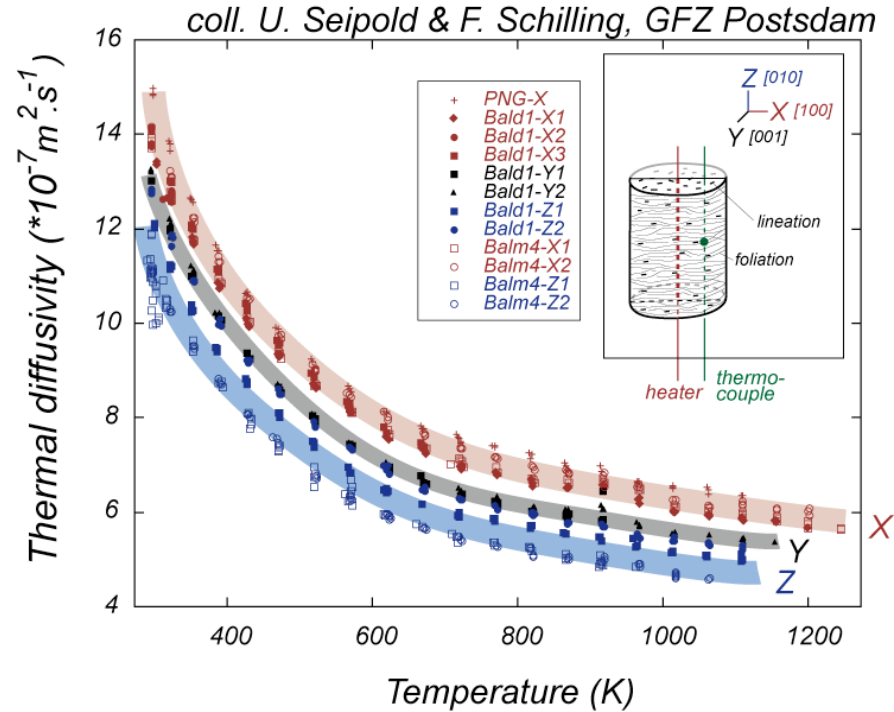
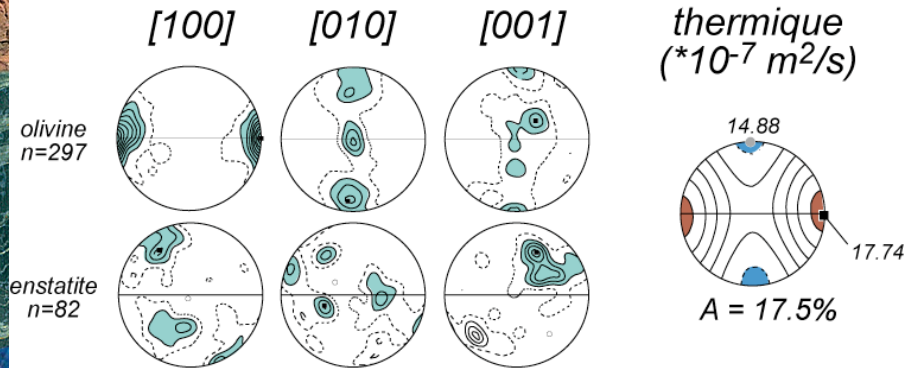
- **essential for localizing strain far from plate boundaries**
- additive contributions = often work together
- thermal gradients = highly effective to localize deformation but shorter lifetime (few 10s m.y. except cratons) & no direct effect on strain regime
- anisotropy = weaker strain localization (strain rates vary by a factor 2-5) but preserved for very long time spans & control strain regime = shearing // to preexisting fabric



Anisotropic thermal diffusivity in the upper mantle



Voigt-Reuss-Hill averaging



Tommasi, Gibert, Seipold & Mainprice, Nature 2001
 Gibert, Seipold, Tommasi & Mainprice, JGR 2003
 Gibert, Schilling, Tommasi & Mainprice, GRL 2003
 Gibert, Schilling, Gratz & Tommasi, PEPI 2005

fastest heat conduction // [100] // to flow direction
slowest heat conduction // [010] normal to flow plane
 • channelling of heat along preexisting faults